GAS SEPARATION THROUGH ZEOLITE THIN FILM MEMBRANES

Margaret E. Welk, Tina M. Nenoff

Sandia National Laboratories, PO Box 5800, MS 0734, Albuquerque, NM 87185-0734
mewelk@sandia.gov

Introduction

The synthesis and testing of inorganic zeolite membranes has been intensely studied because of their potential applications in the domains of gas separation, pervaporation, reverse osmosis and in the development of chemical sensors and catalytic membranes.[1,2,3,4,5] Specifically, development of new technologies, such as zeolite membranes, for H_2 separation and purification has a high priority for the future of H_2 as a fuel source. H_2 is commonly produced by the reformation of hydrocarbons, creating CO_2, CO, CH_4 and H_2O as by-products. A successful membrane for the separation of H_2 from other reformate gases must have both high flux and high selectivity for H_2 in the presence of these other gas species. Inorganic membranes, which have good thermal stability and chemical inertness, are highly attractive. Distinctively, zeolite membranes combine pore size and shape tunability with the inherent mechanical, thermal, and chemical stability necessary for long term separations. The effective pore size distribution, and hence the separation performance, of a defect free zeolite membrane is intrinsically governed by the choice of the zeolitic phase.[6,7,8,9]

Numerous pure gas permeation studies have been performed on MFI-type zeolite membranes that allow ideal selectivities to be calculated.[10,11,12,13,14,15,16,17,18,19,20,21] Typical literature selectivity values of H_2 from CO_2, CH_4 and CO range from 2 to 8, below the values necessary for successful industry integration. It is well recognized that gas mixtures flowing through separation membranes will behave differently than pure gases owing to adsorption effects and other phenomena. Temperature effects on the permeation properties of such membranes also need to be understood. We report here the study of the permeance and selectivity as a function of temperature of both ZSM-5 and silicalite-1 zeolite membranes under the flow of three gas mixtures, two chosen as benchmarks (50/50 mol% H_2/CH_4 and 50/50 mol% H_2/CO_2) and one chosen to emulate an industrial methane reformate stream.

Experimental

Gases. Reagent grade pure gases were purchased from Matheson Trigas. H_2, CO_2, O_2, CH_4, N_2, CO were used to test the permeability of the membranes. SF_6 was used to asses membrane quality, He was used to clean and purge the unit, shown in Figure 1. Three reagent grade gas mixtures pre-mixed by Matheson Trigas were also tested: 50/50 mol% H_2/CH_4, 50/50 mol% H_2/CO_2 , and a four gas component mixture that approximates a methane steam reformate stream, excluding the water vapor (will be referred to as the reformate mixture) : 76.2% H_2, 13.6% CO_2, 6.8%CO, and 3.4% CH_4.

Membrane Synthesis. A thorough description of the silicalite membrane growth has been published elsewhere.[22] The support cleaning, seed synthesis,[12,22] and seeding methodology for the ZSM-5 membranes are identical to the steps for silicalite also can be found in the same reference. A description of the ZSM-5 gel and hydrothermal synthesis of the ZSM-5 membranes is presented here.

In the gel used for the hydrothermal synthesis, the silicon source for the membrane synthesis was colloidal silica Ludox SM-30; the source of aluminum was $Al_2(SO_4)_3{\cdot}18H_2O$, and NaOH is the alkalinity source. Ludox SM-30 was filtered prior to use to remove any SiO_2 flakes; all other reagents were used as received. 2.14 g of NaOH, and 0.832 g of $Al_2(SO_4)_3{\cdot}18H_2O$ were added to 68.4 g of H_2O, and stirred until dissolved. 20 g of Ludox SM-30 was added drop-wise to the mixture while stirring. Each gel was then aged for 24 hours while being stirred at room temperature. Gels that were not aged under agitation did not result in selective membranes. The aged gels in this work were homogeneous and no precipitate had formed prior to the reactions.

The alpha-alumina substrates supplied by Inocermic Gmbh have a 1.8 μm average pore size, a diameter of 13 mm and a thickness of 1 mm. Their high density ensures good mechanical properties and robustness. MFI zeolite seeds were rubbed onto both sides of the cleaned substrates; the seed synthesis and application has been described elsewhere.[23] The seeded substrates were held vertically in the Teflon lined Parr reactor using Teflon holders to prevent sedimentation on top of the membrane. The homogenous gel was then poured in the reactor until the membrane was fully immersed. The hydrothermal syntheses were carried out in Parr reactors with a 23 ml Teflon liner at 170°C for 12 hours under autogenous pressure.

After the hydrothermal synthesis, the two-sided membrane was removed from autoclave, washed with DI water and dried in air at 50°C for few hours. A permeation test on the as-synthesized, uncalcined membrane allows the rapid assessment of its quality before the time-consuming calcination step. At this stage, a good quality membrane should be impermeable for SF_6. The SF_6 kinetic diameter of 5.5 Å is similar to the pore dimensions of the calcined ZSM-5 zeolite (diameter range 5.1 – 5.6 Å). Substantial SF_6 diffusion through the uncalcined membrane indicates the presence of detrimental membrane defects larger than the zeolite pores which will be opened during calcination.[23] Any existing large defects (partial coverage of the substrate and micro-cracks) may be repaired by a second hydrothermal synthesis step, using a shorter reaction time and more diluted starting gel.

Once the quality of the membrane was established, the water was removed from the membrane pores by calcination in air. A calcination temperature of 600°C led to cracks in the membrane and drastic reduction in permeation performance unless a slow temperature ramp rate was used. The stress at the interface between the zeolitic layer and the alumina substrate due to thermal expansion mismatch has to be minimized by using slow heating rates,[24] below 1°C/min. A typical successful temperature profile for the calcination is a heating and cooling rate of 0.5°C/min with a maximum temperature of 600°C maintained for 6 hours. This ensures the removal of water from the pores without creating detrimental defects within the membranes.

Characterization Techniques. The zeolite membranes were characterized by X-ray diffraction (Siemens D500 diffractometer, Cu Kα radiation, Bragg-Brentano geometry) and by Scanning Electron Microscopy (JEOL–6300V equipped with a Link Gem Oxford 6699 EDAX attachment).

Permeation Measurements. The membrane permeations were measured at room temperature using pure gases and a constant trans-membrane pressure of 15 PSI controlled by a backpressure regulator. Each membrane was sealed to a custom stainless steel washer using a silicone elastomer (NuSil) high temperature epoxy. The membrane assembly was then placed in a standard VCR fitting (Swagelok) for testing. The gas flow through the membrane was measured using an acoustic displacement flowmeter (ADM 2000 from J&W) and a digital bubble flowmeter (HP-9301). Between permeation measurements with different pure (SF_6, H_2, CO_2, O_2, CH_4, N_2, CO) and mixed (50/50 H_2/CO_2, 50/50 H_2/CH_4, and the reformate mixture) gases, the whole system was purged, flushed with He and evacuated

several times. For the pure gases, the ideal gas selectivity was calculated as the ratio of the permeances in the steady regime.

Micro Gas Chromatograph. For the mixed gas studies, a Micro Gas Chromatograph (agilent) was attached to the permeate side of the membrane. Three columns were employed: a molecular sieve with Argon as a carrier gas to separate H_2, a molecular sieve with Helium as a carrier gas for CO and CH_4, and a Pora Plot column for CO_2. The permeate was autosampled once every 5 minutes. A constant trans-membrane pressure of 15 PSI was controlled by the back pressure regulator. Calibration curves were generated by flowing the gas mixtures through the permeation unit with a blank support in place of the membrane. Selectivities were calculated as the ratio of the gas species of interest.

Results and Discussion

Both ZSM-5 and Silicalite-1 are MFI type zeolites. Although they have identical structures, the pore chemistry differs owing to the presence of even a small amount of aluminum replacement of the silicon atoms in the ZSM-5 compound. The pore chemistry directly impacts adsorption and therefore, the permeation characteristics of the membranes, particularly the pure gas permeation results. Silicalite-1 membranes have a higher permeance for pure CO_2 than for pure H_2 because of the adsorption of CO_2 to the all-silica pore surfaces, At elevated temperatures, this adsorption effect disappears in the Silicalite membranes. The separation values obtained at between 200 and 300 °C approximate Knudsen separation values. See Figure 1. This is unsurprising given that the pore diameter of the Silicalite membrane is 5.6 Å, slightly larger than the kinetic diameter of H_2, CO_2, CO, and CH_4.

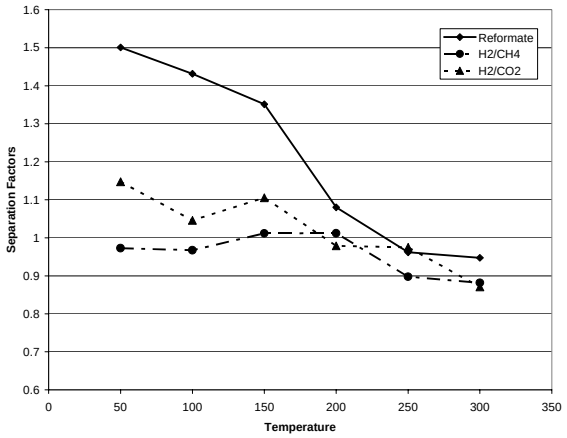

Figure 1. H_2 separation factors as a function of temperature of three gas mixtures: 50/50 mol% H_2/CH_4, 50/50 mol% H_2/CO_2, and a reformate stimulant 76.2% H_2, 13.6% CO_2, 6.8%CO, and 3.4% CH_4.

ZSM-5 has the same crystallographic structure and a similar framework pore diameter, however, exhibits different selectivity factors. Room temperature permeation results show that these ZSM-5 membranes are hydrogen selective beyond Knudsen values, with an H_2/CO_2 ideal selectivity of 15. Mixed gas studies at elevated temperatures are underway. The sodium form of this zeolite which we are studying charge balances the substitution of the Al^{3+} for Si^{4+} with Na^+ ions. These cations reside in the pore structure, thereby diminishing the pore diameter. In addition, the 0.25% substitution of aluminum for silicon adds acidity and therefore a combination of "hopping" sites for cations plus a "polarization" exhibited by the hydrophilic versus hydrophobic nature of the framework. This results in preferential adsorption of molecules onto and through these zeolites.

Conclusions

Further studies on these MFI-type zeolite membranes continue, and include elevated temperatures to 500°C, increased lifetime studies, pressure variations, and additional gas mixtures. The effects of different support materials on membrane performance are also under investigation.

Acknowledgement. Sandia is a multiprogram laboratory operated by Sandia Corporation, a Lockheed Martin Company, for the United Stated Department of Energy under contract DE-AC04-94-AL85000. We thank the DOE/Hydrogen, Fuel Cells, and Infrastructure Technologies Program for continued funding.

References

[1] Armor, J. N. *J. Membr. Sci.* **1998**, *147*, 217.
[2] Caro, J.; Noack, M.; Kolsch, P.; Schafer, R. *Microp. Mesop. Mat.* **2000**, *38*, 3.
[3] Chiang, A. S. T.; Chao, K-J. *J. Phys. Chem. Solids* **2001**, *62*, 1899.
[4] Noack, M.; Kolsch, P.; Schafer, R.; Toussaint, P.; Caro, *J. Chem. Eng. Technol.* **2002**, *25*. 221.
[5] Thoma, S. G.; Trudell, D. E.; Bonhomme, F.; Nenoff, T. M. *Microp. Mesop. Mat.* **2001**, *50*, 33.
[6] Vroon, Z. A. E. P.; Keizer, K.; Gilde, M. J.; Verweij, H. Burggraaf, A. J. *J. Membr. Sci.* **1996,** *113*, 293.
[7] Geus, E. R.; DenExter, M. J.; van Bekkum, H. *J. Chem. Soc. Faraday Trans.* **1992,** *88*, 3101.
[8] Bakker, W. J. W.; Kapteijn, F.; Poppe, J.; Moulijn, J. A. *J. Membr. Sci.* **1996**, *117*, 57.
[9] Bai, C.; Jia, M-D.; Falconer, J. L.; Noble, R. D. *J. Membr. Sci.* **1995,** *105*, 79.
[10] Lai, R. ; Gavalas, G. R. *Ind. Eng. Chem. Res.* **1998**, *37*, 4275.
[11] Hedlund, J.; Noack, M.; Kolsch, P.; Creaser, D.; Caro, J.; Sterte, J. *J. Membr. Sci.***1999,** *159*, 263.
[12] Tuan, V. A.; Falconer, J. L.; Noble, R. D. *Ind. Eng. Chem. Res.* **1999,** *38*, 3635.
[13] Lai, R.; Gavalas, R. *Microp. Mesop. Mat.* **2002,** *38*, 239.
[14] Xomeritakis, G.; Nair, S.; Tsapatsis, M. *Microp. Mesop. Mat.* **2000,** *38*, 61.
[15] Hedlund, J.; Sterte, J.; Anthonis. M.; Bons, A. J.; Carstensen, B.; Corcoran, N.; Cox, D.; Deckman, H.; De Gijnst, W.; de Moor, P-P.; Lai, F.;McHenry, J.; Mortier, W.; Reinoso, J.; Peters, J. *Microp. Mesop. Mat.* **2002,** *52*, 179.
[16] Noack, M.; Kolsch, P.; Schafer, R.; Toussaint, P.; Sieber, I.; Caro, J. *Microp. Mesop. Mat.* **2002,** *49*, 25.
[17] Lai, Z. P.; Bonilla, G.; Diaz, I.; Nery, J. G.; Sujaoti, K.; Amat, M. A.; Kokkoli, E.; Terasaki, O.; Thompson, R. W.; Tsapatsis, M.; Vlachos, D. G. ***Science***, **2003,** *300*, 456.
[18] Xomeritakis, G.; Lai, Z.P.; Tsapatsis, M. *Ind. Eng. Chem. Res.* **2001,** *40*, 544.
[19] Lovallo, M. C.; Tsapatsis, M *AICHE Journal* **1996,** *42*, 3020.
[20] Lovallo, M. C.; Gouzinis, A.; Tsapatsis, M. *AICHE Journal* **1998,** *44*, 1903.
[21] Poshusta, J. C.; Noble, R. D.; Falconer, J. L. *J. Membr. Sci.* **1999,** *160*, 115.
[22] Bonhomme, F; Welk, M. E.; Nenoff, T. M.; *Microp. Mesop. Mat.* **2003,** *66*, 181.
[23] Breck, D.W. Zeolite Molecular Sieves, (John Wiley and Sons, New York 1997).
[24] Dong, J.; Lin, Y. S.; Hu, M. Z. C.; Peascoe, R. A.; Payzant, E. A. *Microp. Mesop. Mat.* **2000,** *34*, 241.

HYDROGEN PERMEATION AND STABILITY OF A COMPOSITE PdCu MEMBRANE

Federico Guazzane, Erik Edwin Engwall, Ivan Peter Mardilovich, and Yi Hua Ma

Center for Inorganic Membrane Studies
Department of Chemical Engineering
Worcester Polytechnic Institute
100 Institute Road
Worcester, Massachusetts 01609 USA)

Introduction

The production of hydrogen from the steam reforming of hydrocarbons in a Pd or Pd-alloy membrane reactor has been proven to be a feasible and economically viable approach for hydrogen production[i,ii]. Composite Pd-Cu alloys have the advantage over Pd and Pd-Ag membranes of being mechanically stable and sulfur resistant[iii]. Morreale et al[iv] recently proved that the low hydrogen permeable Pd-Cu α phase was more resistant to sulfur poisoning than the highly permeable β phase. The $Pd_{60}Cu_{40}$ alloy, having the highest hydrogen permeability, looses its hydrogen transport properties at temperatures above 450ºC due to the β to α transformation. Moreover, the permeability of Pd-0 to 30 wt% Cu alloys decreases as the Cu content increases. Therefore, a low (10-20wt%) Cu content Pd-Cu alloy membrane would preferably be used at high temperatures (>500ºC) and sulfur contaminated atmospheres.

The main objective of this work was to assess the possibility of preparing a thin (<10μm) and stable low Cu content (~10wt%Cu) Pd-Cu membrane on a porous metallic support. Special attention was focused on hydrogen permeance and selectivity stability at 450ºC.

Experimental

The low Cu content Pd-Cu membrane was prepared by the coating and diffusion technique. That is, a 5μm thick palladium layer and a 2μm thick Cu layer were sequentially deposited by the electroless plating method on a porous metal support (0.1μm, Mott Co.). A detailed description on the support preparation and the plating procedures can be found in Ma et al[v] and Mardilovich et al[vi]. The Pd-Cu bimetallic structure was annealed in hydrogen atmosphere following a stage-wise temperature program i.e. the membrane was held for 12-24 hours at 250, 300, 350, 400, 450, 500 and 550ºC. Finally, the annealed Pd-Cu membrane was coated with an additional 3μm of palladium to achieve a leak free membrane. The total surface of the hydrogen permeable membrane was 120 cm^2 and its thickness was estimated to be 10 μm. The Cu content was targeted to be 10wt% although permeation results revealed that the Cu content was close to 5wt%.

The permeation apparatus consisted of a shell and tube stainless steel reactor where the membrane was housed using stainless steel and graphite ferrules. All parameters, pressure, temperature and gas fluxes were continuously logged using National Instruments data acquisition equipment. A detailed description of the permeation system used for membrane characterization was carried out by Mardilovich et al.

The He leak of the membrane was measured either in pure He atmosphere or in hydrogen atmosphere by feeding the shell side with a 99%H_2-1%He mixture gas and analyzing the tube flow with Gas Chromatography (GC). UHP Hydrogen was used as carrier gas and the TCD detector gain was set to high.

Results and Discussion

Hydrogen permeance. The hydrogen permeation rate of the Pd-5wt%Cu membrane was measured at 250, 300, 350, 400 and 450ºC. As seen in Figure 1, no decline in hydrogen permeance was observed at 450ºC over 500 hours indicating that no intermetallic diffusion, migration of support elements into the Pd-Cu layer, occurred for temperatures below or equal to 450ºC.

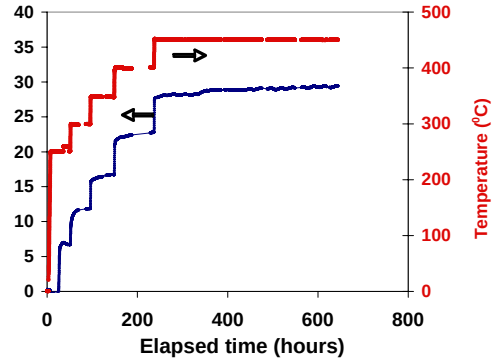

Figure 1. Hydrogen characterization carried out for the Pd-Cu membrane.

Figure 2 shows the hydrogen flux of the Pd-5wt%Cu as a function of $\Delta(P^{0.5})$ at 250, 300, 350, 400 and 450ºC. The hydrogen permeance value of 30 $m^3/(m^2\ h\ bar^{0.5})$ at 450ºC was slightly lower than the hydrogen permeance of a 10μm thick pure Pd membrane previously tested in our laboratory, which showed at 450ºC a hydrogen permeance of 34 $m^3/(m^2\ h\ bar^{0.5})$. The slightly lower hydrogen permeance of the Pd-Cu membrane is consistent with a low Cu content. As seen in Figure 2, the hydrogen flux seemed to be a linear function of $\Delta(P^{0.5})$ indicating that bulk diffusion was the rate limiting step. However, non-linear curve fitting procedure led to hydrogen exponent values of 0.6. The activation energy for hydrogen permeation, assuming Sievert's law, was determined to be 15.6 kJ/mol, which corresponded to a 5-8wt% Cu content. The Cu content was estimated by fitting Ea vs. Cu content experimental data from Howard et al.[vii] with a 3rd degree polynomial function.

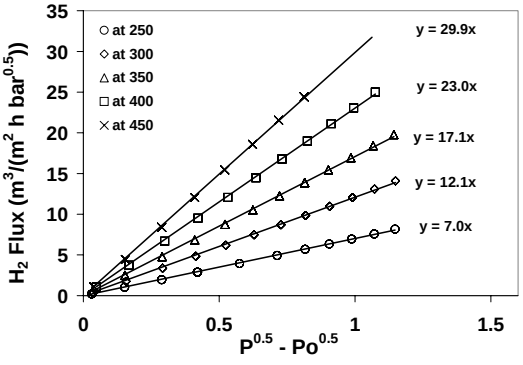

Figure 2. Hydrogen permeance at 250-450ºC for a 10μm thick Pd-5wt%Cu. Numbers beside experimental lines are the hydrogen permeance assuming Sievert's law was followed (n=0.5)

He leak stability. It was of great interest to determine the leak stability of the membrane at low temperatures (250-400ºC) and especially the leak behavior as a function of time at 450ºC in hydrogen atmosphere. The He leak in He atmosphere at 300ºC was equal to 0.0048 $m^3/(m^2$ h bar) (selectivity H_2/He = 1050) after exposure to hydrogen at 300ºC. After measuring hydrogen permeation rate at 350 and 400ºC the He leak was measured at 400ºC in He atmosphere and equaled 0.0054 $m^3/(m^2$ h bar) (selectivity H_2/He = 1760). Since the He leak was almost unchanged up to 400ºC it appeared that the membrane microstructure did not change as temperature was raised i.e. no changes in defects occurred at temperatures between 250 and 400ºC.

The initial He leak at 450ºC, determined with a GC analysis, equaled 0.0046 $m^3/(m^2$ h bar), which was equal to the He leak at 400ºC within the margin of error. That is, the He leak did not increase during the 50 minutes (1ºC/min) of the temperature change. Figure 3 shows separation factor and selectivity (H_2/He) as a function of time at 450ºC in hydrogen.

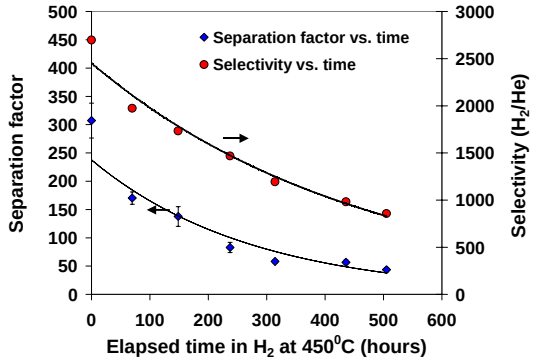

Figure 3. Separation factor and selectivity as a function of time exhibited by the Pd-5wt% Cu membrane at 450ºC in hydrogen atmosphere. The line through experimental points is a guide for the eyes

The separation factor and selectivity steadily decreased as a function of time at 450ºC in hydrogen. The decay seemed not to be linear occurring at a faster rate initially. The increase in leak might have been due related to the formation of pinholes and blisters. An average pinhole size after 500 hours at 450ºC in hydrogen was estimated by performing He and Ar permeation measurements and assuming slip-viscous mechanism (Knudsen and viscous component) for gas diffusion. Both gases led to an average pinhole size of 0.16μm at 450ºC.

Conclusions

The preparation of a low Cu content Pd-Cu alloy membrane was achieved on a porous metal support by the coating and diffusion method. The thin, 10μm, Pd-Cu membrane had a hydrogen permeance as high as 30 $m^3/(m^2$ h $bar^{0.5})$ at 450ºC and was stable for 500 hours. Leaks developed at a very slow rate at temperatures lower than 400ºC, however, the ideal selectivity of the membrane dropped from 2700 to 800 after 500 hours in hydrogen.

Acknowledgement. The authors gratefully acknowledge the financial support provided by Shell Hydrogen and Shell International Exploration and Production, Inc.

References

(i) Kikuchi E. "Membrane reactor application to hydrogen production." *Catalysis Today* **2000** 56(1-3): 97.
(ii) Lin Y. M. and Rei M. H. "Study on the hydrogen production from methanol steam reforming in supported palladium membrane reactor." *Catalysis Today* **2001** 67(1-3): 77.
(iii) McKinley D. L. U.S patent 3,350,845; **1967**
(iv) Morreale B. D., Ciocco M. V., Howard B. H., Killmeyer R. P., Cugini A. V. and Enick R. M. "Effect of hydrogen-sulfide on the hydrogen permeance of palladium-copper alloys at elevated temperatures." *Journal of Membrane Science* **2004** 241(2): 219.
(v) Ma Y. H., Mardilovich P. P., She Y. U.S patent n° 6,1502,987
(vi) Mardilovich P. P., She Y., Ma Y. H. and Rei M. H. "Defect free palladium membrane on porous stainless-steel support". *AIChe journal*, **1998** 44(2) 310-322
(vii) Howard B. H., Killmeyer R. P., Rothenberger K. S., Cugini A. V., Morreale B. D., Enick R. M and Bustamante F. "Hydrogen permeance of palladium-copper alloy membranes over a wide range of temperatures and pressures." *Journal of Membrane Science* **2004** 241(2): 207.

HIGHLY PERMEABLE AND SELECTIVE SILICA MEMBRANES FOR HYDROGEN SEPARATION AT HIGH TEMPERATURE

Yunfeng Gu, Pelin Phacarlioglu, and S. Ted Oyama

Department of Chemical Engineering
Virginia Polytechnic Institute and State University
Blacksburg, VA 24061

Introduction

Hydrogen separation membranes have been the subject of considerable research because of the importance of hydrogen in the refining and chemical industries and because of its potential as a clean, renewable fuel[1]. Many of the reactions that produce hydrogen such as steam reforming, dehydrogenation, and aromatization, are endothermic, equilibrium-limited reactions that could be enhanced by simultaneous reaction and separation. Hence there is particular need for membranes that are stable at the high temperatures (773-973 K) required for these reactions.

Silica-based membranes have been found to have good permeance for hydrogen and have received considerable attention. The first membranes were prepared on porous Vycor glass substrates by the chemical vapor deposition (CVD) of tetraethylorthosilicate (TEOS) at relatively low temperatures (473 K) using co-reagents such as H_2O[2], O_2[3], or O_3[4]. These conditions as well as methods such as the "opposing reactants"[5] or evacuation[6] techniques resulted in the deposition of the silica in the interior of the pores and gave rise to low permeance of the order of 10^{-8} mol $m^{-2}s^{-1}Pa^{-1}$. Improvements were obtained using a thermal decomposition method in which the TEOS was decomposed at high temperature (873-923 K) in an inert atmosphere using Vycor[7] or alumina[8] substrates. The resulting membrane had silica in the form of a thin outer layer of 20-30 nm thickness, and was denoted Nanosil to distinguish it from the previous materials. In this work we report the preparation and properties of a unique Nanosil-type membrane with an intermediate graded alumina substrate architecture which shows high permeability to hydrogen. The permeance at 873 K is high up to 5×10^{-7} mol $m^{-2}s^{-1}Pa^{-1}$, while its selectivity (> 5800 for CH_4) is excellent.

Experimental

Alumina Multilayer Substrate Preparation. The membrane was prepared using as a support a commercial macroporous alumina tube with nominal pore size of 100 nm. A 3-4 cm section of the support was connected to non-porous alumina tubes at both ends with ceramic glass joints. The support was dip-coated successively with a series of boehmite sols of decreasing particle sizes to form a graded multilayer γ-alumina substrate. The boehmite sols were prepared by carefully controlling the hydrolysis of aluminum alkoxides and the subsequent acid peptization of the boehmite precipitate. Three boehmite sols of median particle sizes of 40, 200 and 630 nm were obtained using the conditions listed in **Table 1** at a concentration of around 0.8M. They were denoted S40, S200, and S630. Before the membrane preparation, these original sols were diluted with distilled water and mixed with a polyvinyl alcohol (PVA) solution to form dilute dipping solutions with a 0.15 M concentration of the sol and a 0.35 wt% concentration of the PVA. The alumina support was dipped into the sol solution and was withdrawn after 10 seconds at a rate of 0.01 m s^{-1} using a motor-driven dipping apparatus. The dip-coated alumina was dried in ambient air for 24 h, and then was heated to 923 K in air at a rate of 1 K min^{-1} and calcined at 923 K for 2 h. The dipping-calcining process was repeated using successively smaller sols to form the three-layer γ-alumina substrate. Unsupported γ-alumina reference samples were prepared using the same procedure and parameters as the supported membranes.

Silica Layer Preparation. The final stage of the preparation of the composite membrane involved the deposition of a thin silica layer by the thermal decomposition of TEOS[9]. Briefly, the procedure was carried out in a concentric tubular apparatus with a quartz tube on the outside and the graded γ-alumina substrate on the inside. After heating the assembly to 873 K at a rate of 0.017 K s^{-1}, an argon gas flow (17 μmol s^{-1}) was introduced on the outer annular side and a dilute argon gas flow (17 μmol s^{-1}) with TEOS at a concentration of 0.019 mol m^{-3} was passed on the inner tube side. The TEOS deposition time was 3 h.

Characterization. A dynamic light scattering analyzer (Horiba Model LB-500) was used to measure the particle size of the boehmite sols. Single-gas permeation measurements were carried out at 873 K on H_2, CH_4, CO and CO_2 by admitting the pure gases at 200 kPa into the inner tube side, one end of which was closed, and measuring the quantity of gas flowing into the outer tube with a bubble flow meter at atmospheric pressure. The permeance of gas was obtained from the expression $F_i = (J_i / A)\ \Delta P$, where F_i is the permeance (mol m^{-2} s^{-1} Pa^{-1}), J_i the gas flux (mol s^{-1}), A the surface area (m^2) of the membrane section, and ΔP the gas pressure difference (Pa) between the shell and tube side. Permeation of He, H_2, and Ne was measured in a similar manner at 453-873 K. For low permeances a sweep gas at a known flow rate was used and the composition of the permeate stream was determined with a gas chromatograph (GC). The selectivity was calculated as the ratio of the permeances of H_2 to CH_4, CO or CO_2. A Field Emission Scanning Electron Microscope (FESEM, Leo 1550) was used to observe the cross-sectional microstructural of the membrane.

Results and Discussion

A key step in the synthesis was the formation of colloid boehmite sols of controlled particle size. The particle size of the sols is influenced by reaction conditions such as acid type, acid concentration and hydrolysis time, but past work in this area has yielded conflicting results. The results in **Table 1** show that long hydrolysis time and low acid concentration produce larger sol particles. These colloid sols have a relatively narrow particle size distribution due to the relatively long time of peptization. They were found to be stable for more than six months. The results of nitrogen physisorption on the unsupported γ-alumina references (obtained with a Micromeritics ASAP 2000) indicate that after gelling and subsequent calcination, the resulting γ-alumina membranes had different pore sizes and porosities. The larger the particle size of the sols, the larger the pore size and porosity of the resulting materials.

Table 1. Synthesis Parameters of Boehmite Sols with Different Particle Size

Boehmite Sol	Hydrolysis time / h	Molar ratio of H^+/Al	Median particle size / nm
S40	3	0.15	40
S200	24	0.07	200
S630	24	0.04	630

Cross-sectional images of the silica-on-alumina membrane reveal that three γ-alumina layers with different textures are observable, as shown in **Fig. 1**. There is no evidence of particle penetration into the support, indicating the success of the synthesis strategy of using large particles first. Significantly in this work, the use of dilute solutions (0.15 M) resulted in a relatively thin multilayer structure. The total thickness of the graded γ-alumina multilayer was around 1400 nm (1.4 μm). This is much thinner than

that of typical intermediate alumina layers of 6-10 μm in thickness even though they are not graded.

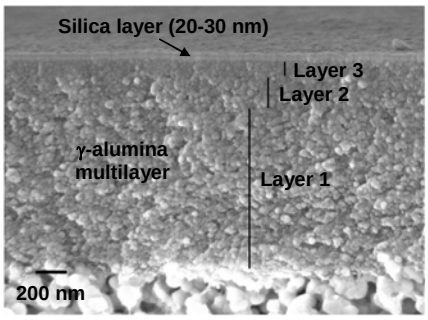

Figure 1. Scanning electron micrographs of fractured sections of the silica/γ-alumina multilayer with a graded three-layer structure.

The top γ-alumina layer has uniform pores and a smooth surface that leads to the formation of a stable silica layer on its surface. The layer is uniform and very thin (20-30 nm). The results here can be contrasted to our previous work with a single, non-graded intermediate layer. In that work again a silica layer of around 30 mm was obtained, however, the silica deposition time required at the same conditions was much longer (12 h vs. 3h) and resulted in a membrane with lower permeability (5-fold) and lower selectivity (2-fold). This implies that for a single intermediate layer a substantial amount of silica needed to be deposited inside the pores of the γ-alumina to repair imperfections before the top layer could be formed. The H_2 permeance was as high as 4.9×10^{-7} mol m^{-2} s^{-1} Pa^{-1} at 873 K, while the selectivities of H_2 over CH_4, CO and CO_2 through the composite membrane reached to 5900, 5100 and 1500, respectively. This indicates that a H_2 purity above 99.9% could be obtained using this composite membrane.

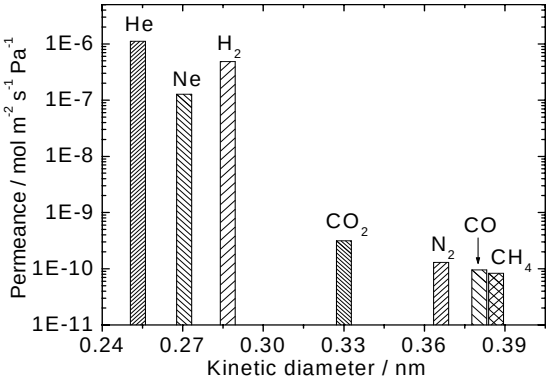

Figure 2. Single-gas permeances at 873 K of the silica-on-alumina membrane.

Fig. 2 shows permeances to single-component gases He, H_2, Ne, CO_2, N_2, CO and CH_4 through the composite membrane. It was found that the smaller the molecular size of the gas, the larger the permeance, demonstrating that a mechanism of molecular differentiation by size selectivity. The huge difference between the permeance of H_2 and CO_2 implies that a critical size in this material is around 0.3 nm. In fact, this size corresponds to the dimensions of the cavities in β-crystoballite, which has been suggested as a model for siliceous glasses similar to the amorphous silica of this membrane.

An unexpected result was the order of permeance of species with molecule size smaller than 0.3 nm, of He > H_2 > Ne, which was unusual since it did not follow the size (He = 0.26 nm, H_2 = 0.289 nm, Ne = 0.275 nm) nor the mass of the species (He = 4.0 au, H_2 = 2.01 au, Ne = 20.1 au). This unusual result can be quantitatively explained by a theory based on a mechanism involving jumps between solubility sites[10]. The governing equation is

$$Q = \frac{1}{6L}\left(\frac{d^2}{h}\right)\left(\frac{h^2}{2\pi m k T}\right)^{\frac{3}{2}}\left(\frac{\sigma h^2}{8\pi^2 I k T}\right)^{\alpha}\frac{(N_S/N_A)}{(e^{h\nu^*/2kT}-e^{-h\nu^*/2kT})^2}e^{-\Delta E_K/RT} \qquad (1)$$

In this equation Q is the permeance of a gas, L the thickness of the membrane, d the jump distance, m the mass of the species, h Planck's constant, k Boltzmann's constant, α is a constant that accounts for imcomplete rotation, σ is the symmetry factor of the species, I the moment of inertia, ν* the vibrational frequency of the species in the passageways between the sorption sites, T temperature, N_s the number of solubility sites available per m^3 of glass volume, N_A Avogadro's number, R the gas constant, and ΔE_K the activation energy for hopping between sorption sites. As shown in **Fig. 3**, the calculated curves, assuming a jump distance of 0.8 nm, fit the experimental points very well.

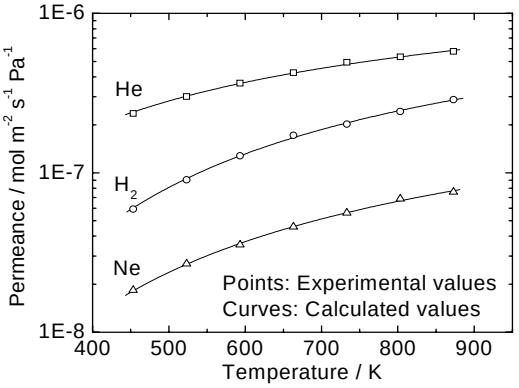

Figure 3. Experimental and calculated He, H_2 and Ne permeances for the silica-on-alumina membrane.

The thin γ-alumina intermediate layer formed by the sequential use of boehmite sols of increasingly small size displayed excellent performance in its role as an intermediate layer connecting the macroporous substrate with the hydrogen-selective Nanosil silica layer. The present Nanosil/Alumina composite membrane displayed much better permeation properties at 873 K in comparison to other silica membranes reported in the literature

References

(1) C. Song, *Catal. Today*, **2003**, 86**,** 211.
(2) M. Tsapatsis, G. R. Gavalas, *J. Membr. Sci.*, **1994**, 87, 281.
(3) W. G. Perkins, D. R. Begeal, *J. Chem. Phys.*, **1971**, 54, 1683.
(4) S-I. Nakao, T. Suzuki, T. Sugawara, T. Tsuru, S. Kimura, *Micropor. Mesopor. Mat.*, **2000**, 37, 145.
(5) G. R. Gavalas, C. E. Megiris, S. W. Nam, *Chem. Eng. Sci.*,**1989**, 44, 1829.
(6) B. K. Sea, K. Kusakabe, S. Morooka, *J. Membr. Sci*., **1997**, 130, 41.
(7) S. T. Oyama, D. Lee, S. Sugiyama, K. Fukui, Y. Iwasawa, *J. Mater. Sci*., **2001**, 36, 5213.
(8) D. Lee, L. Zhang, S.T. Oyama, S. Niu, R.F. Saraf, *J. Membr. Sci*., **2004**, 231, 117.
(9) S. T. Oyama, A. K. Prabhu, U.S. Patent 6,527,833 (**2003**) Assigned to Virginia Tech.
(10) S. T. Oyama , D. Lee, P. Hacarlioglu, R. F. Saraf, *J. Membr. Sci.*, **2004**, 244(1-2), 45.

GAS TRANSPORT AND MECHANICAL BEHAVIOR OF POLYMERIC DENSE FILMS AT ELEVATED TEMPERATURES

Vivek P. Khare, Alan R. Greenberg, Anandh Balakrishnan, Julie Diani and Sudhir Brahmandam*

Department of Mechanical Engineering, University of Colorado, Boulder, Colorado, 80309-0427, USA
*Laboratoire d'Ingénierie des Matériaux (CNRS) - ENSAM Paris, 75013, Paris, France.

Introduction

Polymeric membranes used in gas separation applications are often subjected to the simultaneous and competing effects of compaction and plasticization. Compaction refers to the decrease in membrane thickness due to mechanical deformation, i.e., creep, which occurs upon the application of a suitably high transmembrane pressure gradient. Compaction has been associated with a significant decline in membrane performance over time via a decrease in the free volume of the skin layer and an increase in the skin thickness due to the densification of the porous sublayer. In contrast, plasticization is associated with gases that have a sufficiently high solubility in the polymer to produce a large increase in the free volume and segmental mobility of the polymer matrix. Plasticization generally results in a depression in the glass transition temperature (T_g) [1], and usually leads to swelling and an increase in the permeability of glassy polymers. Literature studies report that prolonged exposure of polymeric membranes to a plasticizing gas leads to membrane "conditioning" that is reflected by a subsequent increase in the permeability of a non-plasticizing gas. Such conditioning results in decreased membrane selectivity and time-dependent performance degradation.

Previous studies of compaction and plasticization have generally employed either off-line mechanical testing or inferential characterization based on flux decline [2,3]; each of these approaches has major disadvantages. While off-line mechanical testing does not provide information about the effect of concomitant phenomena such as plasticization, inferential evaluation could lead to incorrect conclusions about cause-effect relationships, especially if the flux decline occurs due to other phenomena such as concentration polarization or stress-induced crystallization. Moreover, when membrane transport and mechanical responses are not measured simultaneously, it is difficult to establish a meaningful correlation between permselective performance and creep behavior because of the different time-scales involved. Since creep and plasticization are manifested as viscoelastic responses, they should become increasingly significant at elevated temperature, especially those close to the polymer T_g. Since elevated temperature separations offer significant thermodynamic and energetic advantages for many chemical processes, a growing number of applications require membranes that can operate in a high temperature and chemically challenging environment. Characterization of the simultaneous mechanical and transport responses at these high temperatures thus becomes an important input for strategies that optimize the long-term mechanical stability and permselectivity of polymeric membranes. Previous work has described the use of acoustic techniques for obtaining such simultaneous measurements, but the methodology is not easily adapted for high temperature measurements [4]. Consequently, the overall objective of this study is to develop an appropriate methodology for making simultaneous mechanical and transport measurements and to use the results to develop a better understanding of the fundamental factors governing the relationship between creep and gas permeability in polymer dense films at elevated temperatures.

Materials and Methods

Dense films were cast in our laboratory using cellulose acetate (CA) (Eastman Chemical Company; grade 398-10; T_g = 183°C) and poly(methyl methacrylate) (Polysciences; MW = 75000; T_g = 106°C); in addition, polybenzimiadazole (PBI) films supplied by Pall Corporation were used in the as-received condition (T_g ~ 450°C). We utilized a novel technique for conducting simultaneous transport and mechanical property (STAMP) measurements on the polymeric samples (Figure 1). The STAMP protocol was used to study the creep/transport behavior of 60-micron thick PMMA dense films from 25-115ºC, 45-micron thick CA dense films from 25-190ºC, and 50-micron thick PBI dense films from 25-425ºC. In a typical experiment, a dense film sample (50-mm diameter) was loaded into a STAMP permeation cell, and heated to the desired temperature in an inert nitrogen atmosphere and maintained at temperature overnight to establish steady-state conditions. Subsequently, the upstream pressure in the permeation cell was raised to either 4.1 MPa (600 psi) for the PMMA films or 3.1 MPa (450 psi) for the CA and PBI films, and the film thickness and flux were monitored as a function of time for 24 hours. Changes in the film thickness were measured using a linear variable differential transformer (LVDT), and the flux was measured using a pressure-rise technique. Systematic experiments were conducted in which the films were exposed to nitrogen (N_2) and carbon dioxide (CO_2) gases at constant pressure and temperatures. In order to maintain a constant transmembrane pressure gradient, a solenoid valve on the permeate side opened whenever the permeate pressure increased to a set low value. Transport properties are reported as GPU, where 1GPU = 10^{-6} cm^3(STP)/cm^2-s-cmHg.

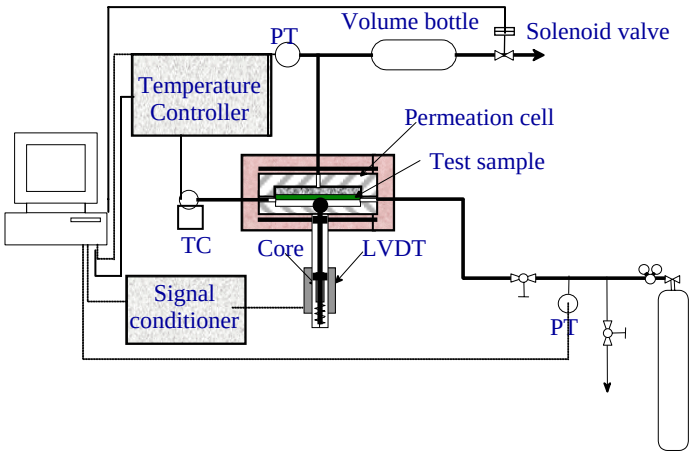

Figure 1. Schematic showing simultaneous transport and mechanical property (STAMP) measurement apparatus.

Results and Discussion

Two samples of the CA films were tested under N_2 pressure at each of the temperatures: 30, 110, 140, 160, 180, and 190 °C, respectively. As expected, an Arrhenius-type dependence of the initial film permeability with temperature was observed. Figure 2 shows the normalized permeance as a function of time at different temperatures. At temperatures <190°C, the permeance decreased by < 3% in 24 hr. In contrast, the permeance decrease was much more pronounced (~ 40%) at 190°C. This response is expected given the structural changes that occur when T > T_g. Likewise, one would expect creep to be more pronounced at 190°C. Figure 3 shows the

creep-time profiles of the films as a function of temperature. Here, creep is reported as percent compressive strain, which is calculated by dividing the measured change in the film thickness by the initial film thickness at the test temperature.

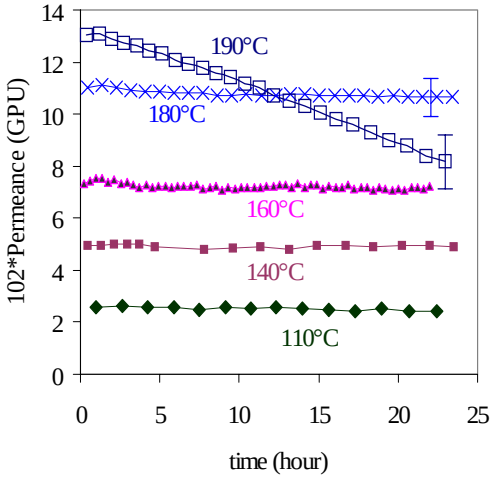

Figure 2. Nitrogen permeance versus time results for cellulose acetate dense films as a function of temperature. Upstream pressure is 3.1 MPa.

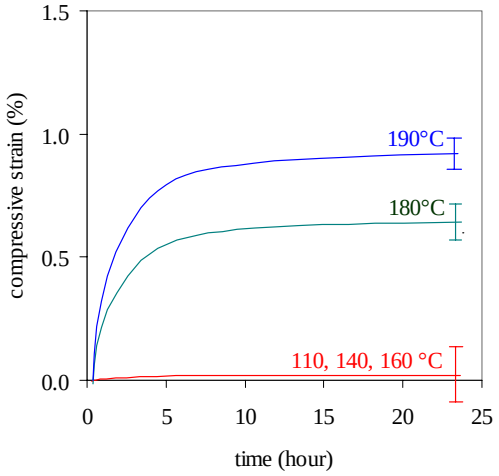

Figure 3. Creep response for cellulose acetate dense films as a function of temperature. Data obtained in nitrogen at an upstream pressure of 3.1 MPa.

As expected, creep is negligible at low temperatures and only the creep-time profiles at 180 and 190 °C evidence significant values of compressive strain, i.e. ~ 0.6 and 1.1 %, respectively. Although the strains are large enough to be measured accurately using the STAMP technique, they are nonetheless too small to explain the extent of the observed permeance decrease, especially at 190°C. If the flux decrease occurs due to a reduction in the polymer free volume, then a 40% flux decrease should imply a decrease of similar magnitude in the free volume, and hence the overall dimensions of the CA film. Clearly, it is difficult to reconcile the small decrease in the film thickness that is observed to the relatively large decrease in the permeance. In contrast to N_2 exposure, no Arrhenius-type relationship was observed under CO_2 pressure. In addition, the permeance increased with time at low temperatures with a maximum value at 25°C, consistent with the largest degree of swelling. For CO_2 exposure a net decrease in permeance with time was only observed at 190°C. The creep measurements corroborated the permeance data; a net increase in thickness was observed at temperatures below 190°C, with the maximum value at 25°. Under CO_2 exposure, film thickness decreased only at 190°C where the creep response (decreased thickness) dominated swelling (increased thickness) due to plasticization.

Similar creep and permeance results were obtained for the PBI and PMMA dense films although the respective magnitudes of the responses are somewhat different. These data support results obtained from preliminary molecular dynamic simulation studies using PMMA that suggest that pressurization leads to a shift in the free volume distribution towards smaller size free-volume elements without a significant change in the total free volume. Additional studies to confirm these results are currently underway.

Conclusions

Data obtained from coupled creep and gas flux experiments suggest that the time scales for mechanical and transport responses are rather different. In addition, the magnitude of observed isothermal permeance decreases at temperatures in the vicinity of T_g does not scale with the magnitude of the measured compressive strain. Results of initial molecular modeling work suggest that the changes in dense film permeance as a function of time may be related to changes in the free volume distribution. Overall, the preliminary studies described in this paper provide important initial insights regarding coupling effects between mechanical and transport behavior at elevated temperature.

Acknowledgement. The authors gratefully acknowledge financial support for this work from the Department of Energy Office of Fossil Energy, administered the National Energy and Technology Laboratory, Morgantown, WV (Project FE-01-0003).

References

(1) Sanders, E.S. *J. Membrane Sci*. **1988**, *37*, 63.
(2) Lawson, K.W.; Hall, M.S.; and Lloyd, D.R. *J. Membrane Sci*. **1995**, *101*, 99.
(3) Fleming, G.K.; and Koros W.J. *Macromolecules* **1986**, *19*, 2285.
(4) Reinsch, V.; Greenberg, A.R.; Kelley, S.; Peterson, R.; and Bond, L. *J. Membrane Sci*. **2000,** *171*, 217.

WATER/ETHANOL SELECTIVITY FOR AN AZEOTROPIC MIXTURE OF ETHANOL/WATER OF NOVEL ORGANIC-INORGANIC HYBRID MEMBRANES FROM POLY(VINYL ALCOHOL) AND OLIGOSILANE -WITH THE AIM OF ALCOHOL FUEL-

Tadashi Uragami, Shohei Yanagisawa, and Takashi Miyata

Faculty of Engineering, Kansai University, Suita, Osaka 564-8680, Japan

Introduction

Membrane separation techniques with easy operation and high energy savings are greatly appreciated in a variety of applications in the medical, food, industrial, energy and environment field. The chemical and physical structures of polymer membranes are engineered to improve membrane performance by several methods.

Alcohol is a clean energy source that can be produced by the fermentation of biomass. However, it needs to be highly concentrated. In general, aqueous alcohol solutions are concentrated by distillation, but an azeotrope (96.5 wt% ethanol) prevents further separated by distillation. Pervaporation, a membrane separation technique, can be used for separation of these azeotropes: pervaporation is a promising membrane technique for the separation of organic liquid mixtures such as azeotropic mixtures[1] or close-boiling point mixtures.[2]

Organic-inorganic hybrid materials are viewed as next generation materials in many applications because they have both the film-forming properties of a polymer and the stability of an inorganic compound. In this study, we prepared novel organic-inorganic hybrid membranes using the sol-gel reaction. It is well-known that poly(vinyl alcohol) (PVA) are highly water/ethanol selective during pervaporation of aqueous ethanol solutions. However, swelling of the PVA membrane in an aqueous ethanol solution results in an increase in both solubility and diffusivity of ethanol, which leads to lower water/ethanol selectivity. In this work, to control swelling of PVA membranes, mixtures of PVA and oligosilane were prepared by the sol-gel reaction and fabricated into PVA/Oligosilane hybrid membranes. The relationship between the structure of the PVA/Oligosilane hybrid membranes and their permeation and separation characteristics for an azeotropic mixture of ethanol/water by pervaporation is discussed in detail.

Experimental

Materials. Poly(vinyl alcohol) (PVA), which was supplied by Nippon Synthetic Chemical Industry Co. Ltd. at an average degree of polymerization of 1650 and a degree of saponification of 99.7 mol%, was employed as the organic component. Oligosilane (**I**), which is Compoceran 1000 supplied from Arakawa Chemical Industry Co. Ltd., was used as the inorganic component. Dimethyl sulfoxide (DMSO) dehydrated by a conventional method was employed as a casting solvent. All other solvents and reagents were purchased from Wako Pure Chemical Industries, Ltd., and were of analytical grade and were used without further purification.

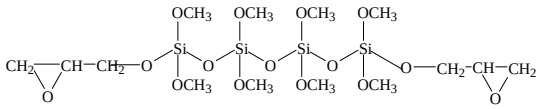

(**I**)

Preparation of PVA and PVA/Oligosilane Hybrid Membranes. PVA powder was dissolved in DMSO at 80°C to make a 2wt% casting solution. After removal of the insoluble impurities using a glass filter, it was stirred for 1 h at 25°C. The PVA membrane was prepared by pouring the casting solution onto Teflon plates, and then allowing the solvent to evaporate completely at 80°C for 24 h.

After the prescribed amount of oligosilane per a weight of PVA was mixed with the PVA dissolved in DMSO at 25°C to a concentration of 2wt%, 1M HCl was added to the PVA/Oligosilane mixture as an acid catalyst for the sol-gel reaction. The PVA/Oligosilane hybrid membranes were prepared by pouring the casting solutions onto Teflon plates, and then allowing the solvent to evaporate completely at 80°C for 30 h.

Permeation Measurements. The pervaporation was carried out using the apparatus described in previous studies under the following conditions: permeation temperature, 40°C; pressure of the permeate side, 5.0×10^2 Pa. The effective membrane area was 13.8 cm^2. An azeotropic mixture of ethanol/water was used as the feed solution. The permeate was collected in a U-tube at liquid nitrogen temperature. The permeation rates of aqueous alcohol solutions during pervaporation were determined from the weight of the permeate collected in the cold U-tube, the permeation time, and the effective membrane area. The compositions of the feed solution and permeate were determined by a gas chromatograph (Shimadzu GC-9A). The results from the permeation of aqueous alcohol solutions during pervaporation were reproducible, and the errors inherent in the permeation measurements were on the order of a few percent.

Contact Angle Measurements. The contact angles for methylene iodide on the surface of PVA and PVA/Oligosilane hybrid membranes were measured using a contact angle meter (Erma, Model G-1) at 25°C. The contact angles, θ, were determined by eq 1:

$$\theta = \cos^{-1}\{(\cos\theta_a + \cos\theta_r)/2\} \quad (1)$$

where θ_a and θ_r are the advancing contact angle and the receding contact angle, respectively.

Cross-link Density of PVA/Oligosilane Hybrid Membranes. The cross-link density, ρ, of the PVA/Oligosilane hybrid membranes was calculated from the network theory of rubber elasticity given in eq. 2:

$$\rho = E'/3d\phi RT \quad (2)$$

where the modulus, E', was determined from measurements with a dynamic mechanical analyzer (Rheogel-E4000 F3, 10 Hz; temperature, 40 °C; d is membrane density, ϕ is the front factor (where $\phi = 1$), R is the gas constant, and T is the absolute temperature.

Annealing of Membranes. The PVA and PVA/Oligosilane hybrid membranes were placed between filter papers and annealed under a nitrogen atmosphere at 100°C for 12h.

Results and Discussion

Effect of Oligosilane Content on the Permeation and Separation Characteristics of PVA/Oligosilane Hybrid Membranes. Figure 1 shows the effects of the oligosilane content on the normalized permeastion rate and the ethanol concentration in the permeate for an azeotrope of ethanol/water through the PVA/Oligosilane hybrid membranes during pervaporation. In all membranes, the ethanol concentration in the permeate was lower than that in the feed. These results suggest that the PVA and PVA/Oligosilane hybrid membranes are high water/ethanol selective. With increasing oligosilane content, the normalized permeation rate increased, but the water/ethanol selectivity decreased.

In **Figure 2**, the effects of the oligosilane content on the concentration in the PVA/Oligosilane hybrid membranes immersed in an azeotrope of ethanol/water and the apparent cross-link density of the PVA/Oligosilane hybrid membranes is shown. The ethanol concentration in the PVA/Oligosilane hybrid membrane increased, but the apparent cross-link density of those membranes decreased, with increasing oligisilane content. Although the crosslinked structure is formed between the hydroxyl groups in PVA molecule and the methoxy groups in oligosilane molecule by the sol-gel reaction, intermolecular hydrogen bonds of PVA molecules are cut because of introduction of oligosilane molecules between the PVA molecular chains. The

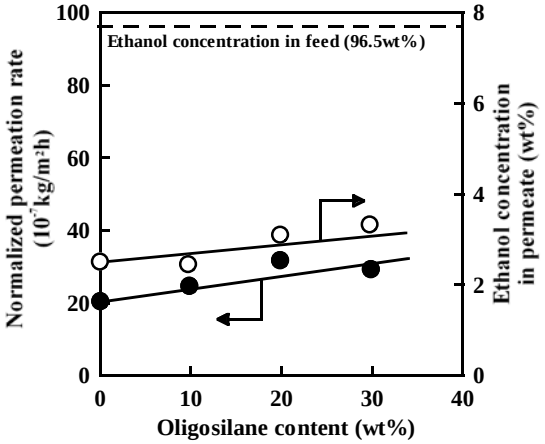

Figure 1. Normalized permeation rate (○) and ethanol concentration in the permeate (●) for an azeotropic mixture of ethanol/water through the PVA/Oligosilane hybrid membranes during pervaporation as a function of the oligosilane content.

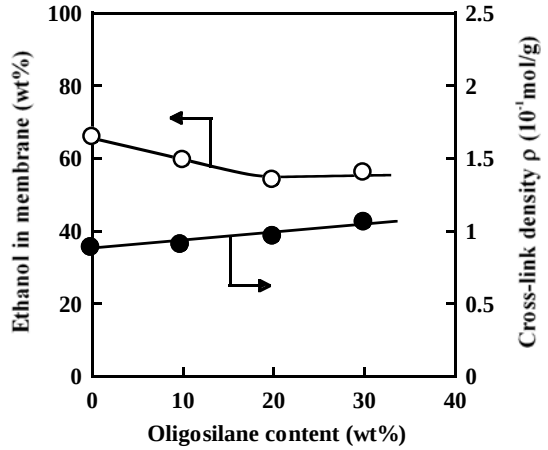

Figure 2. Ethanol concentration in the PVA/Oligosilane hybrid membranes for an azeotropic mixture of ethanol/water (●) and the apparent cross-link density of the PVA/Oligosilane hybrid membranes (○) as a function of the oligosilane content.

decrease in the apparent cross-link density in Figure 2 could be attributed to these facts. On the other hand, the increase in the ethanol concentration in the PVA/oligosilane hybrid membranes is due to the formation of an opened structure with the introduction of oligosilane molecule between the PVA molecules, i. e., the ethanol molecule with larger molecular size as well as the water molecule with smaller molecular size is easily incorporated in the PVA/Oligosilane hybrid membranes.In Figure 1, with increasing oligosilane content, the increase in the normalized permeation rate and the decrease in the water/ethanol selectivity can be attributed to the an opened structure of the PVA/Oligosilane hybrid membranes.

Effect of Annealing of PVA/Oligosilane Hybrid Membranes. Figure 3 shows the permeation and separation characteristics for an azeotrope of ethanol/water through the untreated and the annealed PVA/Oligosilane hybrid membranes as a function of the oligosilane content. The ethanol concentrations in the permeates in all annealed PVA/Oligosilana hybrid membranes were lower than those in the untreaterd PVA/Oligosilane hybrid membranes. These results suggest that the annealing treatment of the PVA/Oligosilane hybrid membranes significantly contributes to an improvement of water/ethanol selectivity for an azeotrope of ethanol/water. On the other hand, the

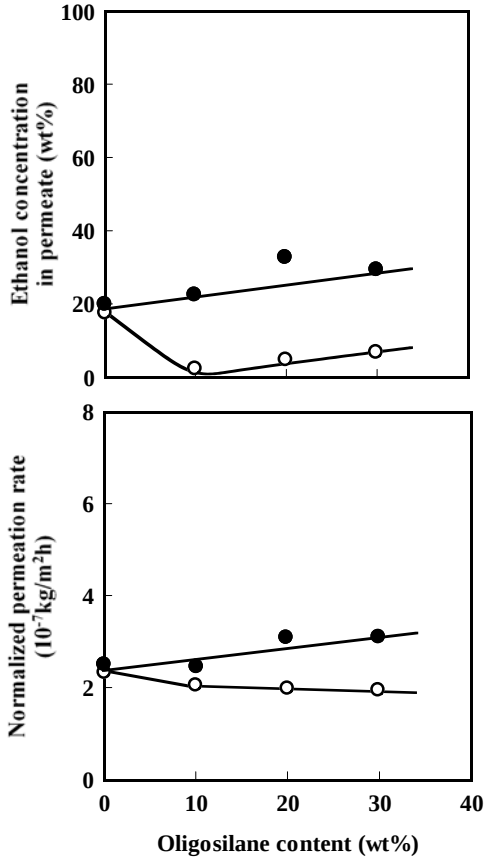

Figure 3. Effects of the oligosilane content on the normalized permeation rate and the ethanol concentration in the permeate for an azeotropic mixture of ethanol/ water through the untreated PVA/Oligosilane hybrid membranes (●) and the annealed PVA/Oligosilane hybrid membranes (○) during pervaporation.

normalized permeation rates of the annealed PVA/Oligosilane hybrid membranes were smaller than those of the untreated PVA/Oligosilane hybrid membranes. This result could be attributed to the fact that the condensation reactions between the PVA molecule and the oligosilane molecule was accelerated by annealing and consequently the structure of hybrid membrane became denser. The measurements of the ethanol concentrations in the untreated and annealedPVA/Oligosilane hybrid membranes for an azeotrope of ethanol/water supported that those in the latter were lower than those in the former.The apparent cross-link density of the latter was significantly higher than that of the former and the degree of swelling of the latter was lower than that of the former. When the PVA/Oligosilane hybrid membranes are annealed, the condensation reactions between the PVA molecules and the oligosilane molecules proceed, the cross-link density of the hybrid membrane increases, the membrane structure becomes denser, the degree of swelling of the hybrid membrane is depressed, and consequently the water/ethanol selectivity for an azeotrope of ethanol/water is improved.

References

1. Psaume, R.; Aurell, Y.; Mora, J. C.; Bersillon, J. L. *J. Membr. Sci.* **1988,** ,36, 373.
2. Blume, I.; Wijmans, J. G;Baker, R. W. *J. Membr. Sci.* **1990**, *49,* 253.

NOVEL MEMBRANE MATERIALS FOR CO_2 REMOVAL FROM MIXTURES WITH H_2

Haiqing Lin[1], Scott Matteucci[1] and Benny D. Freeman[1]
Sumod Kalakkunnath[2] and Douglass S. Kalika[2]

[1]Department of Chemical Engineering
University of Texas at Austin, Austin, TX, 78758
[2]Department of Chemical and Materials Engineering
University of Kentucky, Lexington, KY 40506

Introduction

Polymer membranes are used in many applications, including gas separations, due to their inherently low energy requirements for molecular scale separations. Hydrogen, a potential future energy source, is usually produced by steam reforming of hydrocarbons and requires removal of byproducts such as CO_2 and H_2S.[1] For membrane processes to be applicable to these separations, it is highly desirable to selectively remove CO_2, thereby maintaining H_2 at or near feed pressure to avoid expensive recompression of the desired H_2 product.

Gas permeability, *P*, is the product of gas solubility in the polymer, S, and gas diffusivity, D, as follows: $P=S\times D$.[2] The ability of a polymer membrane to separate two gases, such as CO_2 and H_2, is gauged by the ratio of their permeabilities, which reflects the tradeoff between favorable solubility selectivity (CO_2 is more condensable and, therefore, $S_{CO_2}/S_{H_2}>1$) and unfavorable diffusivity selectivity (CO_2 is larger than H_2, so $D_{CO_2}/D_{H_2}<1$). To achieve very high CO_2/H_2 selectivity, a membrane must exhibit favorable interactions with CO_2 to enhance solubility selectivity, and it must exhibit a very weak size-sieving ability to bring D_{CO_2}/D_{H_2} as close to 1 as possible. To date, the polar ether oxygens in ethylene oxide (EO) units are the best known groups to interact sufficiently strongly with CO_2 to have high solubility selectivity and remain flexible without significantly increasing the size sieving ability of the polymer.[3]

Previously, we have reported on crosslinked copolymers (PEGDA-*co*-PEGMEA) prepared by photopolymerizing mixtures of poly(ethylene glycol) diacrylate (PEGDA: $CH_2=CHCO(OCH_2CH_2)_nOCOCH=CH_2$, n = 14) and poly(ethylene glycol) methyl ether acrylate (PEGMEA: $CH_2=CHCO(OCH_2CH_2)_nOCH_3$, n = 8.5).[4] These materials exhibit very high CO_2 permeability and high CO_2/H_2 pure gas selectivity. In the current report, mixed gas CO_2/H_2 separation performance in these copolymers is evaluated. Decreasing temperature improves CO_2/H_2 mixed gas separation properties. The addition of MgO nanoparticles improves CO_2 permeability considerably with little reduction in selectivity.

Experimental

Film Preparation. Prepolymer solutions were prepared by adding 0.1 wt.% initiator (1-hydroxycyclohexyl phenyl ketone) to mixtures of PEGDA and PEGMEA. This solution was sandwiched between two quartz plates and then exposed to UV light. The detailed procedure has been reported elsewhere.[4] Nanocomposite samples were prepared by mixing MgO nanoparticles with the prepolymer solution and then polymerizing as previously reported.[4]

Permeation and Sorption Measurement. Pure gas permeability was measured using a constant volume/variable pressure apparatus.[5] Mixed gas permeability was measured using a constant pressure/variable volume apparatus.[6] Pure gas sorption isotherms were obtained using a dual-volume, dual-transducer apparatus.[5]

Results and Discussion

Three CO_2/H_2 mixtures (i.e., 10% CO_2/90% H_2, 50% CO_2/50% H_2, and 80% CO_2/20% H_2) have been tested at three temperatures (i.e., 35°C, 10°C and -20°C) in PEGDA-co-PEGMEA samples containing 30 wt% PEGDA and 70 wt% PEGMEA. As reported previously, higher PEGMEA content in the copolymers leads to larger fractional free volume, resulting in increased CO_2 permeability and CO_2/H_2 selectivity.[4] Therefore, this copolymer exhibits relatively high CO_2 permeability and high CO_2/H_2 pure gas selectivity. Furthermore, the PEGMEA content is low enough that this copolymer does not crystallize within the temperature range studied. In contrast, a copolymer containing 91 wt% PEGMEA and the balance PEGDA crystallizes at about 0°C, which has a deleterious effect on gas permeability.

Figure 1 presents CO_2 permeability as a function of CO_2 partial pressure at 35°C, 10°C and -20°C. In general, CO_2 permeability increases with increasing CO_2 partial pressure because of plasticization of the polymer chains by CO_2. The increase becomes more significant at lower temperatures because CO_2 sorption increases with decreasing temperature. Interestingly, at a CO_2 partial pressure of 17 atm, CO_2 permeability at -20°C is higher than that at 10°C and close to that at 35°C. Therefore, lower temperature might not necessarily lead to lower permeability. Additionally, the pure gas and mixture CO_2 permeability appears to fall on the same trend line, suggesting that the presence of H_2 has a negligible effect on CO_2 permeability.

Figure 2 presents H_2 permeability as a function of CO_2 partial pressure at various temperatures. H_2 permeability increases with increasing CO_2 partial pressure. Furthermore, H_2 permeability falls on the same trend line for each temperature, suggesting that the dependence of H_2 permeability on feed composition derives from the amount of CO_2 in the polymer (i.e., plasticization).

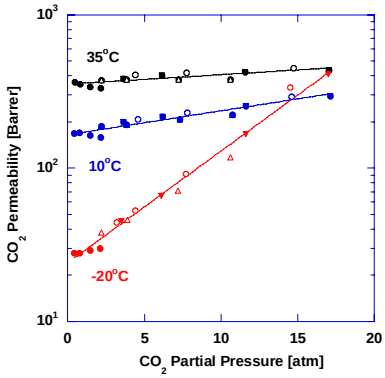

Figure 1. Effect of CO_2 partial pressure on CO_2 pure and mixed gas permeability. ○: pure gas; ●: 10% CO_2/90% H_2; Δ: 50% CO_2/50% H_2; ▼: 80% CO_2/20% H_2. The lines serve as guides to the eye.

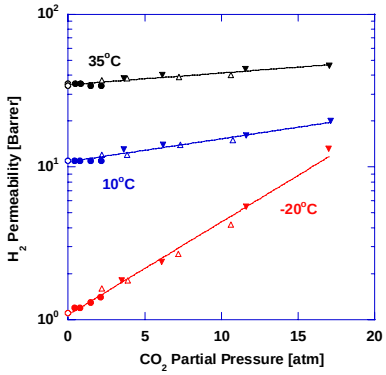

Figure 2. Effect of CO_2 partial pressure on H_2 pure and mixed gas permeability. ○: pure gas; ●: 10% CO_2/90% H_2; Δ: 50% CO_2/50% H_2; ▼: 80% CO_2/20% H_2.

Figure 3 presents CO_2/H_2 selectivity as a function of CO_2 partial pressure at 35°C, 10°C and -20°C. Mixed gas selectivity remains essentially independent of CO_2 partial pressure and mixture compositions at 35°C and 10°C. On the other hand, at -20°C, mixed gas selectivity increases with increasing CO_2 partial pressure and falls on the same trend line for different mixtures. As CO_2 partial pressure increases from 0.4 to 17 atm, CO_2/H_2 mixed gas selectivity increases by 35%, from 23 to 31. Typically, the sorption of a large amount of gas (such as CO_2 in this case) would significantly plasticize the polymer matrix, which is indicated by a decrease in glass transition temperature in the polymer/gas mixture.[7] Such plasticization would reduce the size sieving ability of the polymer, increasing CO_2/H_2 diffusivity selectivity, and, in turn, overall permeability selectivity as indicated in **Figure 3**.

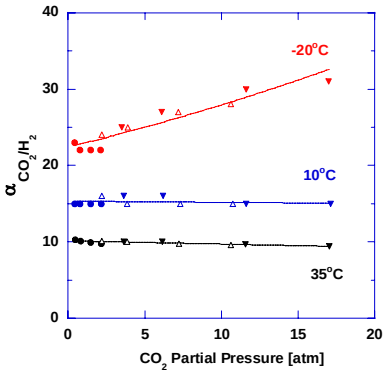

Figure 3. Effect of CO_2 partial pressure on CO_2/H_2 mixed gas selectivity. ●: 10% CO_2/90% H_2; Δ: 50% CO_2/50% H_2; ▼:80% CO_2/20% H_2.

Figure 4 presents a permeability/selectivity map for CO_2/H_2 separation.[8] The upper bound line drawn in the figure predicts the highest pure gas selectivity possible for a given permeability in polymer-based materials, which was calculated based on a model by Freeman.[9] The materials reported here exhibit superior separation performance. The effect of temperature on CO_2 separation properties is also illustrated in the graph. Lower temperature might improve both CO_2 permeability and CO_2/H_2 mixed gas selectivity. The CO_2/H_2 mixed gas selectivity of 31 and CO_2 permeability of 410 Barrers at -20°C and a CO_2 partial pressure of 17 atm is the best separation performance ever reported for CO_2/H_2 mixtures in solid non-facilitated transport polymeric membranes.

Figure 5 presents the effect of MgO nanoparticle content on pure gas CO_2 permeability at 35°C. The polymer matrix (XLPEGDA) is prepared from 100% PEGDA. At low MgO loadings, CO_2 permeability decreases, as predicted by conventional composite models.[10] However, at particle concentrations beyond approximately 32 wt.%, CO_2 permeability increases strongly, while CO_2/H_2 selectivity remains unchanged at about 8. As MgO loading is further increased to 44 wt.%, CO_2 permeability increases by one order of magnitude as compared to that of the particle-free polymer, while CO_2/H_2 selectivity decreases to 4.2. To understand the effect of nanoparticles on gas transport, sorption experiments have been performed for one composite (XLPEGDA with 44 wt.% MgO) at 35°C. Virgin nanocomposite samples sorb high amounts of CO_2. However, such sorption is largely irreversible. The reversible sorption is very similar to that in the pure polymer. Clearly, the strong increase in gas permeability upon adding nanoparticles must be derived in large measure from improvements in gas diffusivity.

Decreasing temperature improves CO_2/H_2 selectivity in the nanocomposite containing 44 wt.% MgO and the balance PEGDA. As temperature decreases from 35°C to -20°C, CO_2/H_2 selectivity increases from 4.2 to more than 10. As illustrated in **Figure 6**, mixed gas CO_2 permeability and CO_2/H_2 selectivity in the nanocomposite increase with increasing CO_2 partial pressure. Additionally, mixed gas CO_2 permeability in the nanocomposite is compared with pure gas CO_2 permeability in the pure polymer at -20°C. This comparison is reasonable because CO_2 permeability values for various compositions fall on the same trend line, as discussed above. Clearly, the addition of MgO nanoparticles improves CO_2 permeability.

References

(1) Kohl, A. L.; Nielson, R. *Gas Purification*, 5th ed.; Gulf Publishing: Houston, TX, 1997.

(2) Wijmans, J. G.; Baker, R. W. *J. Membr. Sci.* **1995**, *107*, 1-21.

(3) Lin, H.; Freeman, B. D. *J. Mol. Struct.* **2005**, *739*, 57-74.

(4) Lin, H.; Freeman, B. D.; Toy, L. G.; Bondar, V. I.; Gupta, R. P.; Pas, S. J.; Hill, A. J. *Polym. Prepr. (Am. Chem. Soc., Div. Polym. Chem.)* **2004**, *45*, 23-24.

(5) Lin, H.; Freeman, B. D. *J. Membr. Sci.* **2004**, *239*, 105-117.

(6) Merkel, T. C.; Gupta, R. P.; Turk, B. S.; Freeman, B. D. *J. Membr. Sci.* **2001**, *191*, 85-94.

(7) Chiou, J. S.; Barlow, J. W.; Paul, D. R. *J. Appl. Polym. Sci.* **1985**, *30*, 2633-2644.

(8) Robeson, L. M. *J. Membr. Sci.* **1991**, *62*, 165-185.

(9) Freeman, B. D. *Macromolecules* **1999**, *32*, 375-380.

(10) Petropoulos, J. H. In *Polymeric Gas Separation Membranes*; Paul, D. R., Yampolskii, Y. P., Eds.; CRC Press, Inc.: Boca Raton, Florida, 1994; pp 17-81.

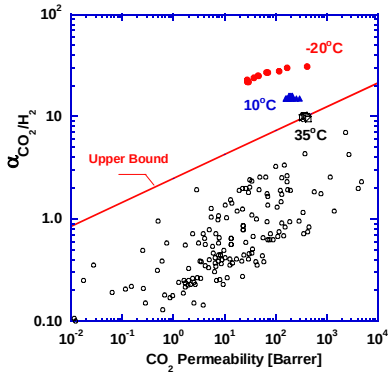

Figure 4. Permeability/selectivity map for CO_2/H_2 separation. Separation performance of PEGDA-co-PEGMEA is also presented at different temperatures.

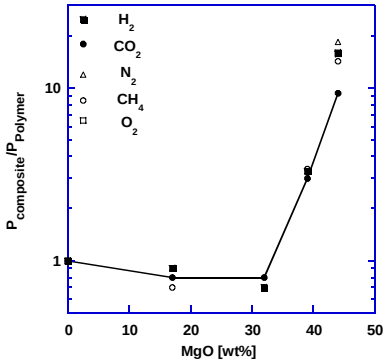

Figure 5. Effect of MgO nanoparticle content in XLPEGDA on pure gas permeability at 4.4 atm and 35°C.

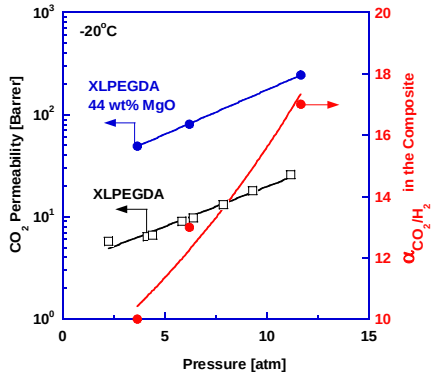

Figure 6. Effect of CO_2 partial pressure on CO_2 permeability and CO_2/H_2 mixed gas selectivity at -20°C in a nanocomposite containing 44 wt.% MgO and the balance PEGDA. The feed gas is 75/25 CO_2/H_2. Data for XLPEGDA are based on pure gas (CO_2) measurements.

HOLLOW FIBER MEMBRANE SIMULATION FOR CO_2 SEPARATION PROCESS

Jun Gyu Park, Hyung-Taek Kim

Dept. of Energy Studies, Ajou University
Wonchon-dong Yeongtong-gu
Suwon, Korea 443-749

Introduction

Separation of Carbon dioxide that is a kind of global warming gas is issued with the effectuation of UNFCCC (United Nations Framework Convention on Climate Change).

There are many methods about separation and recovery of CO_2 within exhaust gas by using fossil fuels. There are the adsorption, the absorption, the distillation, and the membrane separation. But these technologies have many defects up to date. Membrane is the most advanced technology and the most potential process for CO_2 separation from flue gas. Especially, membrane is a good for the facilities about the decrease of CO_2 discharge using the low energy consumption.

In this study, system models are simulated by FORTRAN and Aspen Custom Modeler™. First, we must remove water in front of membrane process. This simulation is changed temperature with pressure done by Aspen Plus™ .A simulation about one membrane module is made progress by using the FORTRAN, using those results, 4 bundles of membrane module is composed like a cascade. It is computed that required membrane area and number of module, permeated CO_2 concentration and the amount of permeated gas. And it is predicted consumption energy of pumps and compresses by Aspen Plus™.

In this study, when condition is fixed permeability and variety selectivity, we estimate required number of module, permeated CO_2 concentration and the amount of permeated gas.

Methods

First of all, we are simulation of dehydration process. Then using those results, 4 bundles of membrane module is composed like a cascade. Thereafter simulation using the FORTRAN is progressed. It is computed that required number of module, permeated CO_2 concentration and the amount of permeated gas by changing selectivity and fixed permeability. Last, it is simulated that the process with the recycle streams by using the FORTRAN. And we predict required energy in this process by Aspen Plus.

At 1 ~ 3 *Stage*

$$L(I,J) = L(I,J-1) + V(I,J-1) + V(I+1,J-1)$$

AT 4 *Stage*

$$L(I,J) = L(I,J-1)$$

I : *i-th Module*

J : *iteration number*

At 1~3 stage have recycle steams but 4 stage don't have it. Therefore, equation of 1~3 stage add recycle steam. The recycle steam composition is the same value of feed steam.

We estimated required number of module, permeated CO_2 concentration and the amount of permeated gas by change selectivity. This method is fixing permeability for 20 and changing selectivity form 20 to 100.

Results and Discussion

Simulation for removal water

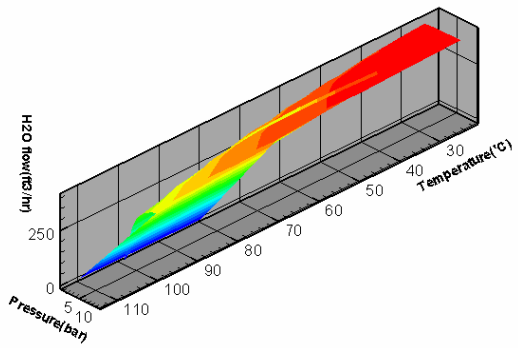

Figure 1. Result of removal water

Water is harmful effect to membrane modules. In front of process, we must remove water. In this case, composition of flue gas is 10% of CO_2, 17% of H_2O and 73% of N_2. Total volumetric flow is 2,410ft^3/hr from LNG power plant. Temperature is 130℃ and vapor fraction is 1. It is simulating by changing temperature and pressure of heat exchanger and flash dram. Temperature range is from 20℃ to 110℃ and pressure is from 1bar to 10bar.

Simulation of membrane process

Table 1. Input Parameters For 1 Membrane Module Process

Parameter	amount	parameter	amount
P_1	6 atm	Number of HF per module	5000
P_2	0.1 atm	Feed rate	1000 m^3/day
Selectivity	20	Length of HF	50 cm
Permeability	20	Pressure ratio	P_2/P_1

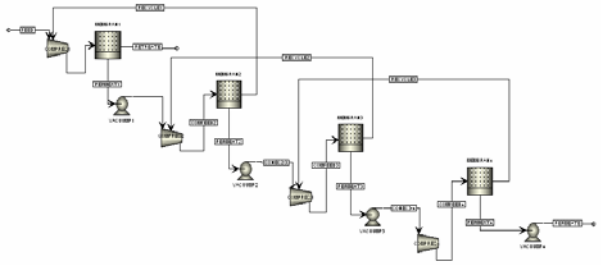

Figure 2. Membrane module process: There are 4 membrane modules and recycle

Fixing permeability for 20 and simulated during changing selectivity

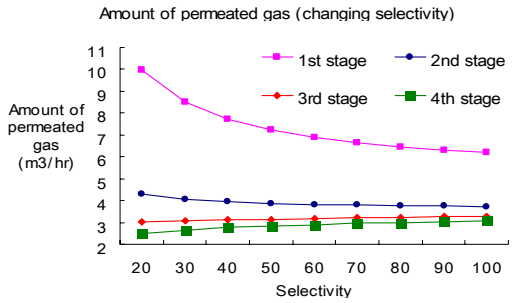

Figure 3. Amount of permeated gas during different selectivity

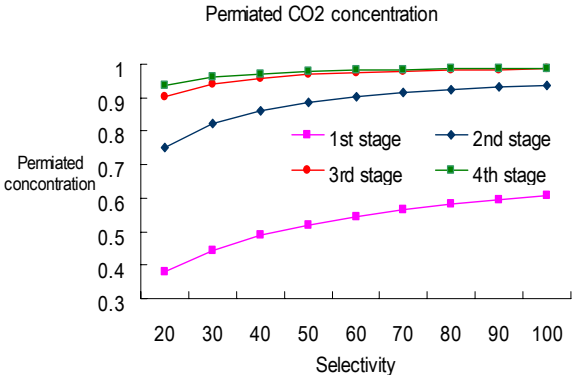

Figure 4. Permeated gas concentration during different selectivity

As selectivity increase, permeability of 1st stage is large decrease and permeability of 2nd stage is small decrease and permeability of 3rd & 4th is increased. Also figure 4, permeated concentration of each stage is increased. At selectivity is 100, CO_2 concentration at last stage is about 98%.

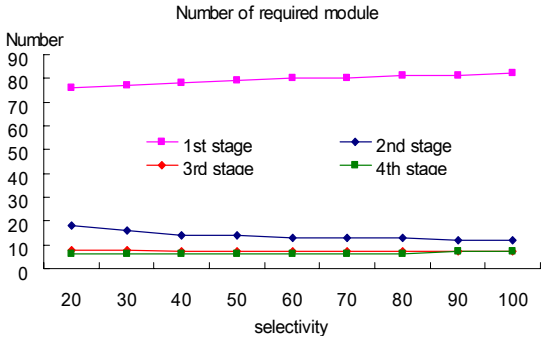

Figure 5. Number of required module during different selectivity

At Figure 5. we can know that number of required module is increased in order to 99% of CO_2 concentration. Because permeated flow is much small, it is more module needed in order to get high purity of CO_2, But when fixed permeability and changed selectivity , the value is not much different each other.

Table 2. Input parameters for energy cost estimation

Parameter	Amount
P1 (Feed pressure)	6 atm
P2(permeated pressure)	0.1 atm
Selectivity	20
Permeability	20
Number of HF per module	5000
Length of HF	50 cm
Number of HF per module	5000
Length of HF	50 cm

Table 3. Required energy consumption

Equipment	Net work requirement (kW)
1st compressor	3.7753
1st vacuum pump	2.9913
2nd compressor	9.0478
2nd vacuum pump	1.339
3rd compressor	3.8497
3rd vacuum pump	0.9876
4th compressor	2.7187
4th vacuum pump	0.8200
Total	25.5244

Total energy consumption is 25.5244kW. As you see Table 3, the required energy in 2nd stage is larger than 1st stage. While 1st stage is pressured form 1atm to 6atm, compressor of 2nd stage is less flow rate than 1st stage. So, energy consumption of 2nd stage is smaller than 1st.

Conclusions

In order to remove water in flue gas, we use cooling method. When temperature goes down about 40℃, almost all water is removed. Next we estimated number of module, permeated CO_2 concentration and the amount of permeated gas as changed selectivity. Membrane process required energy consumption about 25.5244kw for 4 compressors and vacuum pumps.

These results indicate that we can remove more CO_2 and get the high CO_2 concentration. If more bundles are attached, the separation units by using the hollow fiber membrane remove more CO_2 and get the high CO_2 concentration. Therefore, it is very useful that CO_2 separation process by using the hollow fiber membrane.

References

(1) James Marriott; Eva Sorensen; *Chemical Engineering Science 58*, **2003**, 4975-4990.
(2) R. Wang; S. L. Liu; T. T. Lin; T. S. Chung; *Chemical Engineering Science 57*, **2002**, 967-976.
(3) Li Xu; Lin Zhang; Huanlin Chen; *Desalination 148*, **2002**, 309-313.
(4) G. C. Kapantaidakis; G. H. Koops; *Journal of Membrane Science 204*, **2002**, 153-171.

HIGHLY FLUORINATED GRAFT COPOLYMERS AS PROTON EXCHANGE MEMBRANES (PEMs): IMPROVING PEM PROPERTIES THROUGH RATIONAL DESIGN

Tyler B. Norsten, Michael D. Guiver, Jianfu Ding

National Research Council of Canada
Institute for Chemical Process and Environmental Technology
1200 Montreal
Ottawa, ON K1A 0R6

Introduction

Microstructural analysis of Nafion and other newly emerging PEM materials has suggested that both chemical microstructure and nanoscale morphology of ionomer membranes can dictate material performance.[1-3] With this in mind, much current research is aimed at designing and developing alternative polymer materials based on non-fluorinated or partially fluorinated polymeric systems.[4] The majority of this work is based on non-fluorinated polyaromatic hydrocarbon-based condensation polymers that contain ionic functionality randomly located along the polymer backbone (Fig 1a). Generally these polymers can achieve suitable conductivity only at low EW (high degrees of sulfonation) resulting in high water-up take/swelling ratios that are unsuitable for practical PEM applications. It has been suggested that these sulfonated polymers struggle to form defined hydrophilic domains as the rigid polyaromatic backbone prevents co-continuous ionic clustering from occurring.[5]

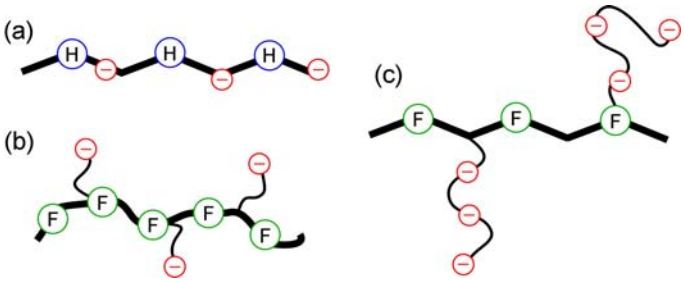

Figure 1. Graphical structure representations of: a) a typical polyaromatic-based PEM displaying a rigid and sulfonated hydrocarbon backbone, b) Nafion-based materials displaying a flexible perfluorinated backbone with short and flexible pendant side chains containing single sulfonic acid groups, and c) our hybrid material based on a highly fluorinated and rigid polyaromatic backbone with long pendant graft polymers containing multiple sulfonic acid groups.

Nafion, on the other hand, is a random copolymer comprised of a perfluorinated hydrophobic backbone that contains a number of short flexible pendant side chains with single hydrophilic/ionic groups (Fig 1b). It is this balance of hydrophobic-hydrophilic properties within the material coupled with the mobility of the sulfonic acid group, as a result of side chain flexibility that, in the hydrated form, leads to a co-continuous network of ionic channels through the material.

The phenomenon of microphase separation of block copolymers can be used to create well defined periodic microdomains of controlled morphology (e.g. cylinders, spheres, lamellae) on the nanoscale (10-100 nm). Recently research has shown that graft copolymers are also capable of creating similar nanoscale morphologies.[6] Herein we report the characterization of a series of highly fluorinated graft copolymers that can be used as proton exchange membranes.

The main chain is comprised of a highly fluorinated polyaromatic backbone, while the graft segments containing the ionic groups are comprised of flexible and monodisperse aromatic polymer side chains (Fig 1c). Like previous polyaromatic PEM structures, this design incorporates the use of a semi-rigid polymer backbone capable of creating mechanically durable high temperature membranes. Unlike most polyaromatic PEMs this design: incorporates a highly fluorinated backbone which provides a high degree of hydrophobicity and chemical stability to the material, ensures little or no sulfonation on the backbone resulting in minimal water-up take into the hydrophobic domains, and employs flexible side chains capable of microphase separating into a continuous ionic network. Furthermore, unlike Nafion, these side chains are reasonably long and contain multiple sulfonic acid groups which were designed to yield increased ionic domain interconnectivity and expected to provide better conductivity at low levels of hydration.

Experimental

Water Uptake and Swelling Ratios. Membrane films were dried at 65°C for 48h prior to the measurements. After measuring the lengths (0.5 cm x 5 cm) and weights of dry membranes, the sample films were soaked in deionized water for 24 h at predetermined temperatures. Before measuring the lengths and weights of hydrated membranes, the surface bound water was removed from the membrane by blotting the surface with a filter paper.

Ion Exchange Capacity. The IEC/EW of the membranes were determined by titration. A piece of membrane typically (4 cm x 4 cm) in the acidic form was immersed in 40 ml of 2.0 M NaCl solution for 24h. Solutions were titrated with 0.025 M NaOH solution to a phenolphthalein end point. After titration, the sample was rinsed with distilled water and dried under vacuum at 65°C until a constant weight (48h).

Conductivity. All conductivity measurements were performed in the longitudinal direction in Milli-Q water (18 MΩ resistivity). Membrane samples (20 mm x 10 mm) were acidified in 2M HCl, rinsed thoroughly and soaked in distilled water for a minimum of 24h before use. Variable temperature measurements were performed in a thermally controlled stainless steel vessel employing a two-electrode (platinum) ac impedance technique using and a Solatron 1260 frequency response analyzer. Spectra were recorded between 10^2 and 10^7 Hz with 10 points per decade at a maximum perturbation amplitude of 100 mV. All conductivities (σ) were calculated using the relation $\sigma = d/RS$, where d and S are the thickness and face area of the sample, respectively and R was derived from the low intersect of the high frequency semi-circle on the complex impedance plane with the Re(Z) axis. The impedance spectra were fitted on the basis of the Rs(C-Rp) equivalent circuit employing the corresponding instant fit function in the Zview 2.80 software by Scribner Associates Inc.

Transmission Electron Microscopy (TEM). Membranes in there sulfonic acid form were immersed in 0.5 M lead acetate solution for 48h and rinsed with water in order to stain the ionic domains. A 1 x 5 mm strip was then cut from the membrane. The thin sample was embedded in bimodal polystyrene by placing the strip in a glass vial containing several PS beads and heating at 120°C until the PS completely embedded the sample. The glass vial was then shattered and the embedded polymer sample collected. Thin films (40-50 nm) of the embedded polymer samples were prepared using an ultramicrotome (Ultracut-E, Reichert-Jung) fitted with a Diatome diamond knife. The slices were picked up with 400 mesh carbon coated copper grids for TEM analysis. The samples were analyzed using a Philips CM20 STEM equipped with a Gatan UltraScan 1000

CCD camera and INCA Energy TEM 200 EDX spectrometer operating at 120 kV.

Small Angle X-Ray Scattering (SAXS). Cu Kα X-rays (1.54 Å) were generated in an Osmic MaxFlux source with a confocal multilayer optic (OSMIC, Inc). Images were taken with a Molecular Metrology, Inc., camera consisting of a 3 pinhole system, 150 cm sample-to-detector distance (calibrated using silver behenate), and a 2 dimensional, multiwire proportional detector (Molecular Metrology, Inc.). The entire X-ray path length was evacuated from the optic to the detector in order to reduce the background from air scattering. This setup allowed neglecting the correction for background scattering as proved by experiment. Two-dimensional images were reduced to one-dimensional form using angular integration. Scattering vectors (q) were calculated from the scattering angles (θ) using $q = 4\pi \sin \theta/\lambda$, and domain periodicities (D) were calculated from Gaussian fits to the principal scattering maxima of the Lorentz-corrected intensities using $D = 2\pi/q$.

Results and Discussion

A series of highly fluorinated graft copolymers were prepared containing weight percents of 18, 25 and 37 graft chain. The graft chains were incorporated randomly into the polymer backbone and were prepared in such a fashion that they were all of uniform length and composition. The conditions for introducing the ionic groups were chosen such that sulfonation of the graft copolymers was selective to the graft chains. This synthetic methodology provided precise control over the amount of hydrophilic side chain that could be incorporated into the hydrophobic backbone.

The sulfonated materials were of high M_n (67000-105000 g/mol) and produced membranes with excellent mechanical properties when solvent cast onto optically flat surfaces. The polymers display good thermal properties with T_g's of 180°C and onset T_d's of 205°C in nitrogen. The IEC capacity of a material is the measure of its exchangeable protons. These protons in conjunction with water are the "vehicles" on which protons are transported through the membrane. Table 1 shows the IEC values for all the graft polymer membranes tested and relates them to N117 under identical test conditions.

Table 1. IEC/EW VALUES AND IONIC INTERDOMAIN DISTANCES FROM SAXS

Polymer	IEC (meq/g) / EW	Ionic Domain Periodicity (nm)
N117	0.96 / 1042	—
18%	0.87 / 1149	19.9
25%	1.41 / 714	15.8
37%	1.75 / 571	13.0

SAXS analysis (Fig 2b) of the lead stained membranes clearly shows that as the amount of ionic graft chain is increased from 18-37% the Bragg scattering vector (q) shifts to larger values indicative of smaller interdomain periodicities. Hence, larger ionic domains concomitantly produce smaller hydrophobic domains, which is a direct measure of the ionic domain periodicities shown in Table 1. This ultimately results in a higher connectivity of hydrophilic proton conducting networks with smaller separation distances.

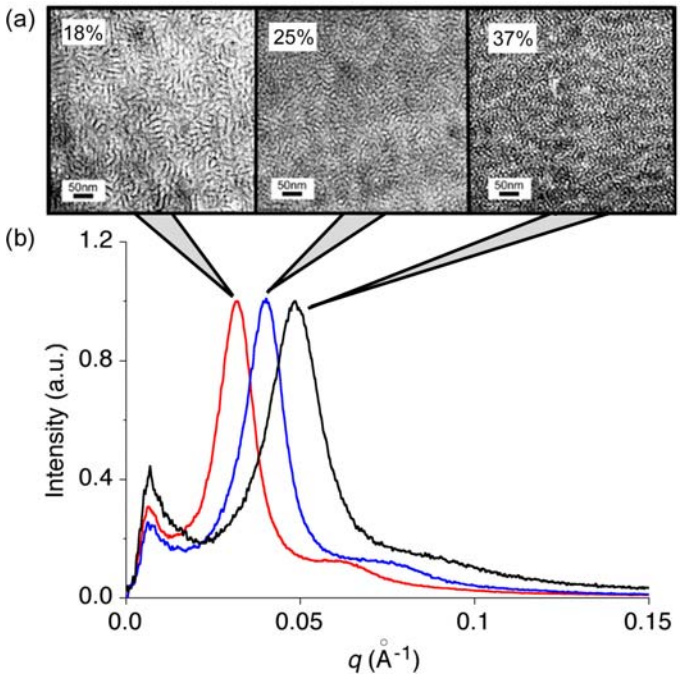

Figure 2. (a) TEM micrographs, the dark regions indicate the ionic domains, and (b) normalized SAXS data of lead stained ionomeric membranes containing 18-37% graft chain content.

The SAXS data is intimately correlated to the TEM micrographs (Fig 2a) which clearly show an increase of ionomeric content on going from 18-37% graft chain and the systematic shrinkage of the hydrophobic regimes. The TEM also indicates that a distinct lamellar morphology results from the 18% material which becomes less pronounced upon incorporation of addition side chain content. This is corroborated by the presence of the broad peak in the SAXS plot at ~2q for the 18% material which systematically flattens on going from the 25% to the 37% materials.

Water management within the membrane is a critical factor in the performance of PEM materials. Although these copolymer materials up-take more water than Nafion their swelling due to water up-take is less in most cases (Fig 3, bracketed numbers). This may be a result of the unique polymer microstructure allowing water only into the hydrophilic domains while the alternating hydrophobic domains serve to maintain dimensional stability. Figure 3 also shows that these materials display excellent proton conductivities over the temperature ranges studied.

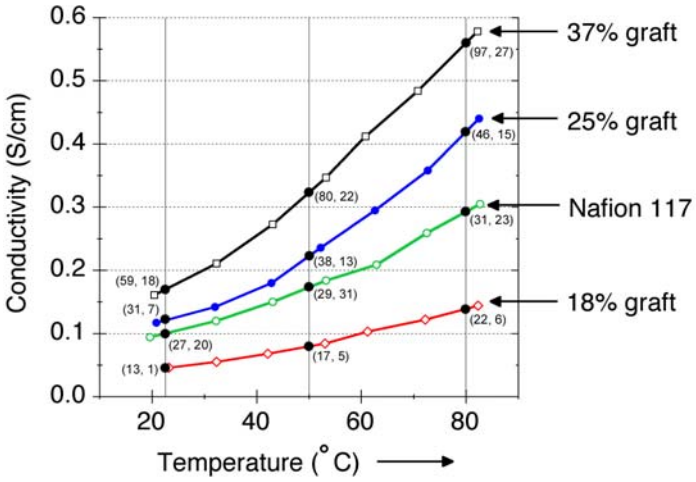

Figure 3. Proton conductivities as a function of temperature for the grafted ionomeric membranes and Nafion 117. The numbers in brackets represent (% water up-take, % swelling) respectively at the specified temperatures.

Conclusions

A series of highly fluorinated graft copolymers have been prepared that show excellent properties as PEM materials. Specifically, these materials display abilities to conduct protons and manage water that is comparable or superior to Nafion. It appears that the unique polymer structure resulting in microphase separation between opposing domains (e.g. hydrophobic and hydrophilic) is responsible for the excellent properties observed for these materials.

Acknowledgement. The authors are grateful to Ben Frankamp for performing SAXS analysis and Dashan Wang for TEM analysis.

References

(1) Mauritz, K. A. and Moore, R. B. *Chem. Rev.*, **2004**, *104*, 4535.
(2) Ding, J.; Chuy, C. and Holdcroft, S. *Chem. Mater.*, **2001**, *13*, 2231.
(3) Eladb, Y. A.; Walker, C. W. and Beyer, F. L. *J. Membrane Sci.*, **2004**, *231*, 181.
(4) Hickner, M. A.; Ghassemi, H.; Kim, Y. S.; Einsla, B. R. and McGrath, J. E. *Chem. Rev.*, **2004**, *104*, 4587.
(5) Kreuer, K. D. *J. Membrane Sci.*, **2001**, *185*, 29.
(6) Xenidou, M.; Beyer, F. L.; Hadjichristidis, N.; Gido, S. P.; Tan, N. B. *Macromolecules*, 1998, *31*, 7659.

NEW SUPER PROTON-CONDUCTIVE, HIGH ACID-CONTAINING FLUOROPOLYMER PEMS FROM CURED LIQUID PRECURSORS

Zhilian Zhou, Raymond N. Dominey and Joseph M. DeSimone

Department of Chemistry
University of North Carolina
Chapel Hill, NC27599

Introduction

Polymer electrolyte membrane (PEM) fuel cells are becoming increasingly popular as candidate solutions to power sources for portable electrical devices, transportation, and distributed power.[1-3] The next generation of fuel cell membranes must outperform today's most widely used material, Nafion®. Although this perfluoro-sulfonic acid based PEM material has many desirable features, several shortcomings limit its utility and performance. Key liabilities include high synthesis and processing costs,[4] diminished proton conductivity under conditions of low water availability,[5-7] high fuel crossover when used in direct methanol fuel cells (DMFC),[8] and limited mechanical strength at elevated temperatures.[9] Furthermore, the flat two-dimensional geometry of current PEM materials severely limits the power generation potential of fuel cells derived from these materials.

To address these deficiencies, we start from a fluoropolymer liquid precursor that is chemically cured into a network. This curing process is solvent-free. No further processing such as melt extrusion or solvent casting is necessary. By employing chemically crosslinked system, membranes with high ion loading can be achieved without dissolution in water. These high acid-containing fluoropolymer PEMs have very high proton conductivity and good mechanical integrity at the same time due to their chemical crosslinked natures. By this liquid precursor approach, flat and 3-dimensional membranes can be easily prepared by photo or thermal curing using soft lithography techniques. Patterned, 3-dimensional membranes can provide a much larger active surface area compared to traditional flat PEMs. Fuel cells comprised of a 3-dimensional membrane should have greater efficiency due to their increased power density.

Experimental

In order to incorporate a crosslinkable functionality, a styrene linkage was added to both chain ends of poly(tetrafluoroethylene oxide-*co*-difluoromethylene oxide) (PFPE) α-, ω- diol by reacting with 4-vinylbenzyl chloride in a phase transfer catalyzed reaction. The resulting product (S-PFPE) is a clear viscous liquid.

In order to make a styrene sulfonic acid precursor that is miscible with S-PFPE, a styrene sulfonate ester was synthesized by reacting 4-vinyl benzenesulfonyl chloride with a fluorinated alcohol.

To make a PEM material, S-PFPE with 1wt% photo-initiator and styrene sulfonate ester were mixed in the desired ratio and chemically crosslinked by irradiation with UV light. The resulting solid membrane is in the ester form, transparent and slightly yellow.

To convert the sulfonate ester group to sulfonic acid, the membrane was soaked in a mixture of NaOH aqueous solution and methanol for 12 h and then refluxed in the same mixture for an additional 10 h. After rinsing with distilled water, the membrane was stirred for a total of 24 h in fresh 20wt% HCl solution. The resulting membrane was in the acid form. Residual HCl was removed by washing with distilled water.

Characterization

Nuclear Magnetic Resonance (NMR) spectra were taken using a Bruker 400 MHz DRX spectrometer. Optical micrographs of the patterned membranes were taken using an Axioskop2 optical microscope equipped with an AxioCam HRm camera.

Ion exchange capacity (IEC) and equivalent weight (EW) of the membranes were determined by titration of the sulfonic acid group. In a titration measurement, a piece of membrane (typically 0.2~0.3g) in acid form was stirred with saturated NaCl solution overnight; the resulting solution was then titrated with standardized 0.01 mol/L NaOH solution using phenolphthalein as the indicator. The titrated membrane was dried in the salt form and the dry weight of membrane was accurately measured. The ion exchange capacity (IEC) and equivalent weight (EW) of the membranes are calculated as follows:

$$EW\ (H^+,\ g\ mol^{-1}) = [Dry\ weight\ /(V_{NaOH}*[NaOH])] - 22$$

$$IEC\ (meq\ g^{-1}) = 1000/EW$$

The thermal stability of the membranes was measured by a Perkin-Elmer Pyris 1 thermogravimetric analyzer (TGA). Dynamic mechanical and thermal analysis (DMTA) measurements were performed with a 210 Seiko dynamic mechanical spectroscopy (DMS) instrument, operating at fixed frequency and film tension mode.

After hydrolysis, the membranes were kept in water until no more weight change was observed. The water uptake of the membranes is calculated as follows:

$$Water\ uptake\ (wt\%) = (Wwet - Wdry)/\ Wdry\ *100$$

Proton conductivity was measured by AC Impedance over the frequency range of 1Hz – 1MHz. Impedance spectra were recorded using Solartron 1287 Impedance and Solartron 1255 HF frequency response analyzer.

Results and Discussion

IEC is the key factor that determines the properties of PEM materials. Membranes with IEC between 0.50 meq/g to 1.82 meq/g (EW= 1900~550) were prepared. It is common for linear PEM materials to dissolve in water if they contain a significant amount of acid groups. Due to the crosslinked nature, however, our PEMs with IEC as high as 1.82 meq/g remained intact after refluxing in methanol-water mixture for 10 h during hydrolysis.

Properties of these new PEMs, such as water uptake, dimensional change, proton conductivity, and fuel cell performance are under investigation and will be reported in the meeting.

Acknowledgement. We would like to thank DuPont for financial support of this project and we acknowledge partial support from the NSF Science and Technology Center for environmentally responsible solvents and processes (Grant No. 4-25151).

References

(1) Appleby, A. J.; Foulkes, R. L. *Fuel Cell Handbook*; Van Nostrand: New York, **1989**.
(2) Jacoby, M. *C&E News* **1999**, *77*, 31.
(3) Malhotra, S.; Datta, R. J. *J. Electrochem. Soc.* **1997**, *144*, L23.
(4) Gil, M.; Ji, X.; Li, X.; Na, H.; Hampsey, J. E.; Lu, Y. *J. Membr. Sci.* **2004**, *234*, 75.
(5) Savadogo, O. *J. New. Mater. Electrochem. Syst.* **1998**, *1*, 47.
(6) Gottesfeld, S.; Zawodzinski, T. A.; Alkire, R. C., Gerischer, H., Kolb, D. M., Tobias, C. W., Eds.; Wiley-VCH, 2002; Vol. 5.
(7) Si, Y.; Kunz, H. R.; Fenton, J. M. *J. Electrochem. Soc.* **2004**, *151*, A623.
(8) Cruickshank, J.; Scott, K. *J. Power Sources* **1998**, *70*, 40.
(9) Hickner, M. A.; Ghassemi, H.; Kim, Y. S.; Einsla, B. R.; McGrath, J. E. *Chem. Rev.* **2004**, *104*, 4587.

THE INTERACTION BETWEEN TIO_2 NANOPARTICLES AND NAFION® IN NAFION COMPOSITE MEMBRANES FOR PEM FUEL CELL APPLICATIONS

Paul W. Majsztrik, Hitoshi Ota, Andrew B. Bocarsly

Chemistry Department
Princeton University
Princeton, NJ 08544

Introduction

Nafion, which to date is the best membrane material for polymer electrolyte membrane fuel cells (PEMFCs), limits the operating temperature of the cell to under 90 °C. Operating a PEM fuel cell in this low temperature range: 1) requires that high-purity hydrogen fuel be used to prevent CO poisoning of the Pt catalyst, 2) produces low quality waste heat, 3) results in decreased catalyst efficiency, and 4) makes water management in the cell difficult. Operation of PEMFCs at elevated temperature (110-150 °C) improves each of these areas. One approach for developing an elevated temperature PEMFC is to create a composite Nafion membrane by the inclusion of metal oxide nanoparticles in Nafion[1,2,3]. Adding certain metal oxide particles (TiO_2, SiO_2, etc.) improves the performance of Nafion at elevated temperature and reduced relative humidity. It has been proposed that the addition of metal oxides increases hydration in the membrane because the metal oxides are hydrophilic[2]. Instead, we propose that metal oxides crosslink the polymer, allowing the polymer to maintain its structure at elevated temperatures and low humidity.

This work investigates the interaction between TiO_2 nanoparticles and Nafion in TiO_2 composite membranes. The purpose of this investigation is to discover how TiO_2 nanoparticles interact with Nafion and if the size or surface characteristics of the particles effects this interaction. Composite membranes prepared using four different size TiO_2 particles are analyzed in order to determine if particle size or surface properties affect the interaction. A mechanism for the thermal decomposition of plain and TiO_2 composite Nafion is suggested.

Experimental

Nafion composite TiO_2 membranes were prepared by recasting using a 5% by weight Nafion solution (Ion Power) mixed with a solvent (either isopropanol (IPA) or dimethyl sulfoxide (DMSO)) and TiO_2 particles. Four different types of TiO_2 particles were used as fillers: 21 nm particles (Degussa-Hüls), 10 nm and 5 nm anatase TiO_2 particles (Nanostructured and Amorphous Materials, Inc.), and 1-2 μm particles (Alfa Aesar). The particles were suspended in a mixture of DMSO or IPA and Nafion by sonication, cast on a flat glass surface, and the solvent was removed at ~80 °C in a vacuum oven (for DMSO) or at 75 °C without vacuum (for IPA). The membranes were then annealed, cleaned, and acid exchanged.

Analysis of the interaction of the TiO_2 particles with Nafion was performed using Thermogravimetric-Mass Spectrometry (TG-MS) analysis ((TG)(Seiko EXSTAR6000), (MS) (Agilent 6890N)) and Thermogravimetric Analysis (TGA) (Perkin Elmer TGA 7). For the TGA scans, a heating rate of 1 °C/min was used and samples were held at 100 °C for 60 minutes to allow for water removal. All TGA runs were performed under Argon. The TG-MS scans were performed on samples dried at 70 °C in a vacuum oven and a scan rate of 10°C/min was used.

The thermogravimetry-mass spectrometry (TG-MS) and temperature programmed desorption or decomposition (TPD-MS) analyses of Nafion/Inorganic composite membrane were performed with the TG-MS system by coupling TG-DTA (Seiko EXSTAR6000) with GC/MS (Agilent 6890N) and the TPD-MS system by coupling the pyrolyzer with GC/MS (Agilent 5973N). The pyrolysis temperature was programmed to increase from 25 to 500°C at a rate of 10°C/min under helium flowing at 60 ml/min. The gaseous decomposition products were introduced directly into the MS unit via a gas transfer tube with a deactivated fused silica capillary. The transfer lines were maintained at 200°C. The MS interface temperature was set at 250°C. The MS system was maintained at about 1×10^{-6} torr.

Results and Discussions

TG-MS data for the thermal decomposition of extruded Nafion and Nafion composite TiO_2 (21 nm particles) membranes are presented in f**igure 2**. From these data, we propose that plain Nafion decomposes in two steps while the Nafion TiO_2 composite decomposes in three steps, as illustrated in **figure 1**.

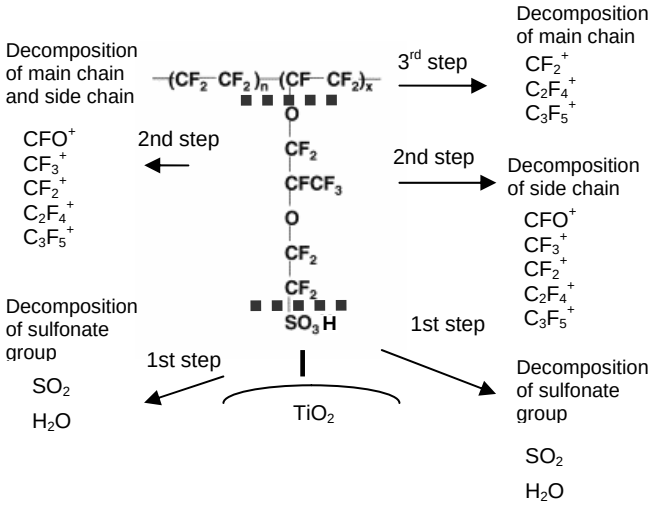

Figure 1. Proposed mechanisms for the thermal decomposition of (left) plain Nafion and (right) TiO_2 composites.

For both plain and TiO_2 membranes, free water is the first to be removed. The sulfonate group is removed next, concomitant with the removal of water bound to the sulfonate. The sharpening and shifting to lower temperature of the water and SO_2 peaks (MS plots) with the addition of TiO_2 indicates that there must be a chemical interaction between the acid groups in Nafion and the surface of the TiO_2 particles and that TiO_2 catalyses the reaction. We propose that there are coordinately unsaturated sites on the surface of the TiO_2 which bond to an O on the sulfonate. Along with the loss of H_2O and SO_2 is CFO from the ether linkages. This is visible as a small peak in the MS plot for the TiO_2 membrane but is not visible for the plain Nafion since the loss of the sulfonate group occurs over a broader temperature range and is thus, present in concentrations beyond the sensitivity of the instrument. Further support for this is seen in TG-MS scans showing the appearance of CF_2 and C_2F_4 along with H_2O and SO_2.

A comparison of the thermal decomposition of Nafion composites prepared with different size/types of TiO_2 (**figure 3**) suggests that the different TiO_2 particles interact differently with Nafion. The addition of 5, 10, and 21 nm TiO_2 particles all result in the bound water and SO_2 loss shifting to lower temperature and

occurring over a smaller temperature range. The 10 and 5 nm particles give the largest slope in the water and SO_2 loss region (~230 °C). This indicates that the 5 and 10 nm particles have the strongest interaction with the sulfonate group. Since the 5 and 10 nm particles have a pure anatase structure, while the 21 nm particles mixed rutile and anatase, this also should affect the interaction.

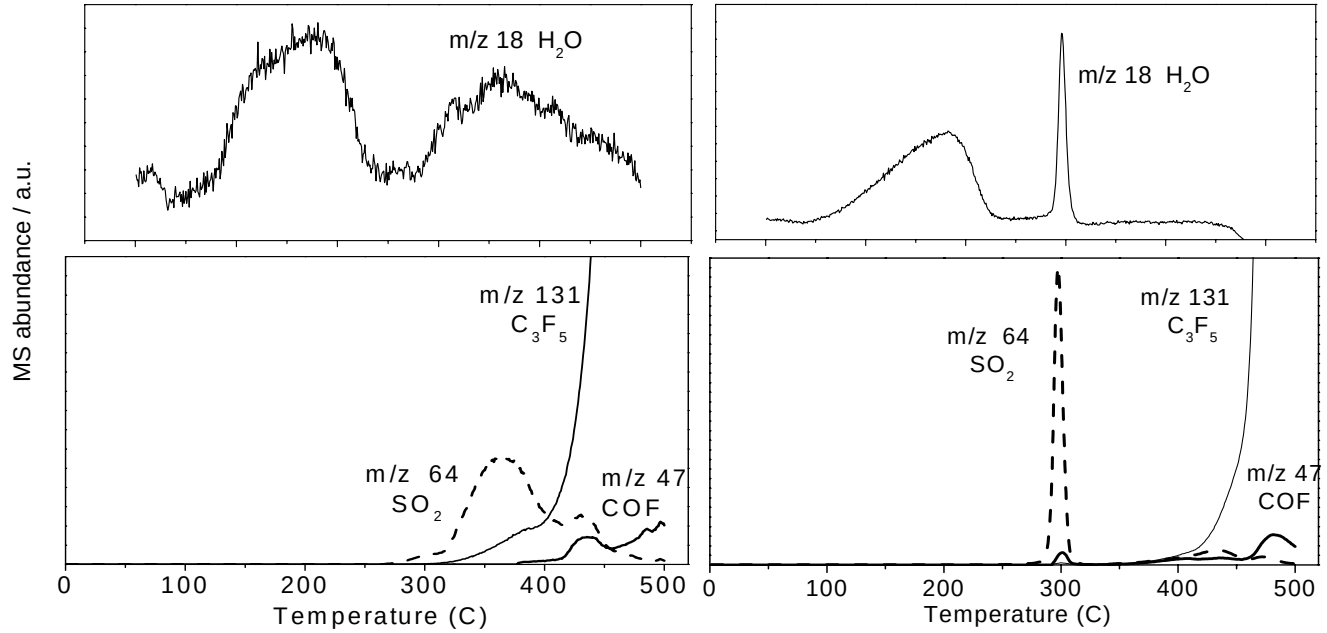

Figure 2. TG-MS scans for plain Nafion and Nafion TiO_2 composite

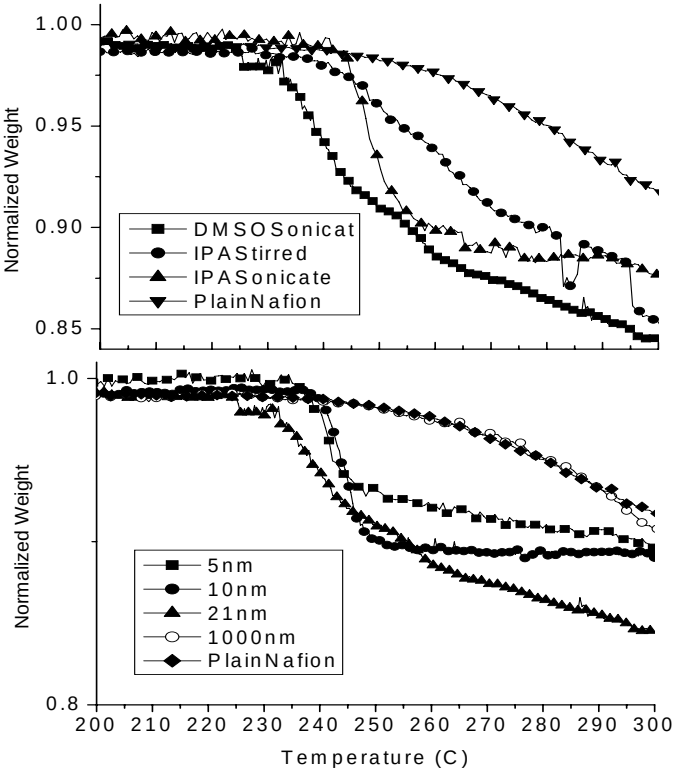

Figure 3. TGA scans (top) comparing Degussa-Hüls composite membranes prepared using different methods and (bottom) composite membranes prepared with different TiO_2 particles.

Perhaps the most interesting result shown here is the comparison of the thermal decomposition of plain Nafion to the Alfa Aesar TiO_2 composite. It was previously reported that membranes prepared with Alfa Aesar TiO_2 filler showed no improvement over plain Nafion when tested at elevated temperature[4]. The TGA curves for plain Nafion and the Alfa Aesar composite are identical (up to 300 °C), indicating that no chemical interaction is occurring between the particles and Nafion. This strongly suggests that it is the chemical interaction between metal oxide particles and Nafion which improves the performance of Nafion.

A comparison was also made between different membrane preparation techniques, namely sonication versus stirring to suspend particles and the use of isopropanol versus DMSO as the recasting solvent. TGA scans indicate that sonication results in better dispersion of particles (loss of sulfonate groups over a narrower temperature range) and that using isopropanol in place of DMSO produces membranes with less interaction between particles and polymer (shift to lower temperature of the sulfonate loss is greater in the case of membranes recast with DMSO).

Acknowledgements

The authors gratefully acknowledge Mitsubishi Chemical Group Science and Technology Research Center, Inc. for the use of instruments to obtain the TG-MS data and Tao Zang for the preparation of the IPA membranes.

References

1. K. T Adjemian, S. Srinivasan, J. Benziger, A. B. Bocarsly, *J. Power Sources*, 109 (2002) 356-364.
2. A.S Arico, V. Baglio, A. Di Blasi, E. Modica, P. L. Antonucci, V. Antonucci, *J. Power Sources*, 128 (2004) 113-118.
3. M. Watanabe, H. Uchida, M Emori, *J. Phys. Chem. B*, 102 (1998) 3129-3137.
4. K. Adjemian, Ph.D. Thesis, Princeton University (2002).

NANO-SCALE MODIFIED INORGANIC/ORGANIC HYBRID MATERIALS AS PROTON CONDUCTORS

Berryinne Chou, Hossein Ghassemi, and Tomas A. Zawodzinski

Chemical Engineering Department
Case Western Reserve University
10900 Euclid Avenue
Cleveland, OH, 44106

Introduction

Proton exchange membrane fuel cells (PEMFC) are considered to be the next generation energy source for transportation and many other applications. Proton exchange membranes are a key component in the fuel cell system. Various perflurosulfonic acid polymers have been used to achieve high proton conductivity, such as Nafion® and Dow membranes. For automotive industrial applications, high operation temperature can help fuel cell release the heat and reduce the size of the cooling system. High temperature also improves the catalytic activity on the electrodes and increases anode CO tolerance. Nafion, however, only gives good proton conductivity when it is fully hydrated and limits the operating temperature to no higher than 80^{o}C. Therefore, developing new materials for high temperature fuel cells (exceeding 100^{o}C) is challenging and very essential. In this work, the surface modified silica particles are bound with polymers to form proton-exchange membranes. Surface modification of silica particles was achieved by sultonation process[1] leading to the production of organic-inorganic hybrid particles with a high IEC value as 2.3 mmol/g. Modified silica particles were blended sulfonated polyether sulfone copolymers (BPSH)[2] with various degree of sulfonation. Membranes with different amounts of silica particles have been prepared by solution casting or melt press technique. These membranes were tested for their proton conductivity and other related properties, such as water up-take. The effect of membrane fabrication condition on their morphology and overall performance has been investigated. Proton conductivity of membranes was measured at different temperatures and humidity and the data was used to understand the proton transfer phenomena.

Experimental

Sultone treated silica particles. The solution which contained 1, 3 propane sultone and dry toluene (molar 1:10) was prepared and mixed with dry aerosil silica, 7 nm, (Degussa). The mixing procedure was performed in a dry box to avoid water absorption before sultone attaches to the silica surface. The chemical reaction was shown in the following scheme. The reaction was heated up at 80^{o}C and stirred for 7 days.

Silica/Polymer composite membrane synthesis. Different polymers have been considered as the binders in this work. Dimethylacetamide (DMAc) was used as a solvent for all the polymers. The sultoned particles are kept in toluene solution before membrane casting. Membranes with different ratios of particles and polymers were cast on glass and dried at 50^{o}C for 4 hours. The membranes were removed from the glass and dried to make sure all the excess sultone and solvents were removed. Before any further membrane characterization, the membranes were boiled at 0.5 M H_2SO_4 for 4 hours to remove all metallic impurities and converted to proton form.

Characterization Methods. Proton conductivity measurements were performed using a Solatron SI 1280B Impedance Analyzer. Voltage was applied with varying frequency from 0.1 to 20,000 Hz and the impedance response. The conductivity measurements were also done at different temperatures and different humidity generated by different LiCl concentration solutions. Water up-take measurements were done by suspending membranes over LiCl solution for 3 days (enough time to reach equilibrium) in a constant temperature chamber at 25°C. Samples to measure the uptake of water in liquid immersed membranes were placed at the bottom of vials filled with distilled water. The membranes were dried, weighed, replaced in vials, and weighed again. The time membranes were exposed to air was minimized to prevent water loss.

Results and Discussion

FT-IR spectra of the particles before and after sulton deposition has been tested and shown at **Fig 1**. In order to determine the surface modification, curve (a) has been subtracted from curve (b) and enlarged three times, as shown as curve (c). There are three peaks 1048, 1117, and 1170 cm^{-1} are the absorption from sulfonate groups. Titration was done to evaluate the ion exchange capacity (IEC) of these sultonated silica particles, 2.3 mmol per gram. Comparing to Nafion 1100 series membrane (0.92 mmol per gram) the sultonated silica particles have a much higher proton density.

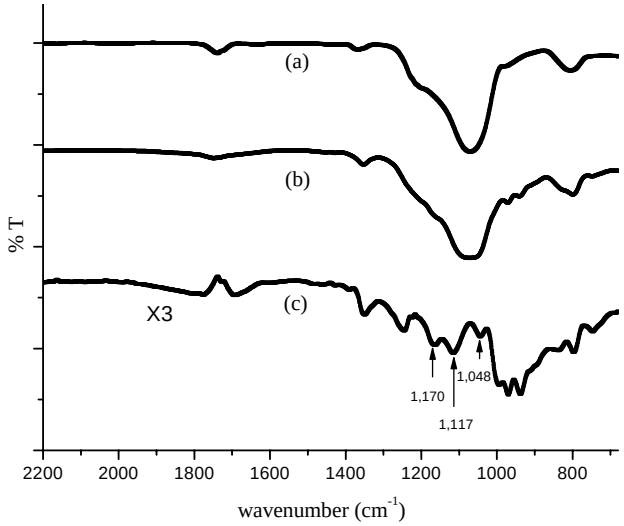

Figure 1. FT-IR of (a) Pure silica particles (b) Sultonated silica particles (c) Curve a Subtracted from curve b.

The conductivity directly tells us whether the protons can transfer through the membranes. The goal of this work is to achieve the conductivity of Nafion, 0.072 Ω^{-1} cm^{-1} in liquid water. Membranes with different BPSH copolymers and different amounts of surface modified silica particles were examined and **Figure 2** shows the conductivity. BPSH 0 is the polymer without any protons, therefore the conductivity must derive from the sulfonic groups from the modified silica surface. BPSH 0 membranes with higher ratios of particles have better conductivity, indicating the modified particles provide the proton and bring the conductivity. Membranes made with BPSH 20 containing different particle loadings also show very similar trends like BPSH 0. But the conductivities are generally higher than BPSH 0 type membranes due to the intrinsic protons from BPSH 20. Pure BPSH 35 and BPSH 60 had very good conductivity because of the high degrees of sulfonation. When the BPSH 35 and BPSH 60 are mixed with modified silica particles, the conductivity drops to a constant value.

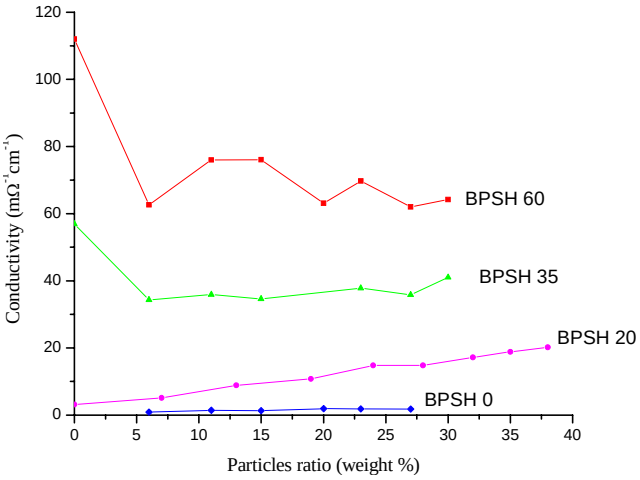

Figure 2. Conductivity with different BPSH with different amounts of surface modified particles. The measurements were done when the membranes were immersed in the liquid water at room temperature.

The water uptake (%) of the membranes were calculated by the weight gain of absorbed water with reference to the dry membrane and reported as weight percent. In order to understand the correlation between water up-take and proton density, IEC values were estimated from the IEC of BPSH with different amounts of modified silica particles. The surface modified silica particles have a very high IEC value, 2.3 mmol per gram. This is higher than BPSH 20, 35, and 60. In **Figure 3**, surface-modified particles help BPSH 20 absorb more water, agreeing the conductivity results shown in **Figure 2**. For the membranes that used BPSH 35 or BPSH 60 as binders, small amounts of surface modified particles lower the water up-take and conductivity. Silica particles prevent membrane from swelling, and the polymer matrix is not able to hold the water easily. As the particle loading increase, the water up-take increase again, possibly due to the high IEC values of the surface modified particles.

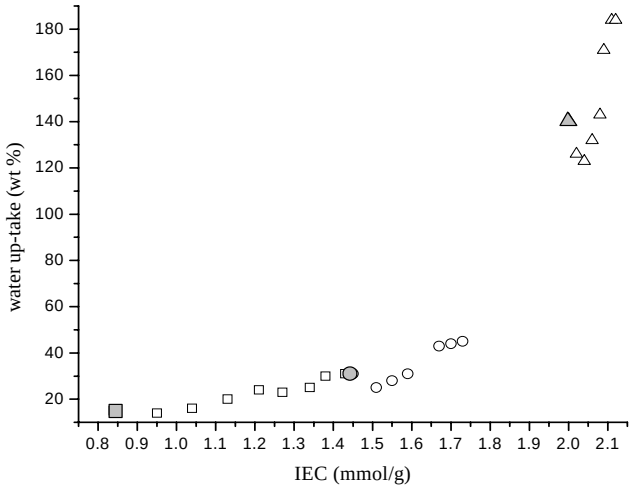

Figure 3. Water up-take of membranes with BPSH 20 (■) with different amounts of surface modified silica (□); BPSH 35 (●) with different amounts of surface modified silica (○); BPSH 60 (▲) with different amounts of surface modified silica (Δ).

Morphology is important to understand how well the particles are dispersed inside the membranes. **Figure 4** shows HRSEM pictures of the membranes with BPSH 20 and BPSH 60 mixed with particles. The original silica particles are 7 nm, and are expected to grow to 9~10 nm after sultonation. The particles' size is around 20~30 nm in **Figure 4** (a); 50~60 nm in **Figure 4** (b). Particle aggregation occurs during the membrane casting, especially in the BPSH 60 type of membranes. The ideal structure of the composite membrane has silica particles well separated and dispersed inside the polymer matrix, but close enough to form the network structure needed in order to provide a proton transfer path. Figure 4 indicates the membrane using BPSH 20 as a binder has better particle dispersion and less particle aggregation comparing to the membranes using BPSH 60 as a binder. The main factor which controls the compatibility between polymers and particles is still not well known in the work.

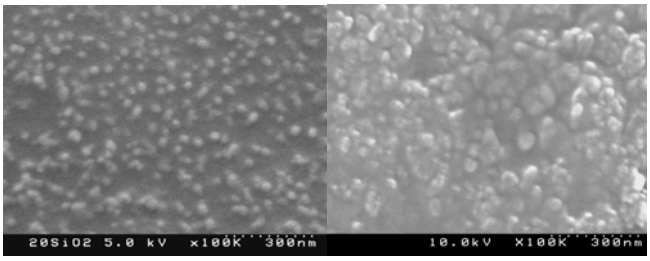

(a) (b)

Figure 4. High resolution scanning electron microscope pictures of (a) BPSH 20 with 38% surface modified silica. (b) BPSH 60 with 30% surface modified silica.

Acknowledgment

This work was supported by U.S. Department of Energy.

References

1. Alvaro, M.; Corma, A.; Das, D.; Fornes, V.; Garcia, H., *Chem. Commum* **2004,** *204*, (8), 956.
2. Wang, F.; Hickner, M.; Kim, Y. S.; Zawondzinski, T. A.; McGrath, J. E., *Journal of Membrance Science* **2002,** *197*, 231.

PARTIALLY FLUORINATED POLY(ARYLENE ETHER SULFONE) COPOLYMERS MODIFIED WITH ZIRCONIUM HYDROGEN PHOSPHATE FOR PROTON EXCHANGE MEMBRANES

Melinda L. Hill, Brian R. Einsla, and James E. McGrath

Macromolecules and Interfaces Institute
Virginia Polytechnic Institute and State University
Blacksburg, VA 24061
Email: jmcgrath@vt.edu

Introduction

Directly copolymerized disulfonated poly(arylene ether sulfone) copolymers have been shown to be advantageous for proton exchange membrane applications due to their excellent thermal and oxidative stability, high proton conductivity, and low methanol permeability.[1,2,3] However, these membranes can be further improved by the addition of an inorganic component. The addition of certain inorganic materials to proton exchange membranes may decrease the water uptake and methanol permeability, while increasing the mechanical strength of the membrane. The permeability to gases, especially oxygen, is an important property in hydrogen/air fuel cell systems, and it has been suggested that this is lowered by the addition of inorganic materials as well. Metal oxides, phosphates, and phosphonates are among the materials that have been investigated for proton exchange membrane additives.[4] The precipitation of zirconium hydrogen phosphate (ZrP) into Nafion membranes through an *in-situ* method has been shown to result in very small particles of ZrP dispersed within the pores of the membrane.[5-7] Nafion/ZrP hybrid membranes prepared by this technique can be used at higher temperatures than pure Nafion membranes.[6] The inorganic component may also prevent dehydration of the membranes at elevated temperatures.[7] The water uptake of the membranes may also be reduced upon addition of ZrP, and this has been shown to be an important factor in PEMFC performance.[8] Herein, we report the fabrication and initial characterization of organic/inorganic composite proton exchange membranes combining disulfonated partially fluorinated poly(arylene ether sulfone) copolymers and ZrP.

Experimental

Materials. 4,4'-Dichlorodiphenylsulfone (DCDPS) was obtained from Solvay Advanced Polymers and was dried at 60 ºC under vacuum for 24 hours before use. Hexafluoroisopropylidene biphenol was provided by DuPont and was dried at 60 ºC under vacuum for 24 hours prior to use. N,N-dimethylacetamide (DMAc, Aldrich) was distilled under reduced pressure over calcium hydride. Potassium carbonate (Aldrich) was dried at 120 ºC under vacuum for 24 hours prior to use. Toluene (Fisher Scientific) was dried over molecular sieves (5 Å, Aldrich). Fuming sulfuric acid (30% free SO_3), zirconyl chloride ($ZrOCl_2$, 30% in hydrochloric acid) and phosphoric acid (H_3PO_4) were purchased from Aldrich and used as received.

Synthesis and acidification of Partially Fluorinated Disulfonated Poly(arylene ether sulfone) Copolymers. Disulfonated poly(arylene ether sulfone) copolymers were synthesized according to a previously reported procedure.[2,9,10] A sample copolymerization reaction for a copolymer in which 35% of the repeat units were disulfonated proceeded as follows: Hexafluoroisopropylidene biphenol (3.3623 g, 10 mmol), DCDPS (1.8666 g, 6.5 mmol), S-DCDPS (1.7194 g, 3.5 mmol), and potassium carbonate (1.5894 g, 11.5 mmol) were charged to a three-neck round-bottom flask equipped with a nitrogen inlet, mechanical stirrer, Dean-Stark trap, and reflux condenser. DMAc (28 mL) and toluene (14 mL) were added, and the reaction mixture was heated in an oil bath at 155 ºC for four hours to reflux the toluene, thereby dehydrating the system. The oil temperature was then increased to 175 ºC for 24-48 h until an increase in viscosity was observed. The viscous solution was precipitated into an excess of deionized water. The resulting copolymer will be referred to as 6FS-XX, where XX represents the mole % of disulfonated repeat units, or the degree of disulfonation. The degree of disulfonation of the copolymers may be varied by changing the ratio of DCDPS to S-DCDPS.

The polymer fibers were dried in a vacuum oven at 100 °C for 24 hours, then dissolved in DMAc (10 wt%). The solutions were filtered through 0.45μm syringe filters and cast onto clean glass plates. The solvent was evaporated under an infrared lamp, and tough, ductile, transparent films were obtained. The films were acidified by boiling in 0.5M sulfuric acid for two hours, then washed in boiling water for two hours. They were dried in a vacuum oven at 100 °C for 48 h before further use. The acidified films are referred to as 6FSH-XX.

Formation of 6FSH-XX/Zirconium Hydrogen Phosphate Composite Membranes. After the dry, acidified films were weighed, they were hydrated in boiling deionized water for one hour. The films were then immersed in various concentrations of $ZrOCl_2$ for eight hours at 80 °C. After a brief rinse with deionized water, the films were then soaked in 0.5M H_3PO_4, resulting in the precipitation of ZrP in the hydrophilic domains of the membrane. The nanocomposite membranes were boiled in deionized water to remove any water-soluble $ZrOCl_2$ or H_3PO_4, and then dried in a vacuum oven at 100 °C for 48 h. After drying, the wt% of ZrP in the membranes was determined from the difference in dry weight before and after the addition of ZrP.

Results and Discussion

The copolymers were successfully synthesized and the structure was confirmed by ^{1}H NMR, and the intrinsic viscosity was measured at 30 °C in NMP with 0.05M LiBr to correct for the ionomer effect (0.6 dL/g). The amount of ZrP that could be incorporated into the membranes increased as the concentration of $ZrOCl_2$ was increased. The amount of ZrP incorporated into the 6FSH-35 membranes increased rapidly with concentration of $ZrOCl_2$ at concentrations below 10%, but subsequently leveled off at 25 wt% when the concentration was further increased, and no additional ZrP was incorporated for $ZrOCl_2$ concentrations as high as 30%.

As expected, the incorporation of ZrP into the disulfonated copolymer membranes resulted in a decrease in the water uptake (Table 1). A significant decrease in the water uptake of 6FSH-35 was observed, lowering it from 38% (with no ZrP) to 30% (for a sample with 25 wt% ZrP).

Table 1. Water Uptake and Thermogravimetric Analysis Data for 6FSH-35/ZrP Composite Membranes

Wt. % ZrP	Water Uptake, %	$T_{5\%}$, °C	Char Yield, %
0	38	385	2.4
15	34	384	8.7
25	30	385	21

The protonic conductivity of the composite membranes was measured as a function of temperature at 100% relative humidity (Table 2). The conductivity increased with temperature, reaching a value of 0.079 S/cm at 80 °C.

Table 2. Protonic Conductivity of 6FSH-35/ZrP Composite Membrane (25 wt% ZrP)

Temperature	Conductivity, S/cm
30 °C	0.019
50 °C	0.025
80 °C	0.079

Conclusions

Different amounts of ZrP were incorporated into partially fluorinated disulfonated poly(arylene ether sulfone) membranes. The amount of ZrP in each composite membrane was dependent on the concentration of the precursor solution, $ZrOCl_2$. An increase in the final amount of ZrP in the membrane was observed up to 10% $ZrOCl_2$, after which point the amount leveled off.

Thermogravimetric analysis showed that the char yield of the composite membranes increased as the amount of ZrP was increased. The proton conductivity of the composite membranes increased as a function of temperature, reaching a high value of 0.079 S/cm at 80 °C under 100% relative humidity.

Acknowledgement. The authors would like to thank the NSF Partnership for Innovation Program (EEC-0332648) and ARO/DARPA (Grant# DAAD19-02-1-0278) for their support of this research.

References

(1) Hickner, M.A.; Ghassemi, H.; Kim, Y.S.; |Einsla, B.; McGrath, J.E. *Chem. Rev.* **2004**, *104*, 4587-4611.
(2) Wang, F.; Hickner, M.; Kim, Y.S.; Zawodzinski, T.A.; McGrath, J.E. *J. Mem. Sci.* **2002**, *197*, 231-242.
(3) Kim, Y.S.; Dong, L.; Hickner, M.A.; Pivovar, B.S.; and McGrath, J.E. *Polymer* **2003**, *44*, 5729-5736.
(4) Alberti, G.; Casciola, M. *Annu. Rev. Mater. Res.* **2003**, *33*, 129.
(5) Grot, W.G.; Rajendran, G. *U.S. Patent 5,919,583*, **1999**.
(6) Costamagna, P.; Yang, C.; Bocarsly, A.B.; Srinivasan, S. *Electrochimica Acta* **2002**, *47*, 1023.
(7) Yang, C.; Srinivasan, S.; Arico, A.S.; Creti, P.; Baglio, V.; Antonucci, V. Electrochemical and Solid State Letters **2001**, *4*, A31.
(8) Pivovar, B.S.; Kim, Y.S. *Proceedings of the 206th Joint International Meeting of the Electrochemical Society*, October **2004**.
(9) Wang, F.; Hickner, M.; Ji, Q.; Harrison, W.; Mecham, J.; Zawodzinski, T.A.; McGrath, J.E. *Macromol. Symp.* **2001**, *175*, 387-395.
(10) Harrison, W.L.; Wang, F.; Mecham, J.B.; Bhanu, V.A.; Hill, M.; Kim, Y.S.; McGrath, J.E. *J. Polym. Sci.: Part A: Polym. Chem.* **2003**, *41*, 2264-2276.

IMPROVEMENT OF DMFC PERFORMANCE AND STABILITY USING MULTI-LAYER STRUCTURE MEMBRANES

Ruichun Jiang,[1] H. Russell Kunz,[1] James M. Fenton[1,2]

[1.] Department of Chemical Engineering,
University of Connecticut, Storrs, CT 06269
[2]. Florida Solar Energy Center,
University of Central Florida, Cocoa, FL 32922

Introduction

Direct methanol fuel cells (DMFCs) are desirable for transportation as well as portable applications such as cell phones, laptops since they use liquid fuel and are simple in system design. However, two major obstacles that currently prevent the widespread commercial applications of DMFCs are low activity of methanol electro-oxidation anode catalysts and crossover of methanol through the polymer electrolyte membrane.[1] Methanol crossover to the cathode not only lowers fuel utilization efficiency but also adversely affects the oxygen cathode, resulting in poorer cell performance.[2] Presently Nafion® is widely used as proton exchange membrane both in hydrogen PEM fuel cell and direct methanol fuel cells. Nafion® membranes have excellent proton conductivity under fully humidified conditions, good mechanical and chemical properties as well as long term stability. However, Nafion® has very high methanol crossover in direct methanol fuel cells. To reduce methanol crossover, thick Nafion® membranes, such as Nafion®117 (175 μm thickness), with higher cell resistance are often used in DMFCs, which also leads to higher cost since Nafion® is an expensive material.

A cheap material, sulfonated poly(ether ether ketone) (SPEEK), was synthesized via the sulfonation reaction of poly(ether ether ketone) (PEEK), and evaluated in DMFCs.[3] Membranes based on SPEEK with different degree of sulfonation (SD) were characterized and tested in DMFCs. SPEEK membranes showed good thermal stability, appropriate mechanical properties, reasonable conductivity, and low methanol permeability.

In this work, we innovated multi-layer structure DMFC membranes with methanol barrier layers based on low SD SPEEK. The thin barrier layer effectively reduced methanol crossover without much IR loss. The conductive layers provided proton-rich membrane/electrode interfaces that ensured less contact resistance with the electrode. DMFC performance and stability were greatly improved by applying this multi-layer structure membrane.

Experimental

SPEEK was obtained through a sulfonation reaction of PEEK (450PF, Victrex US Inc, Greenville, SC). The sulfonation of PEEK was performed by dissolving and modifying the polymer using concentrated sulfuric acid with the degree of sulfonation controlled by reaction time. The sulfonation degree was determined by elemental analysis measurements. SPEEK membranes with different sulfonation degrees were cast by heating and evaporating the solvent from the SPEEK/N-Dimethylacetamide (DMAC) solution in a flat glass dish. Membrane thickness was controlled by varying the solution amount in the casting step.

Two types of multi-layer membranes were prepared. The first type of membranes, with a Nafion®/SPEEK/Nafion® structure were fabricated by sandwiching a thin SPEEK membrane with SD=41% between two Nafion® membranes; while the second type of membranes were prepared by sandwiching a thin SPEEK membrane with SD=41% between two higher SD SPEEK membranes. Multi-layer membranes with the same total thickness (50 μm), but various middle layer thicknesses (5-15μm) were prepared and studied.

The electrodes were prepared by screen-printing the ink containing liquid Nafion® and catalyst onto single-sided ELAT diffusion substrates from E-TEK with an area of 5 cm^2. The MEA was prepared by sandwiching one piece of the membrane between two pieces of gas diffusion electrodes and then hot-pressing at 120°C for 10 minutes at a pressure of 3000 psi. MEAs were tested in a single cell with 5 cm^2 flow channel area (FC05-01SP, Electrochem. Inc., Woburn, MA).

Methanol crossover was determined by the limiting current method using linear sweep voltammetry, with a Solartron SI 1287 electrochemical interface (Solartron Instrument, Houston, TX). The measured limiting current provided the methanol crossover flux of the membrane studied.

Proton conductivity of membranes was calculated from the membrane resistance measured by electrochemical impedance spectroscopy (EIS). The EIS measurements were carried out using a Solartron (Houston, TX) 1250 frequency response analyzer together with the Solartron 1287 electrochemical interface.

MEA fuel cell performance was determined at 60°C and 80°C under ambient pressure with an in-house electrochemical test station that was equipped with a computer controlled Scribner 890B load box. Mean while, the membrane resistance was also measured by current interrupt in the MEA performance test and compared with the results of EIS measurement. DMFC performance with both single layer SPEEK membranes and multi-layer structure SPEEK membranes was investigated.

Results and Discussion

Proton conductivity of SPEEK membranes as a function of temperature with 100% relative humidity was evaluated. The data indicates that the proton conductivities of SPEEK membranes are improved by increasing the sulfonation degree. The SPEEK membrane with a 60% sulfonation degree has proton conductivity slightly lower than Nafion® at temperatures higher than 60°C.

DMFC performance and methanol crossover of single-layer SPEEK membranes were tested. Figure 1 shows the DMFC performance at 60°C and 80°C with 1 M methanol/air, under ambient pressure. Here SPEEK-41 represents SPEEK membranes with 41% sulfonation degree, similar for SPEEK-51 and SPEEK-60. The 41% sulfonation degree SPEEK MEA shows relatively poorer performance due to large IR losses. At 60°C, DMFC performance was improved with increasing sulfonation degree. The cell performance with 60% sulfonation degree SPEEK is much higher than the MEA with the same thickness Nafion® 112 membrane. DMFC performance was improved at 80°C for SPEEK-41, SPEEK-51 and Nafion® 112 due to better reaction kinetics and membrane conductivity. However, cell performance with the SPEEK-60 membrane decreased at 80°C than that at 60°C and showed much lower cell voltage at each current density than that with Nafion® 112 and SPEEK-51 membranes.

Figure 2 shows methanol crossover limiting current results at 60°C and 80°C for the membranes described above. The value of methanol crossover increases slightly at 80°C than 60°C for SPEEK-41. However, a very large increasing of methanol crossover was observed at 80°C for SPEEK-60. The large methanol crossover of SPEEK-60 at 80°C results in a significant cell performance decrease. The large increasing methanol crossover for the SPEEK-60 is due to severe membrane swelling in the methanol solution. Yang et al. measured liquid uptake of Nafion® 115 and SPEEK membranes in 1 M methanol at different temperatures.[4] According to their result, liquid uptake increased slightly for their SPEEK-44 membranes and Nafion® 115 when the temperature was increased from 65°C to 80°C.

However, a large increase was observed for their SPEEK-58 indicating serious membrane swelling at 80°C.

MEAs based on multi-layer membranes were also tested in DMFCs. Figure 3 shows a DMFC cell performance using a multi-layer SPEEK membrane at 60°C and 80°C. Compared with SPEEK-60 membrane alone, improvement of performance can be observed by applying this multi-layer SPEEK membrane. Especially at 80°C, much higher values of cell voltage and power density at each current density were obtained with this sandwiched membrane. The SPEEK-41 barrier layer in the middle swells less in the higher temperature methanol solution and effectively slows down methanol crossover. The outer layers provided proton rich electrode-membrane interfaces, thus reduced contact resistance and improved catalyst utilization as well.

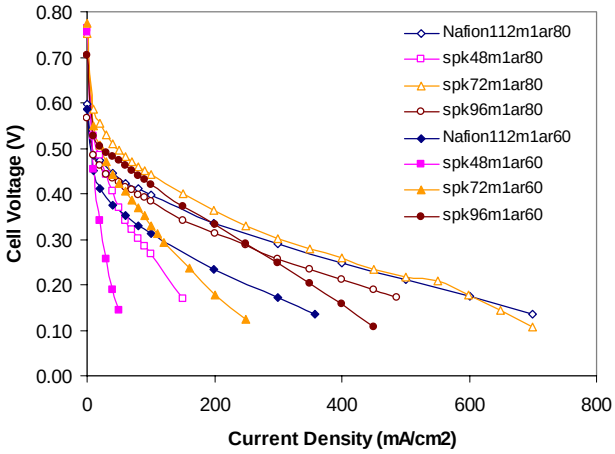

Figure 1. DMFC performance with Nafion® and SPEEK membranes at 60°C and 80°C in 1 M methanol/air at ambient pressure.

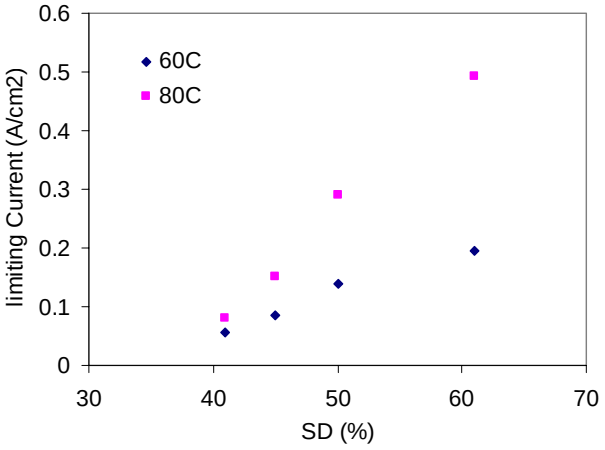

Figure 2. Methanol crossover of SPEEK membranes at 60°C and 80°C with 1 M methanol solution.

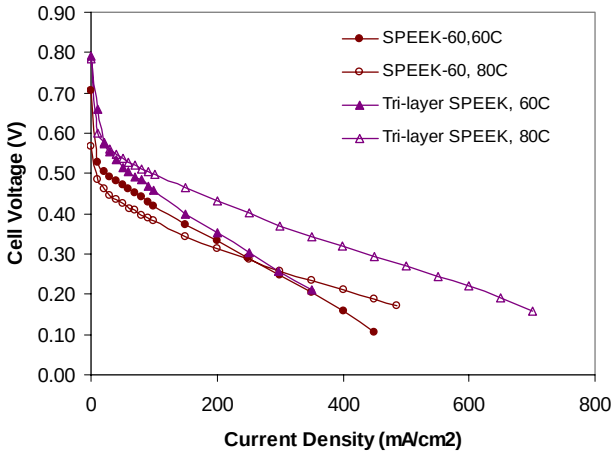

Figure 3. MEA performance with SPEEK multi-layer membrane [SPEEK-60(20μm)/SPEEK-41(10μm)/SPEEK-60(20μm)] with 1 M methanol/Air under ambient pressure.

Conclusions

SPEEK membranes with sulfonation degrees ranging from 40% to 60% show good potential for DMFCs applications. However, the DMFC performance with higher SD showed decreased performance at higher temperature (80°C) due to high methanol crossover. This largely increased methanol crossover was induced by severe membrane swelling of the higher SD SPEEK membrane in the higher temperature methanol solution. With the lower SD SPEEK membrane, DMFC performance becomes better at higher temperature (80°C) than that at 60°C. Due to the effect of less membrane swelling for the lower SD SPEEK membranes, their methanol crossover values increased in a much smaller scale with the increasing temperature than that with higher SD.

A series of multi-layer structure membranes with a thin and lower sulfonation degree (SD=41%) SPEEK barrier layer showed suppressed methanol crossover and acceptable cell resistance. The MEA with a 10 μm thickness SPEEK-41 middle layer showed much better performance than that with a same thickness single SPEEK-60 membrane. The SPEEK-41 barrier layer effectively blocked methanol crossover, especially at 80°C, less swelling of the barrier layer helped to significantly slow down methanol crossover. The MEA with the multi-layer membrane achieved improved methanol utilization and enhanced DMFC performance, and used less costly materials as the proton exchange electrolyte compared to Nafion®. Multi-layer structure membranes also show a promising strategy for DMFC improvement with other hydrocarbon based membrane materials.

References

(1) X. Ren, M. S. Wilson, S. Gottesfeld, J. Electrochem. Soc., **1996**, 143, L12.
(2) D. Chu and S. Gilman, *J. Elelctrochem. Soc*., **1994**, 141, 1770.
(3) R. Jiang, H. R. Kunz and J. M. Fenton, The 204th Meeting of Electrochemical Society, Orlando, Oct. **2003**, (Abstract No. 1024).
(4) B. Yang and A. Manthiram, *Electrochem. Solid-State Lett*., **2003**, 6 (11)**,** A229.

MOLECULAR ARCHITECTURE FOR POLYPHOSPHAZENE ELECTROLYTES FOR SEAWATER BATTERIES

Mason K. Harrup, Frederick F. Stewart, Thomas A. Luther, Christopher J. Orme, and Eric S. Peterson*

Department of Chemical Sciences, Idaho National Laboratory, P. O. Box 1625, Idaho Falls, ID 83415-2208

Introduction

Batteries which use seawater not only as the electrolyte but also as the oxidant with inert cathodes have existed for a long time. Among the better examples of these cells are C. L. Optiz's magnesium/steel wool batteries from the late 1960's and M. A. Walsh's Rope Battery. These cells are attractive power sources for a variety of underwater applications as they have a potential for high energy density, moderate cost, and infinite storage properties when kept dry. The difficulty for these systems in seawater is that an adherent calcareous film forms upon them which reduce the current necessary to protect the structure, resulting in cathode performance deterioration. Lithium is particularly attractive as a battery anode material because of its light weight, high voltage, high electrochemical equivalence, and good conductivity. In such a lithium/seawater batteries, lithium serves as the anode and the cathode is the seawater. For lithium, the principal reactions are:

Anode	Li	-	e^-	$\rightarrow$	Li^+		
Cathode	H_2O	+	e^-	$\rightarrow$	OH^-	+	$\frac{1}{2}H_2$
Overall	Li	+	H_2O	$\rightarrow$	LiOH	+	$\frac{1}{2}H_2$

However, as apparent from the overall electrochemical reaction, lithium and water will also react directly with one another, essentially resulting in parasitic corrosion of the anode when exposed to water. The corrosion reaction is highly undesirable because it produces no useful electrical energy and consumes active lithium. Further, the reaction is highly exothermic and can have detrimental effects on the battery. Accordingly, the principal challenge with respect to reactive metal-water batteries is development of techniques that minimize this direct lithium-water reaction. Research in liquid electrolytes has typically focused on non-aqueous additives that enhance or result in formation of a calcareous film upon the outer surface of the lithium metal as a means of protecting the metal from direct contact with water. Unfortunately, the use of such non-aqueous liquid electrolytes results in the need for complex battery designs to retain the additives employed within the battery while still affording access to the water to allow the battery to function.

Given this, development of practical lithium/seawater batteries hinges upon developing novel solid polymer electrolytes with the appropriate physical and chemical properties. The membranes paradoxically must allow lithium atoms to pass from the metallic surface, oxidize to the ionic form, and then pass through the membrane to the water outside. At the same time, the membrane must exclude water, tramp ions, and gases such as oxygen and carbon dioxide. Also, the calcareous deposits noted above are avoided due to the presence of the membrane. Recent research at the INL has developed deliberately modified polymer electrolytes based upon the phosphazene family of polymers which have a high probability of addressing the above paradox. Initial studies were performed to determine the impact of molecular architecture within the polyphosphazene structure. The startling magnitude of the differences in electrolyte performance due to molecular architecture is discussed in this paper.

Experimental

Polymer Synthesis. The dichlorophosphazene polymer was made by ring-opening polymerization of phosphonitrilic chloride trimer (Strem) using previously described methods.[1-2] An average of 40-45% conversion to the linear polymer, $(PNCl_2)_n$ was achieved. The organophosphazenes (**1**-**4**) were made using standard literature procedures. A typical synthetic scheme is given here. A solution of was made with toluene. To this was added to a solution of *p*-methoxyphenoxide formed from the reaction of *p*-methoxyphenol and sodium hydride in dry THF. Once added the mixture was stirred for 3 hours. A solution of sodium 2-(2-methoxyethoxy)ethoxide was then prepared via reaction with sodium hydride in dry THF. This solution was then added to the polymer solution followed by heating at 108 °C for 18 hours. Once substitution was complete, the polymer was precipitated into water twice and hexane twice sequentially from THF to obtain a tan colored gum. The MEEP polymer (**1**) was synthesized according to the general procedure above but was isolated and purified in 66% yield via a novel route exploiting the lower critical solubility temperature (LCST) behavior of this material in aqueous solution.[3]

Water Permeation Measurements. The polymer membranes were cast directly on porous supports with an average thickness of 50 μm. These supported membranes were loaded into cells obtained from Millipore and modified for pervaporation experiments. Modification to the Millipore cells consisted of a pumping system to flow feed solution over the membrane at approximately 50 mL/min. A diaphragm vacuum pump capable of providing a transmembrane pressure differential of 550 mmHg was installed on the system with a cryo-trap between the pump and the cell. Permeates were collected for six to eight hours and quantified gravimetrically. Transmembrane fluxes are reported in terms of L/m^2h, where L = volume of permeate, m^2 = membrane area (0.0017 m^2), and h = experimental time.

Electrochemical Measurements. Each polymer was dissolved in dry THF and anhydrous $LiBF_4$ was added to the solution. A range of concentrations was employed, typically from 4 to 10 wt% salt vs polymer weight. Films of the salted polymers were cast directly on SS316 steel electrodes measuring 1.00 cm^2 and dried in a vacuum/Argon oven for several hours. A second steel electrode was placed on top of the films and impedance measurements were taken with a PARC model 273A potentiostat coupled to a Solartron SI 1260 impedance/gain-phase analyzer, with computer control provided by Z-plot for Windows (Scribner Assoc.). A frequency sweep technique was employed with a range of 10kHz to 1Hz. Conductivity reported is for the salt loading level that exhibited maximum conductivity for each individual polymer.

Results and Discussion

In formulating polymer electrolytes for seawater battery applications, the material must both conduct lithium ions as well as minimize water permeation. For polyphosphazenes, this requirement is met by incorporating some pendant groups that impart a hydrophobic nature along with some pendant groups that are highly polar to afford lithium ion conduction. How to best incorporate both of these opposing groups into one polymer was a question of molecular architecture that was the subject of our investigations. Since organophosphazenes can be considered to have three principal components – the backbone, the hydrophobic region and the conductive region. Three alternate molecular architectures result from this situation. The first of these architectures is to form a homopolymer from a single pendant group that incorporates both components. Groups of this type are readily commercially available as non-ionic surfactants. However, with this design, one has the

choice of connecting the surfactant moiety to the phosphazene backbone either through the hydrophobic portion, resulting in a core of hydrophobicity and a conductive region that is shifted away from the backbone; or through the conductive portion, resulting in a backbone centered ion channel surrounded by a hydrophobic sheath. Representatives of both molecular architectures were synthesized and are shown in Figures 1 and 2.

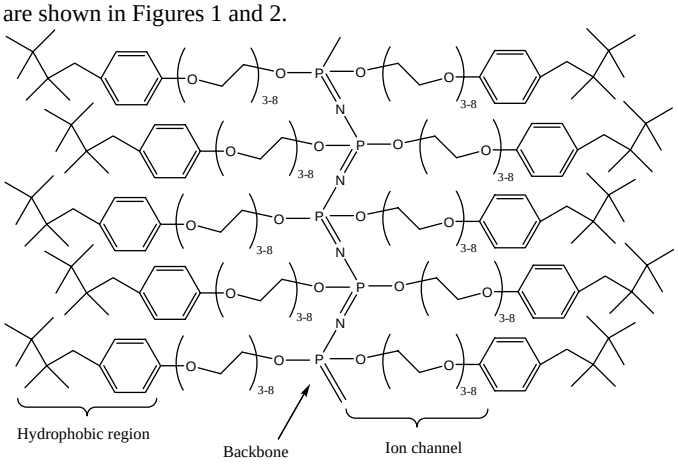

Figure 1. Structure of the triton polymer. This electrolyte possesses the correct molecular architecture to maximize ion conduction.

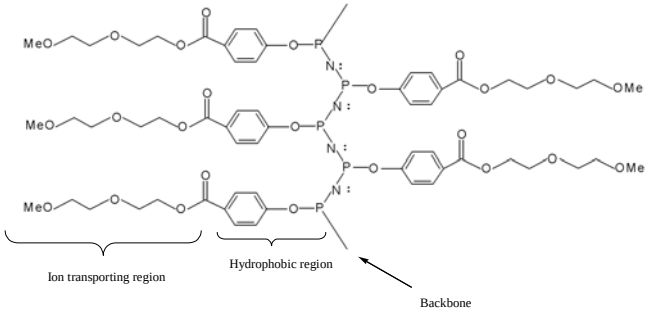

Figure 2. Structure of the DEG ester polymer. In this molecular architecture, the ion channel is "shifted" away from the backbone, resulting in the poorest conductivity.

The third choice for molecular architecture is to form a simple heteropolymer by mixing to different pendant groups – one polar and one hydrophobic. To complete our series for evaluation, a representative of this molecular architecture was prepared as well as shown in Figure 3.

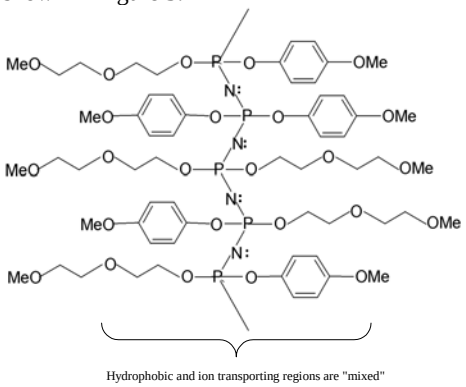

Figure 3. Structure of the 50/50 polymer. In this molecular architecture, the ion channel is "clogged" leading to reduced conductivity.

The water permeability and lithium ion conductivity were measured for these three representative polymers and the results are given in Tables 1 and 2. The well-studied MEEP polymer was also evaluated as a benchmark. As shown in Table 1, the water permeabilities for the three molecular architectures were very similar. This is attributed to the fact the ratio of hydrophobic portion to the conductive portion was very similar for all three polymers, and water transport can be understood to be reflective of this ratio. However, the ionic conductivity of the three polymers was very different – different by a factor of over 15,000. This is explained through the impact of molecular architecture. The mechanism of lithium ion conduction is dependant on a key role played by the nitrogen atoms in phosphazene backbone. This backbone assisted transport mechanism (BIM) affords much more facile ion transport than that via other possible transport mechanisms, such as a hand-to-hand mechanism. As a consequence, when the conductive region is centered on the backbone, the BIM becomes dominant and conductivity is markedly increased. When the conductive region is remote from the backbone, other transport mechanisms dominate and conductivity is lower. In the intermediate architecture, some of the conductive region is near the backbone, but there is no clear all-conductive region – resulting in an ion channel that is "clogged" by hydrophobic moieties. In this instance some BIM transport is possible, but other mechanisms must be responsible for moving through/around the hydrophobic portions. This mixed transport situation leads, logically, to an intermediate conductivity.

Table 1. Water Permeability of Polymer Electrolytes

Polymer Tested	Water Flux (L/M^2*h)
MEEP (**1**)	Dissolves readily
Triton (**2**)	0.013
50/50 DEG/MeOP (**3**)	0.011
DEG Ester (**4**)	0.040

Table 2. Conductivity of Polymer Electrolytes

Polymer Tested	Conductivity (nS/cm)
MEEP (**1**)	43,000
Triton (**2**)	850
50/50 DEG/MeOP (**3**)	41
DEG Ester (**4**)	0.054

Conclusions

Through this work, we have demonstrated that the molecular architecture within the polyphosphazene is critical to performance as an electrolyte membrane suitable for lithium seawater batteries.[4] From these studies, the backbone centered ion channel (BIM) mechanism of lithium transport was developed. Further studies have since confirmed this lithium transport mechanism[5], so all future polyphosphazenes for seawater battery applications will posses this correct molecular architecture.

Acknowledgement. This work was supported by the U.S. Department of Energy, under DOE-NE Idaho Operations Office Contract DE-AC07-05ID14517.

References

(1) Allcock, H. R., *Phosphorous-Nitrogen Compounds*, Academic Press, New York, **1972**.
(2) Singler, R. E.; Schneider, N. S.; Hagnauer, G. L.; Polym. Sci. Eng.**1975**, *15(5)*, 321.
(3) Harrup, M. K.; Stewart, F. F.; J. Appl. Poly. Sci., **2000**, *78(5)*, 1092.
(4) Harrup, M. K.; Stewart, F. F.; Peterson, E. S. *U. S. Patent # 6,146,787*, November 14, **2000**.
(5) Luther, T. A.; Stewart, F. F.; Budzien, J. L.; LaViolette, R. A.; Bauer, W. F.; Harrup, M. K.; Allen, C. W.; Elayan, A.; *Journal of Physical Chemistry B*, **2003**, *107*, 3168-3176.

PROTON CONDUCTING BEHAVIOR OF WATER FREE PEM: POLYPHOSPHORIC ACID IMBEDDED P(VDF-co-HFP) THIN FILM

Zijie Lu[1], Han Hong[2], and Daocheng Luan[2]*

1. PennState University, University Park, PA 16802 USA
2. Xihua University, Chengdu, Sichan, 610039 P.R. China

Introduction

The fuel cell based on 85~95 vol% phosphoric acid as proton electrolyte had shown certain success in temperature region of 180~200°C.[1] Recently using H_3PO_4 to dope various polymer electrolyte membranes for proton exchange membrane (PEM) fuel cell (PEMFC) and directly methanol fuel cell (DMFC) had received much attention for preparing high temperature-tolerance PEM.[2,3] It was found that polybenizimidazol (PBI) doped with H_3PO_4 at high doping level of 5.7 (mol ratio of H_3PO_4/repeat unit) the proton conductivity could reach 7.9×10^{-2} S/cm at 200°C.[4] The problem was that those PEMs could not be entirely anhydrous, as water played as a necessary plasticizer for improving conductivity and mechanical properties. In addition, only two H_3PO_4 has chance to bond to the polymer for each unit and the remaining "free acid" can be easily washed away. Meanwhile the methanol crossover could not be avoided for DMFC. To prevent the exudation of H_3PO_4, a porous film of PBI was made and the doping level could reach 14.6.[5] Again water is needed to have proton conductivity. However H_3PO_4 could be squeezed out of the film if it was applied in fuel cell stack. In sum, although H_3PO_4 doped polymer electrolytes are promising candidates for high temperature PEMs, the water issue would bring a series problem in fuel supply and heat recovery of fuel cell as well as the exudation of H_3PO_4, and thus reduce the power efficiency. Accordingly, preparing a good PEM based on H_3PO_4 still remained a big challenge.

Here we reported a water-free PEM based on a short chain polyphosphoric acid (PPA, the structure is shown as below) that was imbedded in the polymer matrix.

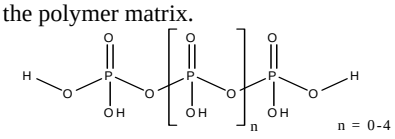

PPA was of 0%wt of free water and was highly soluble in organics. The mobility of PPA in polymer was so small that it could not move out of polymer matrix. Provided that the proton of OH groups along the backbone has certain capability to exchange, one would have chance to get the proton conductivity when the content of PPA and its distribution allow the formation of percolation.

Instead of PBI, the polymer matrix used here was poly(vinyledene difluoride-co-hexafluoropropene) [P(VDF-co-HFP)]. It is a good candidate for high temperature-tolerance PEM due to its excellent thermal stability and inertness to O_2 as well as strong acid.

Experimental

Materials. Polyphosphoric acid (115% equivalent), acetone, methyl ethyl ketone, dioxane and diethylene glycol dimethyl ether were purchased from Sigma-Aldrich company and used after being dried over 4A zeolite. P(VDF-co-HFP) was synthesized from free radical polymerization. In order to get good PPA distribution, low content –OH groups was introduced in to P(VDF-co-HFP) by coplymerization with trifluorovinyl comonomer bearing OH group.

Characterization. -OH functional structure was conformed by ^{1}H-NMR, ^{19}F-NMR in D_6-acetone (Bruker AVANE 300). Impedance of the PEM was measured with Solartron frequency response analyzer (1255B).

Preparation of PEM. According to the desired formulation, certain quantity PPA and functional P(VDF-co-HFP) were mixed in a mixture solvent (such as Acetone/MEK/dioxane/DMG). After casting on a glass substrate, a carefully drying process was carried out to prevent any bubbles. The film was easily peered off from glass surface when it was completely dried.

Results and Discussion

Film-forming behavior of P(VDF-co-HFP) with OH functional groups. It turned out to be every difficult to make a good film from normal P(VDF-co-HFP) with PPA at a content above 5%wt. But with OH functional P(VDF-co-HFP), a good film was made at PPA content 15.0%wt. as shown in figure 1. The OH functional structure was conformed by the small peak at δ = 3.84 ppm assigned to -C**H**$_2$-OH in ^{1}H-NMR as shown in figure 2.

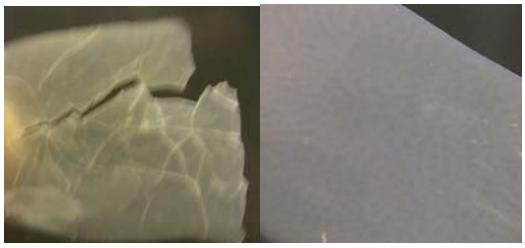

(a) **(b)**

Figure 1. The photos of the films from (a) commercial P(VDF-co-HFP) with 5.0%wt PPA and (b) OH functional P(VDF-co-HFP) with 15.0%wt PPA.

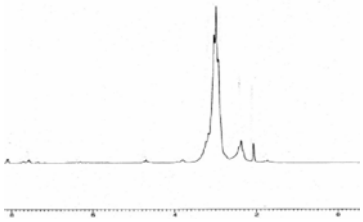

Figure 2. ^{1}H-NMR of OH functional P(VDF-co-HFP).

The SEM image showed that there was no obvious defect and no big hole in the film. This means the distribution of PPA was rather homogeneous.

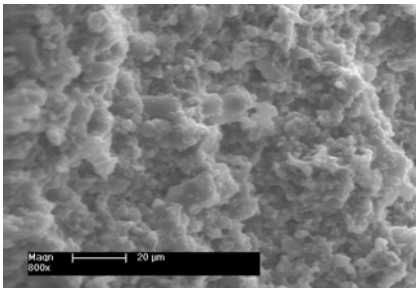

Figure 3. SEM image of the cross section of film from OH functional P(VDF-co-HFP) with 15.0%wt PPA.

Proton of OH groups in PPA. The key point of proton conductivity should lie on the exchanging ability of the proton on the PPA. Based on the studies of ATP, it was claimed that this kind proton exchanging did exist among the polyphosphoric acid segment as shown in figure 3. In this study, we also found that under completely dry conditions, the film did show charge movement within the film.

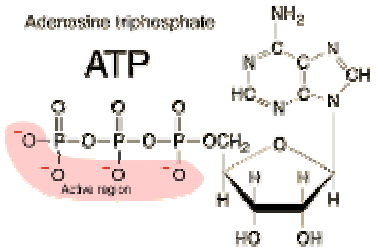

Figure 4. Proton exchanging possibility of the polyphosphoric acid segment.

Proton conducting behaviors. The proton conducting behavior of PPA/P(VDF-co-HFP) was investigated in comparison with Nafion 117 membrane at ambient temperature. In those samples, the effective dc resistance was determined by fitting the semicircular portion of the Nyquist plot (Figure 5) to an equivalent circuit model composed of a resistor, R, in parallel with a constant phase element (CPE). The data points of the low frequency region, where electrode effects are strong or dominant, were excluded from fitting. The un-imbedded P(VDF-co-HFP) polymer was an insulator, as expected. While PPA/P(VDF-co-HFP) showed certain ionic conductivity at room temperature (Table 1). Though the conductivity was two orders lower than wet Nafion, this composite polymer showed promise for further development because it was completely anhydrous. Since high temperature usually helped the increasing of mobility of protons, considering the thermal stability of both polymer matrix and PPA, it was likely for this kind of composite film to use as PEM at high temperature after optimizing the percolation issues of the PPA in polymer matrix to get high proton conductivity.

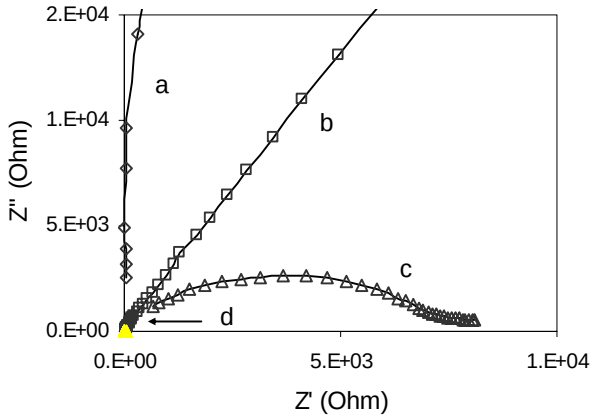

Figure 5. Nyquist plots of impedance measured using two-electrode method at room temperature. a: un-imbedded P(VDF-co-HFP) polymer; b: dry Nafion 117 with 2wt% H_2O; c: PPA/P(VDF-co-HFP); d: Nafion 117 soaked in water with 35wt% H_2O.

Table 1. The comparison of ionic conductivity of PPA imbedded P(VDF-co-HFP) with Nafion 117.

Materials	σ (S/cm) at 25°C
PPA/P(VDF-co-HFP)	1.3×10^{-4}
P(VDF-co-HFP)	2.4×10^{-8}
Wet Nafion (35wt% H_2O)	9.0×10^{-2}
Dry Nafion (2wt% H_2O)	2.3×10^{-5}

Conclusions

A composite film from P(VDF-co-HFP) imbedding inorganic oligomer polyphosphoric acid (15.0%wt) was made. The film showed very good morphology and mechanical properties. It also showed remarkable proton conductivity under completely dry conditions. Compared with the film from Nafion 117, whose proton conductivity was strongly depended on water content, the proton conductivity behavior of water-free film from PPA/P(VDF-co-HFP) was rather encouraging. Optimizing the percolation issues of the PPA in polymer matrix and investigating of temperature effect on the proton conductivity was undergoing.

References

1. Kinoshita, K. *Electrochemial Oxygen Technology*, New York: Willey, **1992**
2. Kawahara, M.; Morita, J.; Rikukawa, M.; Sanui, K.; Ogata, N. *Electrochem. Acta*n**2000,** *45*,1395
3. Tanaka, R.; Yamamoto, H.; Shono, A.; Kubo, K.; Sakurai, M. *Electrochem. Acta*n**2000,** *45*,1385
4. He, R.; Li, Q.; Xiao, G.; Bjerrum, N. J. *J. Membr. Sci.* **2003**, *226*, 169
5. Mecerreyes, D.; Grande, H.; Mihuel, O.; Ochoteco, E.; Marcilla, R.; Cantereo, I. *Chem. Mater.* **2004**, *16*, 604

PROTON EXCHANGE MEMBRANE FOR DMFC AND H_2/AIR FUEL CELLS: II. SYNTHESIS AND CHARACTERIZATION OF PARTIALLY FLUORINATED DISULFONATED POLY (ARYLENE ETHER BENZONITRILE) COPOLYMERS

*Mehmet Sankir, Yu Seung Kim[1], William L. Harrison[2], Anand S. Badami and James E. McGrath**

[1]Los Alamos National Lab (LANL), Los Alamos NM 87544,
[2]NanoSonic Inc, Blacksburg VA 24060
Macromolecules and Interfaces Institute,
Virginia Polytechnic Institute and State University,
Blacksburg, VA 24061, USA
jmcgrath@vt.edu

Abstract

Partially fluorinated disulfonated poly(arylene ether benzonitrile) copolymers were synthesized by direct nucleophilic substitution copolymerization reactions. The 2,6-dichlorobenzonitrile and 3,3'-disulfonated 4,4'-difluorodiphenyl sulfone (SDFDPS) and control amounts of 4,4'-biphenol and hexafluoroisopropylidene diphenol (hexafluorobisphenol A, 6F) were used to produce partially fluorinated disulfonated copolymers with various degrees of fluorination (0-100 mol% 6F). NMR analysis coupled with titration of sulfonated moieties confirmed both chemical structure and copolymer composition. The copolymers produced ductile films. Intrinsic viscosity analyses indicated high molecular weight copolymers were synthesized. Water uptake of membranes and cell resistance of MEAs were lowered by partial fluorination. The influence of this on direct methanol fuel cell performance was demonstrated. Characterizations including TGA, water uptake, proton conductivity and morphology will be presented.

Introduction

Proton exchange membrane fuel cell membranes require several qualities, such as good mechanical properties/stabilities, good proton conductivities, and have low permeabilities of the reactant fuels. Currently, perfluorinated sulfonic acid polymers are employed despite their reported limitations. Our research group and others have been investigating novel commercially viable proton conducting membranes for polymer electrolyte fuel cells. Alternative PEMs are primarily based on aromatic engineering polymers, such as poly ether sulfones and poly ether ketones that have been chemically modified to contain sulfonic acid groups along the main chain. In contrast, our approach has been to control the degree of sulfonation by copolymerizing sulfonated monomers. It has also been demonstrated that exact control (distribution) of sulfonation over the entire sequence is better via direct copolymerization versus post-sulfonation by titration and NMR studies [1-4]. The synthesis and characterization of high molecular weight, nitrile-functional copolymers using 3,3'-disulfonated 4,4'-difluorodiphenyl sulfone (SDFDPS), 2,6-dichlorobenzonitrile and 4,4'-hexafluoroisopropylidene diphenol (hexafluorobisphenol A, 6F) [5] and its nonfluorinated analogue [6] have been reported by our group. In this contribution, we report the synthesis and characterization of partially fluorinated disulfonated poly (arylene ether) copolymers and their direct methanol fuel cell (DMFC) performances.

Experimental

Reagents. 4,4'-biphenol was kindly provided by Eastman Chemical, 2,6-dichlorobenzonitrile was purchased from Aldrich and both were used without any purification. The 4,4'-hexafluoroisopropylidene diphenol (hexafluorobisphenol A), received from Ciba, was purified by sublimation and dried *in vacuo*. The disodium salt of 3,3'-disulfonated 4,4'-dichlorodiphenyl sulfone (SDCDPS) was synthesized through the reaction of 4,4'-difluorodiphenyl sulfone (Solvay Advanced Polymers) and fuming sulfuric acid, as described previously [7]. All other reagents were obtained from commercial sources and purified, as needed, via common procedures.

Synthesis of Partially Fluorinated Disulfonated Poly (arylene ether benzonitrile). Partially fluorinated disulfonated poly (arylene ether benzonitrile) copolymers were achieved at 35 mol percent disulfonation with various degrees of fluorination (0-100 mol% 6F) via direct copolymerization. A typical copolymerization is presented for 25 mol % 6F incorporated in 35 mol percent disulfonated poly(arylene ether benzonitrile). 2,6-dichlorobenzonitrile (1.3487 g, 7.8 mmol), 3,3'-disulfonated 4,4'-difluorodiphenyl sulfone (SDFDPS) (1.9350 g, 4.2 mmol), 4,4'-biphenol (1.6846 g, 9 mmol), 4,4'-hexafluoroisopropylidene diphenol (1.0139 g, 3mmol) and 1.9172 g potassium carbonate (15% mol excess) were transferred to 3-neck flask equipped with a mechanical stirrer, a nitrogen inlet and a Dean Stark trap. Dry NMP (15 mL) was used as the polymerization solvent while toluene (7.5 ml) was the azeotrope. The reaction mixture was refluxed for 4 h at 150 ºC to complete the dehydration process. The reaction temperature slowly increased to 180 ºC for 16 h just after the removing of the toluene gradually. The viscous reaction product was cooled and diluted with NMP and precipitated in deionized water as swollen fibers. After washing several times with deionized water, the precipitated copolymers were boiled in deionized water for 4 h to remove the salts. Copolymers were isolated by filtration then dried in a vacuum oven at 120 ºC for 24 h.

Film Casting and Membrane Acidification. Membranes in the potassium sulfonate form were prepared by first redissolving the copolymer in DMAc to afford 5-10% (w/v), filtered, then cast onto clean glass substrates. The transparent solutions were carefully dried with infrared heat at gradually increasing temperatures (up to ~ 60 ^{o}C) under a nitrogen flow, until the film was fairly dry. The sulfonated poly(arylene ether sulfone) copolymer films were converted to their acid form by boiling the cast membranes in 0.5 M sulfuric acid for 2 hours, followed by 2 hours extraction in boiling deionized water, which has been referred to as Method 2 [8].

Characterization

Intrinsic viscosities were determined in NMP containing 0.05 M LiBr at 30 ºC using an Ubbelohde viscometer. The thermo-oxidative behavior of both the salt-form (sulfonate) and the acid-form copolymers was performed on a TA Instruments TGA Q 500. Dried, thin films (5 to 10 mg in salt form) were evaluated over the range of 30 to 800 ^{o}C at a heating rate of 10 ^{o}C/min in air. Titration of the sulfonic acid groups was performed on acidified membrane samples of known mass by exchanging with sodium sulfate then back titrating with 0.01M NaOH. Thin film conductivity measurements were conducted on acidified membranes while submerged in deionized water using a Hewlett Packard 4129A Impedance/Gain-Phase Analyzer recorded from 10 MHz to 10 Hz. DMFC performances were evaluated at LANL.

Results and Discussion

Direct nucleophilic polycondensation was used to synthesize several series of high molecular weight partially fluorinated disulfonated poly(arylene ether sulfone) copolymers (Table 1). The chemical structure of disulfonated poly(arylene ether benzonitrile) copolymer can be seen in Figure 1a. Disulfonation was kept constant

at 35 mol percent for partially fluorinated copolymers. However, biphenol and 4,4'-hexafluoroisopropylidene diphenol were used together to obtain a series of partially fluorinated copolymers (Figure 1b)

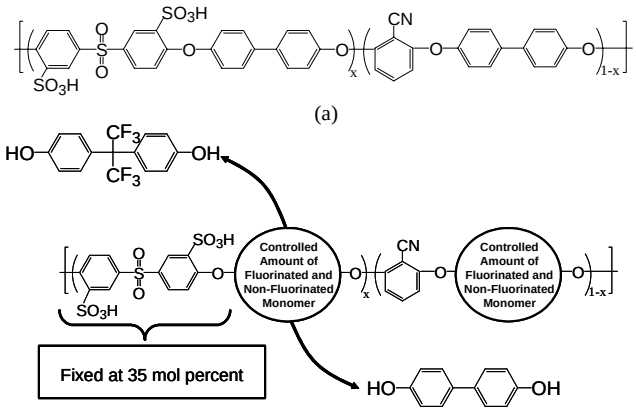

Figure 1. Chemical structure of (a) 35 mol percent disulfonated poly(arylene ether benzonitrile) and (b) 35 mol percent disulfonated partially fluorinated poly(arylene ether benzonitrile)

Copolymers showed very high thermooxidative stabilities. The five percent weight loss temperature for acid form of PAEB35, PAEB35+6F25 and PAEB35+6F50 was 350ºC. Thermooxidative stability was increased with increasing fluorination and the five percent weight loss temperature reached up to 400 ºC for PAEB35+6F75 and PAEB35+6F100 which is more than enough for 120 ºC fuel cell operation.

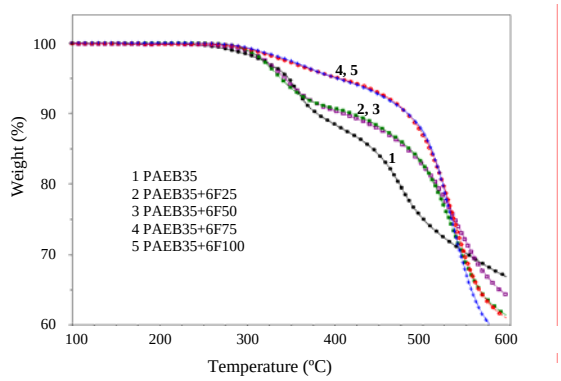

Figure 2. Influence of partial fluorination on thermooxidative stability of acid form of PAEB copolymers (10 ºC/min in air)

Table 1 shows membrane properties such as water uptake, proton conductivity, ion exchange capacity (IEC), methanol permeability as a function of degree of fluorination. Partial fluorination decreased water uptake which was important for long term performance. Although ion exchange capacities of the membranes decreased with increasing degree of fluorination, the decrease in proton conductivities was about 20 mS/cm. The minimum conductivity, 70 mS/cm, was sufficient for fuel cell applications. Hence, the water uptake was controlled without loosing much the proton conductivity.

Table 1. Influence of the Partial Fluorination on Several Features (XX denotes the mol percent 6F)

PAEB 35+XX	Intrinsic Viscosity dL/g	Water Uptake (wt. %)	IEC meq./g	Proton Cond. (mS/cm)	Membrane thickness (micrometer)	Methanol Limiting current (mA/cm2)	Methanol permeability x10^{-6} (cm^2/s)
0	1.00	40	1.87	90	55	65	1.2
25	0.87	35	1.70	80	55	63	1.2
50	0.70	31	1.56	80	55	71	1.3
75	0.65	27	1.44	70	50	89	1.4
100	0.65	24	1.33	70	51	77	1.4
Nafion 112	NA	19	0.92	110	50	190	3.3

The methanol permeabilities of partially fluorinated PAEB 35 copolymers (Table 1) were 2-3 times lower than Nafion 112. Nafion dispersions were used to make membrane electrode assemblies. Cell resistances were decreased and stabilized by increasing degree of fluorination due to better adhesion at catalyst layer-membrane interface (Figure 3). Higher initial cell performances were observed compared to Nafion due to the lower methanol permeabilities of copolymers (Figure 4). The initial performances were further improved with increasing degree of fluorination because of the interfacial effect.

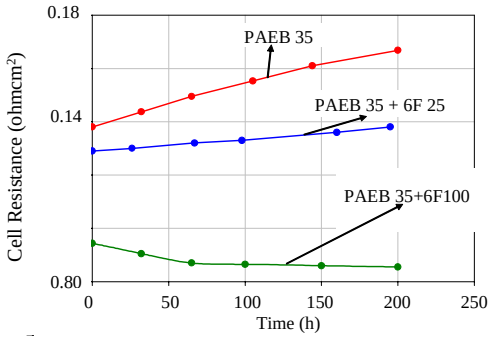

Figure 3. Cell resistance was lowered and stabilized with partial fluorination

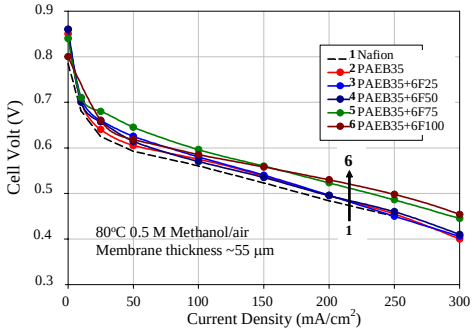

Figure 4. Initial cell performances were improved with partial fluorination

Partial fluorination also improved longer term performances (200 h). This effect was mainly attributed to the decrease in water uptake with increasing fluorination. It has been proposed that the

water uptake of a membrane was the critical factor for its long term performance [9]. Interfacial delamination between electrode layer and membrane occurred when their water uptake values were not close to each other. Hence, the water uptake depression with increasing fluorine content decreased the dimensional mismatch between the electrodes and the membrane (Figure 5).

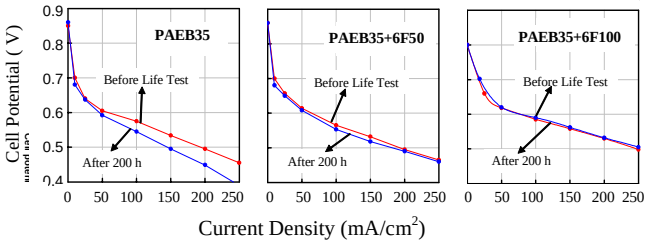

Figure 5. Long term performances were also improved with partial fluorination (Same studies have been conducted up to 2000 h)

Conclusions

The benzonitrile-containing, thermally stable, ductile, high molecular weight partially fluorinated disulfonated copolymers were successfully synthesized. These copolymers showed better initial and long term performances than Nafion 112 due to their lower methanol permeabilities. The partial fluorination has two important effects on a proton exchange membrane and/or membrane electrode assembly: It reduces the cell resistance and also lowers the water uptake of membrane. The former one is important for initial performance, while the latter is crucial for long term performance.

Acknowledgement. The university authors would like to thank the National Science Foundation "Partnership for Innovation" Program (HER-0090556) and the Department of Energy (DE-FC36-01G01086) for support of this research effort.

References

(1) Hickner, M.A.; Ghassemi, H.; Kim, Y.S.; Einsla, B.R.; McGrath, J.E. *Chemical Reviews*, 2004, 104, 4587
(2) Wang, F.; Hickner, M.; Kim, Y. S.; Zawodzinski, T. A.; McGrath, J. E. *J. Membr. Sci*. **2002**, 197, 231
(3) Wang, F.; Hickner, M.; Ji, Q.; Harrison, W.; Mecham, J.; Zawodzinski, T.; McGrath, J. E. *Macromol. Symp*. **2001**, 175(1), 387.
(4) Harrison, William L.; Wang, Feng; Mecham, Jeffery B.; Bhanu , Vinayak A.; Hill, Melinda; Kim, Seung Yu; McGrath, J.E. *J. Polym. Sci.: Part A: Polym. Chem.* **2003**, 42, 2264.
(5) Sumner, M.J.; Harrison, W.L.; Weyers, R.M.; Kim, Y.S.; McGrath, J.E.; Riffle, J.S.; Brink, A.; Brink, M.H. *J. Membrane Science* **2004**, 239, 199.
(6) Sankir, M.; Harrison, W. L.; Wiles, K. B.; Li, Y.; McGrath, J. E. Preprints of Symposia ACS **(2004)**, 49(2), 526-527
(7) Sankir M. et al , *Journal of Applied Polymer Science* (accepted)
(8) Kim, Y.S.; Wang, F.; Hickner, M; McCartney, S.; Hong, Y.T.; Harrison, W.; Zawodzinski, T. and McGrath, J.E. *J. Polym. Sci.; Part B: Poly. Phys.* **2003**, 41, 2816.
(9) Kim, Y.S., Advances in Materials for PEM Fuel Cell Systems, ACS Asilomar CA **2005**; Kim, Y.S.; Sumner, M.J.; Harrison, W.L.; Riffle, J.S.; McGrath, J.E.; Pivovar, B.S. *J. Electrochem. Soc.* **2004**, 151, A2150

DIRECT COPOLYMERIZATION OF WHOLLY AROMATIC AND PARTIALLY FLUORINATED DISULFONATED POLY(ARYLENE ETHER SULFONE)S

*Brian R. Einsla, Linda A. Harris, Melinda L. Hill and James E. McGrath**

Macromolecules and Interfaces Institute
Virginia Polytechnic Institute and Stated University
Blacksburg, VA 24061
*jmcgrath@vt.edu

Introduction

Proton exchange membrane (PEM) fuel cells are becoming increasingly important as alternative energy sources for stationary, automobile and portable power. The proton conducting PEM must possess several characteristics to be considered for fuel cell applications; including thermal, oxidative and hydrolytic stability, and mechanical durability. High temperature aromatic polymers are used in many areas such as microelectronics, automotive, structural adhesives and aerospace industries due to their excellent thermal and chemical resistance and superior mechanical integrity. These properties suggest that appropriate aromatic polymer systems should be good candidates for proton exchange membranes.[1]

The disulfonated poly(arylene ether sulfone) family of copolymers have great potential as PEMs.[2] These copolymers are prepared by direct copolymerization, which allows for increased control over the chemical composition and hence the ion exchange capacity (IEC). The result is higher acidity of the sulfonic acid sites, lower water uptake, and improved conductivity compared to post-sulfonated poly(arylene ether)s.[3] In particular, the wholly aromatic BPSH copolymers show similar DMFC performance to Nafion, while having lower methanol crossover.[4] A variation on the BPSH copolymers is the 6FSH series, which adds a hexafluoroisopropylidene linkage to every repeat unit of the backbone.[5] This partially fluorinated copolymer series may enhance the stability of membrane electrode assemblies (MEAs) prepared with Nafion electrodes.[4] It has been suggested that the compatibility of the MEA could be improved due to the similar fluorinated backbones and water uptakes. Although the water uptake values of these materials are lower than post-sulfonated polymers, the directly polymerized copolymers go through a percolation threshold at higher levels of disulfonation where the water uptake increases dramatically (above 100%) and mechanical strength is lost, as illustrated in Figure 7-1.

Experimental

Materials. 4,4'-Dichlorodiphenyl sulfone (DCDPS) was kindly provided by Solvay Advanced Polymers and dried under vacuum at 60 °C before use. 4,4'-Biphenol was obtained from Honshu Chemical Ind. Co. and dried under vacuum at 60 °C. 4,4'-(Hexafluoroisopropylidene)diphenol (6F) was obtained from DuPont and dried under vacuum at room temperature. Potassium carbonate was purchased from Aldrich and vacuum dried at 120 °C for 24 hours before use. N,N-Dimethylacetamide (DMAc, Fisher) was distilled under reduced pressure over calcium hydride prior to use. Fuming sulfuric acid (27% SO_3), sodium chloride, sodium hydroxide, and toluene were used as received from Aldrich.

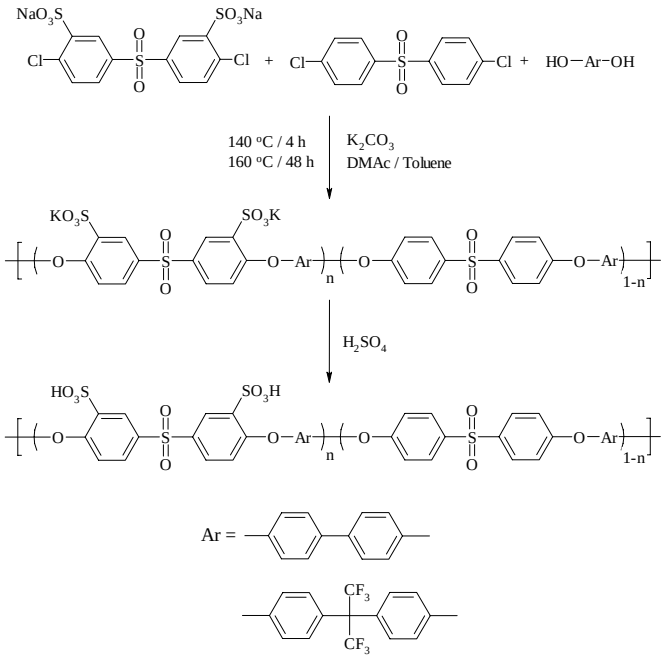

Figure 1. Direct synthesis of random disulfonated poly(arylene ether sulfone) copolymers.

Monomer Synthesis: Disodium-3,3'-disulfonate-4,4'-dichlorodiphenylsulfone (S-DCDPS). In a typical reaction, DCDPS (28.7 g, 99 mmol) was dissolved in 60 mL (390 mmol SO_3) of fuming sulfuric acid (27% SO_3) in a 100-mL, three neck flask equipped with a mechanical stirrer, condenser, and a nitrogen inlet/outlet. The solution was heated to 110 °C for 6 h to produce a homogeneous solution. The reaction was cooled to room temperature, dissolved into 400 mL of ice water, and 180 g of sodium chloride were added to produce a white precipitate of the product. The powder was filtered, redissolved in 400 mL of deionized water and neutralized to a pH of ~6-7 with aqueous 2 N sodium hydroxide. An excess of sodium chloride (~180 g) was added to salt out the sodium form of the disulfonated monomer. The crude S-DCDPS was filtered and dried at 120 °C for 48 h. The dry monomer was dissolved into 500 mL of hot methanol, filtered, and then allowed to cool to room temperature overnight. S-DCDPS was isolated by filtration and recrystallized in a mixture of isopropanol and water (6/1, v/v). The resulting pure product was dried at 120 °C under vacuum for at least 24 h.

Synthesis of Disulfonated Poly(arylene ether sulfone) Copolymers. A direct copolymerization of a 60 mol% partially fluorinated (6F-BisA) copolymer is discussed. First, SDCDPS (4.9120 g, 10 mmol), DCDPS (1.9145 g, 7 mmol) and 6F-BisA (5.6043 g, 17 mmol) were introduced into a 250-mL, three-necked flask equipped with a mechanical stirrer, a Dean-Stark trap, condenser and a nitrogen inlet/outlet. Potassium carbonate (2.77 g, 20 mmol) and 62 mL of DMAc were added to the reaction flask to afford a 20% (w/v) solid concentration. Toluene (31 mL) was added to the flask as an azeotroping agent. The Dean-Stark trap was filled with toluene and the reaction mixture was heated to 150 °C to dehydrate the system. After 4 h at 150 °C, the Dean-Stark trap was emptied and the oil bath temperature was heated to 175 °C for 48 h. The resulting viscous solution was cooled to room temperature, diluted with DMAc and precipitated into an excess of deionized water (3 L). The precipitated copolymer was collected by filtration and dried under vacuum at 80 °C for 24 h and 100 °C for 24 h. Yield: 98%.

Membrane Preparation. Membranes were prepared by solution casting the copolymers from DMAc. The solvent was evaporated under infrared heat at 40 °C. The membranes were removed from the glass substrates by submersion in deionized water and then vacuum-dried at 120 °C for 24 h. The copolymer membranes were converted to their acid form by immersion in boiling 0.5 M H_2SO_4 for 2 h followed by boiling deionized water for 2h. In all cases, tough, ductile, transparent membranes were obtained.

Characterization. ^{1}H NMR spectra were recorded on a Varian Unity 400 instrument operating at 399.952 MHz, in deuterated dimethylsulfoxide (DMSO-d_6). Intrinsic viscosity (IV) measurements were conducted in 0.05 M LiBr/NMP at 25 °C using a Cannon Ubbelohde viscometer. The water sorption values of the membranes were determined at 30 °C. The membranes were vacuum-dried at 120 °C for 24 h, weighed and immersed in deionized water at room temperature for 24 h. The wet membranes were wiped dry and quickly weighed again. The water uptake of the membranes was calculated in weight percent as follows: *water uptake = [(mass$_{wet}$ - mass$_{dry}$) / mass$_{dry}$] * 100*. Proton conductivity measurements were performed on membranes after being soaked in deionized water at 30 °C. An impedance spectrum was recorded from 10 MHz to 10 Hz using a Hewlett-Packard 4129A Impedance/Gain-Phase Analyzer.

Results and Discussion

The synthesis of disulfonated poly(arylene ether sulfone) copolymers has been reported. At high degrees of disulfonation (> 40%), it initially was difficult to synthesize high molecular weight copolymers using S-DCDPS in the partially fluorinated systems. Another procedure was introduced using the highly activated but more costly difluoro monomers (DFDPS and S-DFDPS) to produce high molecular weight copolymers. Herein, an alternative method to obtain high molecular weight copolymers from S-DCDPS at high ion exchange capacities (IECs) is presented. The conversion of DCDPS to S-DCDPS by the reported conditions was quantitative with no side-products.[6] The only impurity introduced was sodium chloride upon precipitation and isolation. A method was described to calculate the amount of salt present in S-DCDPS and use this monomer to produce high molecular weight copolymers.[6] Another procedure is described herein where the S-DCDPS was recrystallized in methanol to remove the salt impurity (Figure 2). The crude S-DCDPS was dissolved in hot methanol, filtered to remove sodium chloride, and allowed to cool to room temperature, which crystallized pure S-DCDPS. After filtration, excess methanol could also be removed by vacuum distillation or crystallization to obtain pure S-DCDPS. High molecular weight copolymers were generated using this purified monomer (Figure 1), as judged by the intrinsic viscosity (IV) values (Table 1). For example, the IV of the 6FSH-60 copolymer was measured in pure NMP and 0.05 M LiBr/NMP at 25 ºC. The IV of 6FSH-60 in NMP was 2.7 dL/g, which is close to the value previously reported for the copolymerization using the highly activated S-DFDPS (2.5 dL/g).[5] The dilute solution viscosity measurements were also conducted in 0.05 M LiBr/NMP to eliminate the polyelectrolyte effect in these sulfonated copolymers. The IV in LiBr/NMP was 0.91 dL/g.

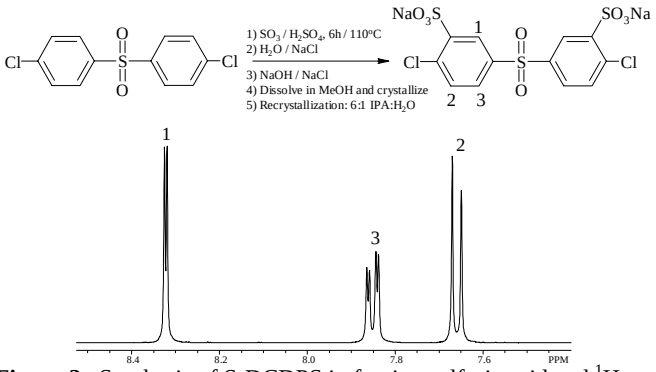

Figure 2. Synthesis of S-DCDPS in fuming sulfuric acid and ^{1}H NMR to confirm the structure (DMSO-d_6).

Table 1. Intrinsic Viscosity, Water Uptake and Proton Conductivity of Selected Copolymers

Copolymer	I.V. (dL/g)*	Water Uptake (%)	Proton Conductivity (S/cm)
BPSH-35	1.05	37	0.08
BPSH-40	0.98	58	0.10
6FSH-35	1.02	35	0.07
6FSH-60	0.91	200	-

*0.05 M LiBr in NMP at 25 oC

Conclusions

A revised procedure was developed to synthesize consistently high molecular weight copolymers derived from pure S-DCDPS. Recrystallization of S-DCDPS in methanol was utilized to remove the salt impurities. It was shown that very transparent, high molecular weight copolymers could be synthesized at lower temperatures in DMAc, as opposed to the previously reported high-temperature conditions in NMP.

Acknowledgement. The authors appreciate the support of this research by the NSF Partnership for Innovation (contract # EEC-0332648), UTC Fuel Cells (contract # PO 3651) and the Department of Energy (contract # DE-FC36-01G011086).

References

[1] Hickner, M.A.; Ghassemi, H.; Kim, Y.S.; Einsla, B.R.; McGrath, J.E. *Chem. Rev.* **2004**, *104*, 4587.
[2] Kim, Y.S.; Hickner, M.A.; Dong, L.; Pivovar, B.S.; McGrath, J.E. *J. Membr. Sci.* **2004**, *243*, 317-326.
[3] Kim, Y.S.; Wang, F.; Hickner, M.; McCartney, S.; Hong, Y.T.; Harrison, W.; Zawodzinski, T.A.; McGrath, J.E. *J. Polym. Sci., Part B: Polym. Phys.* **2003**, *41*, 2816-2828.
[4] Kim, Y.S.; Sumner, M.J.; Harrison, W.L.; Riffle, J.S.; McGrath, J.E.; Pivovar, B.S. *J. Electrochem. Soc.* **2004**, *151*, A2150-A2156.
[5] Harrison, W.L.; Wang, F.; Mecham, J.B.; Bhanu, V.A.; Hill, M.; Kim, Y.S.; McGrath, J.E. *J. Polym. Sci.: Part A: Polym. Chem.* **2003**, *41*, 2264-2276.
[6] Sankir, M. Bhanu, V.A.; Ghassemi, H.; Wiles, K.B.; Hill, M.L.; Harrison, W.; Sumner, M.; Glass, T.E.; Riffle, J.S.; McGrath, J.E. *ACS Div. Polym. Chem., Polym. Preprs.* **2003**, *44*, 1079-1080; *J. Appl. Polym. Sci.* **2005**, *accepted.*

PARTIALLY FLUORINATED DISULFONATED POLY（ARYLENE ETHER SULFONE）COPOLYMERS WITH CONTROLLED MOLECULAR WEIGHTS AND THEIR APPLICATIONS TO PROTON EXCHANGE MEMBRANE FUEL CELLS

Yanxiang Li[1], Juan Yang[1], Abhishek Roy[1], Brian Einsla[1], Feng Wang[2], and James E McGrath[1]*

[1]Macromolecular Science and Engineering & Macromolecules and Interfaces Institute
Virginia Polytechnic Institute and State University
Blacksburg, VA 24061
[2] PPG Industries Inc., 440 College Park Drive, Monroeville, PA 15146
*jmcgrath@vt.edu

Introduction

The electrochemical and mechanical properties of sulfonated copolymers such as Nafion™ , sulfonated polyethersulfones, etc. has become increasingly important as their potential application in proton exchange membrane fuel cells(PEMFC) becomes more evident[1,2]. Molecular weight is a fundamental parameter affecting all mechanical behavior of polymers as is well known. Most reports of new proton exchange membrane materials have included information on ion content (EW or IEC), protonic conductivity, and water uptake. Despite the large body of research on this topic, there is almost nothing in the PEM literature describing molecular weights of candidate materials, even including Nafion and other systems[3].

Sulfonated poly(arylene ether sulfone) copolymers are good candidates for PEMs due to their good acid and thermal oxidative stabilities, high glass transition temperatures and excellent mechanical strength[4]. Partially fluorinated 6F bisphenol monomer in the copolymer may improve certain properties of proton exchange membrane (PEM), such as providing a more hydrophobic membrane surface that will lower the water uptake. Furthermore the fluorine rich surface will be more compatible with electrodes that contain Nafion and may permit more durable electrode membrane assembly (MEAs), which display lower interfacial losses.

In this paper, the synthesis of partially fluorinated poly(arylene ether sulfone) disulfonated copolymers with controlled number average molecular weights (M_n) was described. M_n values of the copolymers were controlled by changing the amount of the monofunctional monomer, tert-butylphenol endcapper relative to the difunctional monomer[5] and were characterization by combination of proton NMR and intrinsic viscosity measurements. In our group, we have begun to utilize NMP with 0.05 M LiBr to measure intrinsic viscosity of ion-containing copolymers instead of simple dilute solution viscosity measurements in pure solvents. The small amount of salt effectively suppressed the polyelectrolyte effect allowing improved characterization of the ion containing materials[3]. Furthermore, we have also begun to examine the influence of molecular weight on several different critical parameters important for proton exchange membranes, such as water uptake, swelling ratio, protonic conductivity, and mechanical properties.

Experimental

Materials. Highly purified 4,4'-dichlorodiphenyl sulfone (DCDPS) was kindly provided by Solvay Advanced Polymers. The 6F bisphenol was provided by DuPont. Both were well dried in a vacuum oven before use but otherwise used as received. The 4-tert-butyphenol (BP) end capper was obtained from Aldrich and purified by sublimation before copolymerization. The 3,3'-disulfonated 4,4'-dichlorodiphenyl sulfone (SDCDPS) was synthesized as reported earlier[6-8]. The solvent N,N-dimethylacetamide (DMAc, Fisher) was vacuum-distilled from calcium hydride onto molecular sieves. Potassium carbonate was dried *in vacuo* before polymerization. Toluene and methanol were obtained from Aldrich and used as received.

Copolymerization. The step growth copolymerization employed a modified procedure from that reported previously[5]. A typical copolymerization for a controlled molecular weight of 40 kg/mol copolymer is described as follows: The 6F bisphenol (5.000g, 14.871mmol), 4,4'-dichlorodiphenyl sulfone (2.596 g, 5.287 mmol), 3,3'-disulfonated 4,4'-dichlorodiphenyl sulfone (2.820 g, 9.818 mmol), and 4-tert-butylphenol (0.071g, 0.469 mmol) were added to a three neck flask equipped with mechanical stirrer, nitrogen inlet and a Dean Stark trap. 1.15 equivalent of potassium carbonate and dry DMAc were introduced to afford 20% solid concentration. Toluene (DMAc/Toluene = 2/1) was used as an azeotropic agent. The reaction mixture was heated under reflux at 160 ^oC for 4 hours to dehydrate the system. Then, the bath temperature was raised slowly to 175 ^oC for 48 hours, which caused the DMAc to reflux. The solution became viscous and was cooled to room temperature, then diluted with DMAc to form about a 20% copolymer solution. The copolymer was isolated by precipitation in deionized water, filtered, and dried in a vacuum oven for 24 hours at 120 ^oC. The crude dry copolymer was then ground to a powder and washed with ethanol and deionized water extensively to remove any potential free endcapping agent and salt. The copolymer was finally vacuum dried at 120 ^oC for 24 hours. The resulting copolymers were designated as 6FS35-XX (salt form) or 6FSH35-XX (acid form), where the mole ratio of disulfonated monomer in the repeat unit was fixed at 35% for all copolymers and XX represents the target number average molecular weight (kg/mol). The molecular weight was controlled by varying the amount of monofunctional monomer 4-tert-butylphenol and the ratio of the difunctional monomers.

Characterization. ^{1}H NMR spectra were conducted with a Varian Unity 400 NMR spectrometer. Intrinsic viscosities (IV) were determined in NMP with 0.05 M LiBr at 25 ºC using an Ubbelohde viscometer.

Results and Discussion

Figure 1 shows the reaction scheme for the step growth polymerization of tert-butylphenol terminated poly(arylene ether sulfone)s containing 35% sulfonate groups. By changing the amount of endcapping regent, tert-butylphenol, according to the modified Carother's equation[9], and the stoichiometry of the feed comonomers, tert-butylphenyl terminated copolymers with different molecular weights (20 ~ 50 kg/mol) were successfully synthesized. Since 6F bisphenol monomer has low reactivity due to the strong electronegativity of -CF_3 groups, the reaction needed much longer reaction times, typically 48 hours or longer than biphenol system. The crude dry copolymers were ground to a powder and washed extensively with ethanol and deionized water to remove any possible free endcapping reagent and residual salt. This step may be important to obtain accurate NMR integration values to calculate molecular weight (M_n).

The molecular weight of the copolymer was calculated from the relative ^{1}H NMR integrals of the tert-butyl endgroups and the aromatic resonances. An example of a proton NMR spectrum of 6FS35-50 is shown in Figure 2. The calculation followed our literature method[5] : There are 18 methyl protons on the two end tert-butyl groups, the average aromatic protons per repeat unit is 15.3 and 15.3 aromatic protons are attached on the terminal phenyl rings. Thus, the following equation can be used to calculate the number of repeat unit:

$$(15.3n + 15.3)/18 = 136.94/2.00$$

Where n is the number of repeat unit and was calculated to be 79.55. Accordingly the average number molecular weight (M_n) of 6FS35-50 was calculated to be:

$$M_n = 79.55 \times 621.4 \text{ g/mol} + 585.4 \text{ g/mol} = 50{,}020 \text{ g/mol}$$

Where the average molecular weight per repeat unit is 621.4 g/mol and the molar mass of the endgroups is 585.4 g/mol. The molecular weights of 20 to 40 kg/mol copolymers were all calculated using the same method and listed in Table 1. It was reassuring that the experimental molecular weights was in close agreement with the target values.

The ^{1}H NMR spectrum in aromatic region and its assignment of 6FS35-50 copolymers was also shown in Figure 3. The chemical composition is exactly as expected. The degree of disulfonation was calculated based on the integration values of k, and a, b proton peaks[10]. The mol content of sulfonated unit in 6FS35-50 is 32.7%. The content of sulfonated unit in other copolymers were also calculated and listed in Table 1. The calculated values are in good agreement with the feed ratio, which suggests that the starting monomers were successfully incorporated into the copolymer chain.

Conclusions

Partially fluorinated poly(arylene ether sulfone) copolymers with different molecular weights were successfully prepared via direct step growth polymerization. The molecular weights were controlled by addition of the monofunctional monomer, tert-butylphenol, together with offsetting the stoicheometry of the feed comonomer ratios. The molecular weights were characterized by proton NMR and intrinsic viscosity measurement. The improved intrinsic viscosity measurement method in 0.05 M LiBr/NMP allows conventional extrapolates to zero concentration due to suppression of the polyelectrolyte effect. The experimental values were in close agreement with the theoretical values. The influence of the molecular weight on the properties of proton exchange membrane, such as water swelling and conductivity, will also be discussed at the meeting.

Acknowledgements. The authors appreciate the support of this research by the Department of Energy (contract # DE-FC36-01G011086) and UTC Fuel Cells (contract #PO 3651).

References

(1) Savadogo O. *J New Mater Electrochem Syst* 1998; 1: 47
(2) Y. S. Kim, L. Dong, M.A. Hickner, B.S. Pivovar, J.E. McGrath, *Polymer*, 2003, 44, 5729-5736
(3) M.A. Hickner, H. Ghassemi, Y.S. Kim, B.R. Einsla, and J.E. McGrath, Alternative polymer systems for proton exchange membranes (PEMs), *Chem. Rev*., 2004, 104, 4587
(4) J.J. Dumais, A.L. Cholli, L.W. Jelinski, J.L. Hedrick, and J.E. McGrath, *Macromolecules*, 1986, 19,1884
(5) F. Wang, T. Glass, X. Li, M. Hickner, Y.S. Kim, J.E. McGrath, *Polymer Preprint*, 2002, 43(1), 492-493
(6) F. Wang, Q. Ji, W. Harrison, J. B. Mecham, R. Formato, R. Kovar, P. Osenar, and J.E. McGrath, *Polymer preprints*, 2000, 41(1), 237
(7) F. Wang, M. Hickner, Q. Ji, W.L. Harrison, J. Mecham, T. Zawodzinski, and J.E. McGrath, *Macromolecular Symposia*, 2001,175, 387-395
(8) F. Wang, M. Hickner, Y.S. Kim, T. Zawodzinski, and J.E. McGrath, *J. of Membr. Sci*, 2002, 197,231-242
(9) F. Wang, J. Mecham, W. Harrison, and J.E. McGrath, *Polymeric Materials: Science & Engineering* **2001**, *84*, 913
(10) W.L. Harrison, F. Wang, J. Mecham, V.A. Bhanu, M. Hill, Y.S. Kim, and J.E. McGrath, *J. of Poly. Sci. Part A*, 2003, 41, 2264-2276

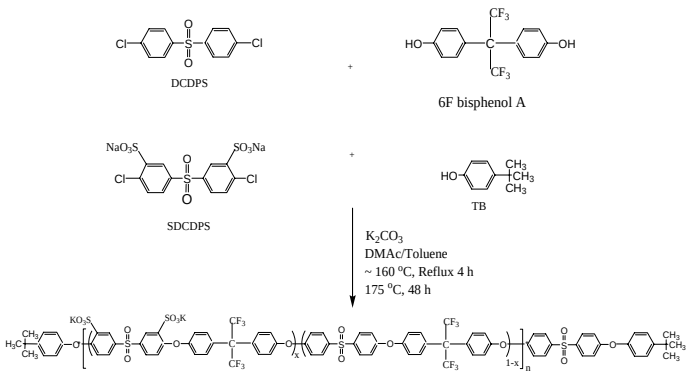

Figure 1. Synthesis of tert-butylphenol terminated partially fluorinated poly(arylene ether sulfone) containing sulfonate groups (x = 0.35)

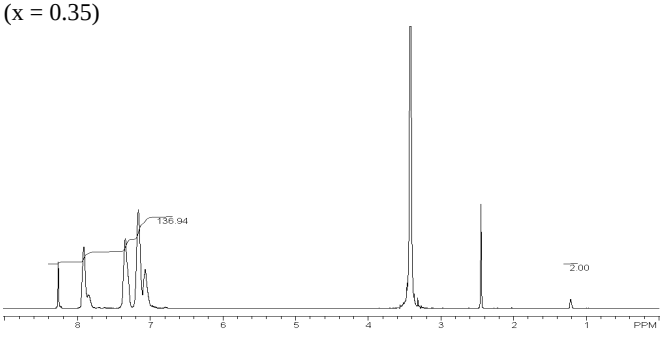

Figure 2. The molecular weight of the copolymer can be calculated from the relative ^{1}H NMR integrals of the tert-butyl endgroups and the aromatic resonances. (6FS35-50 copolymer in DMSO-d_6)

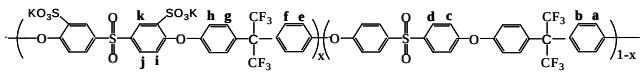

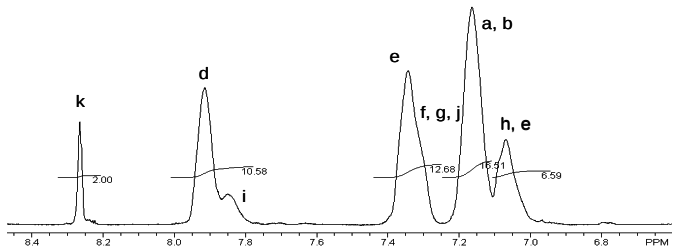

Figure 3. ^{1}H NMR spectrum of 6FS35-50 copolymer (aromatic region)

Table 1. **Characterization of 6FS35 series copolymers**

M_n (kg/mol)	M_n by NMR (kg/mol)	IV[a] (dL/mol)	Degree of sulfonation[b] (%)	
			Target	Calculation
20	19.9	0.25	35	32.5
30	28.5	0.39	35	33.7
40	41.1	0.52	35	34.1
50	50.0	0.58	35	32.7

a Intrinsic viscosities were determined in 0.05 M LiBr/NMP solution at 25 °C.
b Mole % of sulfonated monomer in repeat unit

NEW FUNCTIONALIZED LIQUIDS FOR PROTON EXCHANGE MEMBRANES IN FUEL CELLS

Jennifer Y. Kelly[1], Raymond N. Dominey[2], Paul R. Resnick[3], and Joseph M. DeSimone[1,4]

[1]Department of Chemistry
University of North Carolina at Chapel Hill
Chapel Hill, NC 27599-3290
[2]Department of Chemistry
University of Richmond
Richmond, VA 23173
[3]DuPont Fluoroproductsr
Fayetteville, NC 28306
[4]Department of Chemical Engineering
North Carolina State University
Raleigh, NC 27695

Introduction

There is a growing interest in materials for use as proton exchange membranes in fuel cells. Fuel cells are being targeted to power small electronic devices such as cell phones, laptops, military devices, and automobiles to name a few. DuPont's Nafion® (Figure 1) is the current benchmark material for proton exchange membranes due to its durability, high ionic conductivity and super selectivity. Nafion® is an amorphous copolymer of tetraflouroethylene (TFE) and perfluoro-2-(2-fluorosulfonylethoxy)propyl vinyl ether (PSEPVE) (Figure 1). There are opportunities however for improving the properties of Nafion®. At temperatures above 100 °C Nafion®'s mechanical stability is degraded and its conductivity compromises due to dehydration, thus Nafion® based PEM fuel cells are normally operated at 80 °C or below. Fuel cells running at these lower operating temperatures exhibit decreased catalytic activity both due to generally higher activation losses at lower temperatures but also, for typically envisioned hydrogen feedstocks, due to carbon monoxide poisoning of the platinum catalyst.. Another challenge for Nafion® membranes is methanol (MeOH) permeability. Severe MeOH crossover drastically decreases the open circuit potential and thus the power density of the fuel cell decreases. This results in unattainable optimum performance when Nafion® is used in direct methanol fuel cells.

Herein we report the low temperature synthesis of fluorinated oligomers in supercritical carbon dioxide ($scCO_2$). Our research efforts focus on synthesizing polymers containing TFE or vinylidene fluoride (VF_2), PSEPVE, and a cure site monomer. These liquid, fluorinated oligomers are subsequently crosslinked to form solid membranes. The membranes are hydrolyzed into the proton conducting form for use in hydrogen and methanol fuel cells.

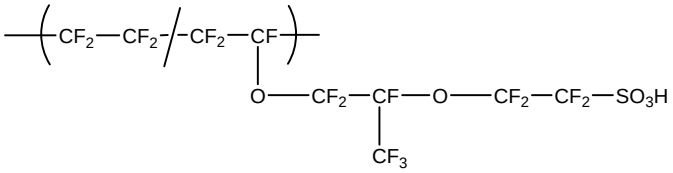

Figure 1. DuPont's Nafion.

Experimental

Materials. TFE was obtained by DuPont as a 50 weight-% mixture in CO_2 and used as received. PSEPVE was provided by DuPont and purified by passing through a neutral alumina column. 2-Bromotetrafluoroethyl trifluorovinyl ether (EVEBr) was obtained from Matrix Scientific and was used as received. α,α,α-Trifluorotoluene was obtained from Aldrich and used as received. Vinylidene fluoride was obtained from Synquest and used as received. SFC purity CO_2 was obtained from Air Products. Bis(perfluoro-2-N-propoxypropionyl) peroxide (dimer peroxide) was prepared in 1.1.2-triichloro-1,2,2-trifluoroethane according to a published procedure[1] and stored over dry ice. The concentration was determined by iodometry and was typically 20 weight-%.

Instrumentation. Infrared spectra were collected using a BIO-RAD FTS-7 spectrometer. Nuclear Magnetic Resonance spectra were collected using a Varian Unity Inova 600 NMR spectrometer.

Synthesis. The experimental set-up is shown in Figure 2. Polymerizations were carried out in a 25 mL high-pressure reaction vessel equipped with a stir bar, thermocouple, rupture disk and a sapphire window which permits visual observation of the reaction mixture with an endoscope. In a typical reaction the high pressure cell was purged with CO_2 to remove oxygen, then the cell was cooled to 15 °C and PSEPVE and EVEBr were charged via syringe while purging with argon. After sealing the cell TFE/CO_2 mixture (50 wt.-%) or vinylidene fluoride (VF_2) was introduced with a manual pump (HIP, Model 62-6-10) under stirring. To add the desired amount of TFE the pump was pressurized to 103 bar (psig). The volume of the TFE/CO_2 mixture was calculated from the density at 103 bar. By repeating opening of the valve between the pump and the reaction vessel and repressurizing to 103 bar the desired volume was introduced. To add the desired amount of VF_2 the pump was pressurized to 48 bar (700 psig). The volume of the VF_2 was calculated from the density at 48 bar. By repeating opening of the valve between the pump and the reaction vessel and repressurizing to 48 bar the desired volume was introduced. The reaction vessel was then heated to the desired reaction temperature which was typically 35 °C and the initiator solution was transferred via syringe to a small addition tube connected to the CO_2 line. The reaction view cell was then filled with CO_2 using an automatic syringe pump (ISCO, Model 260 D) while simultaneously introducing the initiator. After the reaction, the CO_2 was slowly vented.

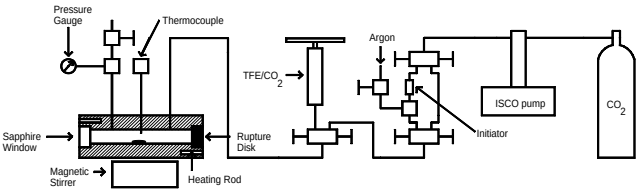

Figure 2. Experimental Set-Up for Synthesis of TFE or VF_2 Containing Terpolymers in $scCO_2$..

Results and Discussion.

Low molecular weight oligomers that are liquids at room temperature have tremendous utility. Such liquids can take on any shape and when containing a cure site monomer (CSM), can subsequently be crosslinked to form a chemically and mechanically robust, fluorinated, solid membrane. Carbon dioxide as a reaction medium for polymerization has enormous benefits. Using CO_2 instead of traditional organic solvents or aqueous based systems affords an environmentally friendly approach which avoids the use of fluorinated surfactants or fluorinated solvents. One can exploit the unique properties of CO_2 especially when used in the supercritical phase in that it has gas-like viscosities and liquid-like densities. Handling TFE as a 50 wt.% mixture in CO_2 enables safer management of this monomer. Furthermore low temperature polymerizations are possible in CO_2 which affords the ability to

minimize β scission and thus minimize acid chain ends that are thought to be involved in PEM ionomer degradation.

All monomers discussed are soluble in $scCO_2$. The reaction mixture is homogenous throughout the reaction. A viscous, slightly cloudy liquid is left after slow venting of CO_2. The products are soluble in α,α,α-trifluorotoluene and subsequently filtered to give a clear solution. The yields of terpolymers containing TFE, PSEPVE, and EVEBr ranged between 12 and 17 % depending on mole ratios charged, whereas when VF_2 was used instead of TFE, yields of at least three times more were obtained. The mole ratios of monomer to initiator of initiator charged ranged between 5 and 10 %. NMR and IR spectroscopy confirmed monomer incorporation into the oligomers.

Conclusions.

Low molecular oligomers containing TFE or VF_2, PSEPVE, and a CSM have successfully synthesized in $scCO_2$ at low temperatures. Product yield increased at least threefold when polymerizations were charged with VF_2 instead of TFE of the same mole %. The viscous liquds were diluted with trifluorotoluene.

Acknowledgement. Nafion® is a registered trademark of DuPont. We would like to thank DuPont for financial support of this project and we acknowledge partial support from the NSF Science and Technology Center for environmentally responsible solvents and processes (Grant No. 4-25151).

References.

[1] Zhao, C.; Zhou, R.; Pan, H.; Jin, X.; Qu, Y.; Wu, C.; Jiang, X. *J. Org. Chem.* **1980**, *47*, 2009-2013.

SYNTHESIS AND CHARACTERIZATION OF MULTIBLOCK COPOLYMERS FOR PROTON EXCHANGE MEMBRANES

*Xiang Yu, Abhishek Roy, James E. McGrath**

Institute for Polymeric Materials and Interfaces, Virginia Polytechnic Institute and State University, Blacksburg, Virginia 24061
jmcgrath@vt.edu

Introduction

Proton exchange membranes (PEM) as the key component for fuel cells have attracted considerable interest recently. Much effort has been made to develop PEMs that combine high proton conductivity, high chemical, thermal, and hydrolytic stability, and low cost[1,2]. Although Nafion, the currently state of the art PEM, shows good chemical and mechanical stability as well as high proton conductivity at relatively low ion exchange capacity (IEC), it suffers from some disadvantages including high cost, high methanol permeability, and limited operating temperature (80 ^{o}C).

Among the polymers developed as alternative PEMs are poly(arylene ether sulfone)s, synthesized by the direct random copolymerization of bisphenol monomers with disulfonated and unsulfonated 4,4'-dichlorodiphenylsulfone (DCDPS)[3-5]. While showing proton conductivity comparative to that of Nafion, the copolymers with high degrees of disulfonation were found to swell dramatically or even dissolve in water, and consequently lose their mechanical strength, making them unacceptable as PEMs[4-6]. This was noted when the percolation limit was exceeded, at which point the ionic domains aggregate and form a continuous phase[6]. Thus control of the copolymer morphology is important, namely, nanophase separation is desired to prevent the ionic phase aggregation.

On the other hand, although the poly(arylene ether) membranes with medium degrees of sulfonation showed satisfactory proton conductivity under fully hydrated conditions, it generally decreased rapidly with decreasing relative humidity or increasing temperature, and was much lower than that of Nafion. This is not surprising considering that, in this type of random copolymer, the ionic proton conducting sites are distributed randomly, with virtually no sequence length. Thus more "free water" needs to be present to maintain good proton conductivity[7]. Nafion, in comparison, reportedly has ionic channels dispersed in the hydrophobic matrix, a structure that greatly facilitates proton conductance at low relative humidity[8-10].

It is therefore desirable to design a PEM which contains proton conducting channels, but which should not swell too strongly in water. We will report in this article, and in the accompanying paper by Roy et al., that block copolymers may show the desired behavior. The synthesis and characterization of amphiphilic multiblock copolymers, containing disulfonated poly(arylene ether sulfone) as the hydrophilic block and perfluoro poly(arylene ether) as the hydrophilic block, will be discussed. Such copolymers are expected to produce nanophase separated morphology which should help reduce membrane swelling, as well as long sequences of sulfonic acid groups that form ionic channels[11].

Experimental

Materials. 4,4'-Isopropylidenediphenol (BPA), obtained from Dow Chemical, was recrystallized from toluene and dried in *vacuo* before use. Decafluorobiphenyl was purchased from Aldrich and dried overnight in *vacuo* at 60 ^{o}C before use. 4,4'-dichlorodiphenylsulfone (DCDPS) was obtained from Solvay Advanced Polymers and used as received. 3,3'-disulfonated-4,4'-dichlorodihenylsulfone (SDCDPS) was synthesized from DCDPS according to a process reported elsewhere[5]. 4,4'-biphenol was obtained from Eastman Chemical and used as received. N-methyl-2-pyrrolidone (NMP), purchased from Aldrich, was vacuum-distilled from calcium hydride and stored under nitrogen.

Synthesis of the perfluoro hydrophobic macromonomer. A typical polymerization procedure was as follows: BPA (1.174g, 5.142 mmol) was added to a three neck round bottom flask equipped with a mechanical stirrer, a condenser, a nitrogen inlet and a dean-stark trap. 10 mL of NMP was added to the flask and the mixture was stirred up to obtain a clear solution. Then K_2CO_3 (1.183g, 7.20mmol) was added, followed by 5 mL of toluene. The reaction bath was heated to 150 ^{o}C and kept at this temperature for 2 hours to dehydrate the system. The bath temperature was then raised to 160 ^{o}C to distill off most of the toluene. The reaction was cooled to 50 ^{o}C and decafluorobiphenyl (2.046g, 6.124mmol) was added, after which the bath temperature was raised to 110 ^{o}C and the reaction was allowed to proceed at this temperature for 5 hours. The mixture was precipitated into 200mL of water/methanol (50/50 volume fraction) and rinsed with water and methanol. The precipitated polymer was stirred overnight in methanol and then dried in *vacuo* at 100 ^{o}C.

Synthesis of the BPS hydrophilic macromonomer. A three neck round bottom flask, equipped with a mechanical stirrer, a condenser, a nitrogen inlet and a dean-stark trap, was charged with biphenol (0.412g, 2.213mmol), 3,3'-disulfonated-4,4'-dichlorodiphenylsulfone (SDCDPS) (0.912g, 1.856mmol), and 10 mL of NMP. The mixture was stirred until dissolved, then K_2CO_3 (0.430g, 3.12mmol) and 5 mL of toluene was added. The reaction bath was heated to 150 ^{o}C to dehydrate the system. The bath temperature was then slowly raised to 190 ^{o}C by the controlled removal of toluene. The polymerization was allowed to proceed at this temperature for 16 hours, and the resulting oligomer was used in the block copolymer synthesis without isolation.

Synthesis of the multiblock copolymer. The reaction bath for the hydrophilic macromonomer synthesis was cooled to 80 ^{o}C, and the highly fluorinated hydrophobic macromonomer (1.050g, 0.350mmol) was dissolved in 10 mL of NMP and added to the same reaction flask. The bath temperature was raised to 95 ^{o}C and kept at this temperature for 9 hours. The reaction mixture was precipitated into 300 mL of isopropanol to obtain a brownish fibrous polymer. The product was stirred in deionized water for 12 hours and in acetone for 12 hours, and dried in *vacuo* at 120 ^{o}C for 24 hours.

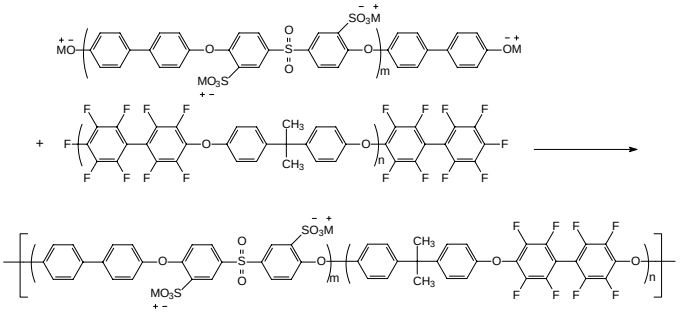

Scheme1. Synthesis of multiblock copolymers

Results and Discussion

Phenoxide terminated poly(arylene ether sulfone) (BPS) macromonomers with 100% degree of disulfonation were synthesized following a procedure similar to our group's earlier work.. Excess biphenol was reacted with SDCDPS to afford oligomers with a variety of target molecular weights. Similarly, fluoro-terminated telechelic macromonomers with different molecular weights were synthesized by reacting BPA with excess

decafluorobiphenyl, but under milder conditions, due to the much higher reactivity of the activated difluoride monomer.

As shown in Scheme 1, multiblock copolymers were obtained through the coupling reaction between the end groups of the two telechelics. At the end of the hydrophilic BPS oligomer synthesis, the amount of fluoro-terminated hydrophobic oligomer to be added was calculated from the target molecular weights of both telechelics and the amount of hydrophilic BPS oligomer that should have been obtained, such that a stoichiometry close to 1:1 was ensured, an important factor in high molecular weight polymer synthesis. The reaction time it took to obtain a viscous solution was longer for copolymers with higher block lengths, probably due to the lower concentrations of end groups available.

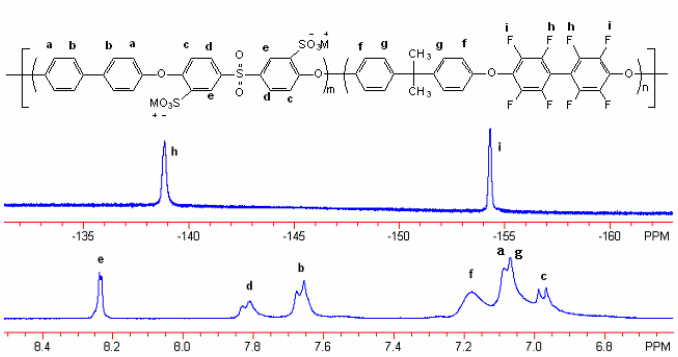

Figure 1. ^{19}F(upper) and ^{1}H(lower) NMR spectra of block copolymer XU1

Figure 1 shows the ^{1}H and ^{19}F NMR spectra of the multiblock copolymer XU3, as well as those of the hydrophobic and hydrophilic macromonomers used to produce it. The peaks due to protons in both oligomers (not shown) are present in the copolymer's spectra, whereas the protons at the hydrophilic oligomer chain ends diminish. These verify the copolymer's composition and support the success of the polymerization.

In Table 1 we can see that the proton conductivity of the block copolymers decreased from XU1 through XU3, reflecting the differences in the ion exchange capacity (IEC). This in turn is in agreement with the changes in block lengths, for although both hydrophobic and hydrophilic block lengths increase from XU1 to XU3, the hydrophilic/hydrophobic ratio actually decreases. Thus proton conductivity in liquid water should mainly be a function of IEC.

Table 1. Characterization of the multiblock copolymers

Polymer	Block lengths[a] (g/mol)	IV (dL/g)	Mn(GPC)[b] (g/mol)	IEC[c]	Water uptake	Proton Conductivity[d] (S/cm)
XU1	3k:3.5k	0.86	30k	1.61	71%	0.13
XU2	3.5k:4k	1.50	40k	1.58	42%	0.11
XU3	5k:5k	0.86	30k	1.38	58%	0.10

a: Block lengths are expressed in the form hydrophobic:hydrophilic
b: Polystyrene was used as the standard
c: Measured from ^{1}H NMR
d: Measured in liquid water at 30 °C

Figure 2 displays the proton conductivity of the block copolymers XU1 and XU3, as well as Nafion 117 as a function of relative humidity. The copolymers show conductivity slightly lower than that of Nafion, yet, in contrary to the results in liquid water, XU3 is the higher of the two, even though it has lower IEC. This indicates that the hydrophilic block length plays a more important role in the proton conductivity under partially hydrated conditions. This agrees with our expectations that, due to the shortage of "free" or "freezing" water in such cases, the proton conductance may rely more upon the ionic channels, which should be easier to form in polymers with longer hydrophilic block lengths.

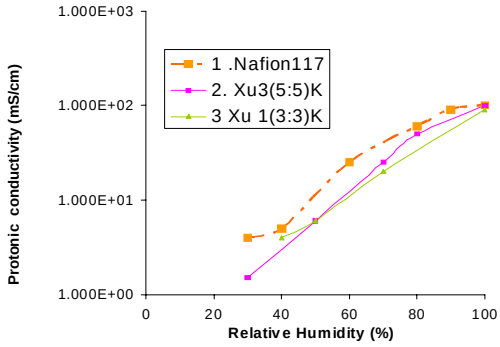

Figure 2. Proton conductivity vs. relative humidity for XU1, XU3 and Nafion 117

Conclusions

Multiblock copolymers with varying block lengths were synthesized by the coupling reaction between hydrophilic BPS and telechelic hydrophobic poly(arylene ether) oligomers. These polymer membranes possess high proton conductivity and relatively low water uptake, and show good potential as candidates for proton exchange membranes. Measurements under different conditions showed opposite trends in proton conductivity of the three polymers, suggesting that block lengths have a larger impact on conductivity in partially hydrated polymers, where the proton conductance should occur mainly through channels formed in between the hydrophilic domains. Since the BPA units in the hydrophobic blocks may not have long term stability, part of our future research will be focused on using alternative bisphenol monomers.

References

(1) Hickner, M. A.; Ghassemi, H.; Kim, Y. S.; Einsla, B. R.; McGrath, J. E. *Chem. Rev.* **2004**, *104*, 4587.
(2) Kerres, J. A.; *J. Membr. Sci.* **2001**, *185*, 3.
(3) Wang, F.; Hickner, M.; Ji, Q.; Harrison, W.; Mecham, J.; Zawodzinski, T.; McGrath, J. E. *Macromol. Symp.* **2001**, *175*, 387.
(4) Wang, F.; Hickner, M.; Kim, Y. S.; Zawodzinski, T. A.; McGrath, J. E. *J Membr Sci* **2002**, *197*, 231.
(5) Harrison, W. L.; Wang, F.; Mecham, J. B.; Bhanu, V. A.; Hill, M.; Kum, Y. S.; McGrath, J. E. *J. Polym. Sci. Polym. Chem. Ed.* **2003**, *41*, 2264
(6) Kim, Y. S.; Hickner, M. A.; Dong, L; Pivovar, B. S.; McGrath, J. E. *J. Membr. Sci.* **2004**, *243*, 317.
(7) Kim Y. S.; Dong, L.; Hickner, M. A.; Glass, T. E.; Webb, V.; McGrath, J. E. *Macromolecules* **2003**, *36*, 6281.
(8) Mauritz, K. A.; Moore, R. B. *Chem. Rev.* **2004**, *104*, 4535.
(9) Ioselevich, A. S.; Kornyshev, A. A.; Steinke, J. H. G. J. Phys. Chem. B 2004, 108, 11953.
(10) Moore, R. B.; Martin, C. R. *Macromolecules* **1989**, *22*, 3594.
(11) Ghassemi, H.; Harrison, W. L.; Zawodzinski, T. A.; McGrath, J. E. *Polym. Prepr (Am. Chem. Soc. Div. Polym. Sci.)* **2004**, *45(1)*, 68.

SYNTHESIS AND CHARACTERIZATION OF SEGMENTED SULFONATED POLY(ARYLENE ETHER)-B-POLYIMIDE COPOLYMERS AS PROTON EXCHANGE MEMBRANES

*Hae-Seung Lee, Brian Einsla, and James E. McGrath**

Department of Chemistry and
Macromolecules and Interfaces Institute,
Virginia Polytechnic Institute and State University
Blacksburg, VA 24061
*jmcgrath@vt.edu

Introduction

The proton conductive polymer membrane is one of the most critical components in polymer electrolyte fuel cells (PEFCs) and direct methanol fuel cells (DMFCs).[1] A high performance proton conductive polymer membrane has some essential requirements such as high proton conductivity, low water swelling, and good mechanical properties. The perfluorinated copolymers such as Dupont's Nafion™ have been most frequently used as fuel cell membranes because of their high performance, including high proton conductivity and good thermal and chemical stability. However, some problems limit further applications, such as high methanol permeability and a relatively low hydrated T_g. To address these weaknesses much attention has been given to polyimides for DMFC applications. Polyimides are well known for their high performance properties such as excellent thermal and oxidative stability, high mechanical strength, very low fuel permeability, and superior chemical resistance to solvents.

One aspect of our research has focused on disulfonated six-membered ring polyimide copolymers,[2] which show high proton conductivity and low methanol permeability (**Figure 1**). However, they hydrolytically degrade if they contain disulfonic acid groups at 80 °C due to the ease of hydrolysis of imido rings and limited suitability for fuel cell. Yet, their low methanol permeability is attractive and alternative methods to enhance their hydrolytic stability are the focus of our current research.

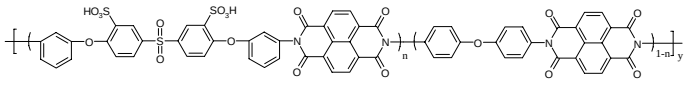

Figure 1. Structures of sulfonated polyimide copolymers.

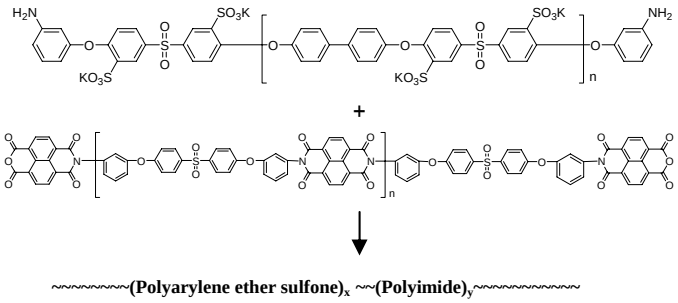

Scheme 1. Synthesis of segmented sulfonated poly(arylene ether)-B-polyimide.

As **Scheme 1** indicates, we are investigating multi phase segmented block copolymer systems which may afford higher hydrolytic stability under acidic conditions. The polyimide portion of the membrane allows for good mechanical properties and low fuel permeability and the sulfonated poly(arylene ether) permits the transport of protons by specific water transport mechanism. This paper describes the synthesis and properties of disulfonated six-membered ring polyimide copolymers. In addition to these, preliminary researches on segmented poly(arylene ether)-B-polyimide are addressed here as well.

Experimental

Materials. 4,4- dichlorodiphenylsulfone (DCDPS, BP-Amoco) and 4,4-biphenol (BP, Eastman Chemical) were all obtained in monomer-grade purity and were dried prior to use. Fuming sulfuric acid (SO_3 content~30%) was obtained from Alfa Aesar and used as received. *m*-Aminophenol (*m*-AP) was received from Aldrich and purified by sublimation. DMAc and toluene (both from Merk and Aldrich) were dried overnight over calcium hydride with a nitrogen purge and distilled at reduced pressure. Potassium carbonate (Aldrich) was dried in vacuum oven at 130 °C for twelve hours.

Sulfonated monomer synthesis. The reaction was conducted in oil bath at the stipulated temperature, using a 100 mL three necked flask fitted with an overhead stirrer and condenser. The temperature was monitored using a thermocouple. The reaction was carried at 110 °C for 6 hrs. The reaction mixture was cooled after the reaction, poured into a mixture of 200g ice and 200 mL de-ionized water, and the crude product was salted out by adding 60g sodium chloride. The product was stirred for 30 minutes and filtered. Finally recrystallization was carried in IPA/H_2O solution for purification.

Synthesis of poly(arylene ethers) of controlled molecular weights. For various molecular weights of poly(arylene ethers), different amounts of BP, DCDPS, and *m*-AP were used. A sample polymerization is as follows: 40.5mmol BP, 44.0mmol DCDPS, 7.1mmol m-AP and 51mmol potassium carbonate (15mol% excess) were dissolved in 70 ml of distilled DMAc and 35ml of toluene in a 3-necked flask equipped with condenser, Dean Stark trap, nitrogen outlet and mechanical stirrer. The reaction mixture was heated at 150ºC for 4 hours with refluxing toluene as the azeotropic agent. The reaction temperature was slowly increased to 180ºC by distillation and removal of toluene and allowed to react for 20 hours. The resulting viscous reaction mixture was diluted with DMAc and precipitated in vigorously stirring methanol and water mixture (1:1). The fibrous polymer was filtered and dried in a vacuum oven at temperatures up to 100ºC.

Characterization Methods. Proton NMR spectra were obtained with a Varian UNITY 400 MHz spectrometer using DMSO-d_6 as a solvent (5% w/v polymer solutions). Intrinsic viscosity (IV) measurements were obtained in NMP at 25ºC using a Cannon Ubbelohde viscometer.

Results and Discussion

Properties of sulfonated polyimide copolymers. Several properties of sulfonated polyimide copolymers were examined to determine their potential for fuel cell applications. It was found that the proton conductivity of the membranes increased at elevated temperature, high relative humidity and high IEC. Sulfonated polyimide copolymer membranes whose IEC were ~1.9 meq/g showed conductivities close to 0.1 S/cm in water at elevated temperatures and this result is equivalent to Nafion 1135 (**Figure 2**). The initial DMFC performance of several copolyimides was investigated, and it was found that these membranes had lower methanol permeability and performed comparably to Nafion 117 **(Figure 3)**. However, their hydrolytic stability at 80 °C was still much lower than Nafion or analogous poly(arylene ether)s.

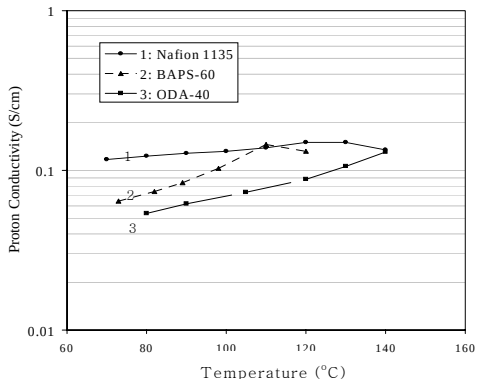

Figure 2. Proton conductivity of sulfonated polyimide copolymer and Nafion 1135 at elevated temperature and 100% RH.

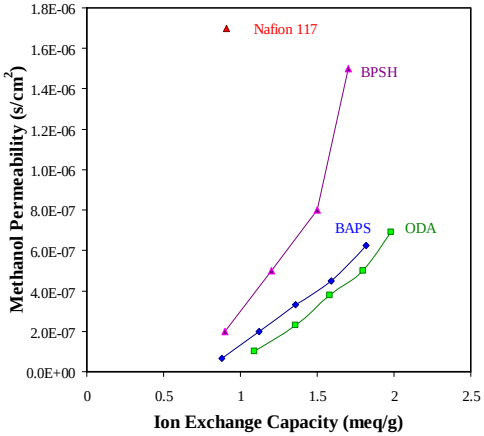

Figure 3. Methanol permeability of sulfonated polyimide copolymer(BAPS, ODA), sulfonated poly(arylene ether) (BPSH) and Nafion 1135.

Synthesis of poly(arylene ethers) with telechelic amine functionalization. A series of controlled molecular weight primary amine terminated poly(arylene ethers) were synthesized as controls (**Scheme2**).

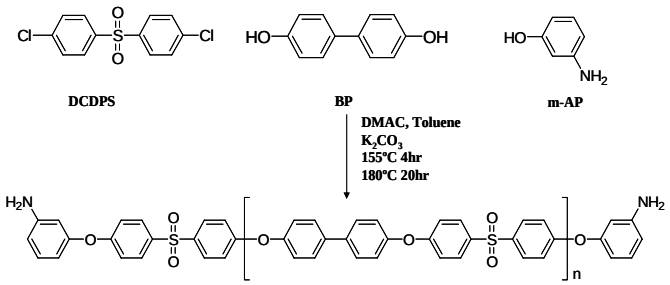

Scheme 2. Polymerization of primary amine terminated poly(arylene ether)

The telechelic primary amine functionality will allow the incorporation of these oligomers in segmented poly(arylene ether)-*b*-polyimide as shown in **Scheme 1**. Number average molecular weights($\overline{M}_n$) of 5,000, 10,000, 15,000, and 20,000 grams per mole were targeted and successfully synthesized. Characterization of molecular weight was estimated by intrinsic viscosity measurements. A more quantitative evaluation of $\overline{M}_n$ was achieved by integration of selected peaks of ^{1}H NMR spectra. As was observed, number average molecular weights matched well with the targeted molecular weights. A summary of the molecular weight characterization is shown in **Table 1**.

Table 1. **Molecular weight characterization of the polymers.**

Targeted Mn (g/mol)	Mn by NMR Analysis (g/mol)	Intrinsic Viscosity (dL/g)
5,000	5,880	0.22
10,000	12,370	0.37
15,000	18.120	0.42
20,000	19,960	0.47

Conclusions

Sulfonated polyimide copolymers showed high proton conductivity and low methanol permeability. Unfortunately, its performance was damaged under aqueous acidic condition because of poor hydrolytic stability. To address this drawback, synthesis of segmented sulfonated poly(arylene ether)-*b*-polyimide is underway. In the preliminary research for the synthesis of controlled molecular weight primary amine terminated telechelic poly(arylene ethers) were successfully synthesized. ^{1}H NMR and intrinsic viscosity measurements confirmed that control of molecular weight from 5K to 20K was successful.

Acknowledgment

The authors wish to acknowledge the support of the Army Research Laboratories under subcontract to General Technical Services LLC, PO# 05-1-084.

References

1. M.A. Hickner, H. Ghassemi, Y.S. Kim, B. Einsla and J.E. McGrath, *Chemical Reviews* **2004**, 104(10), 4587-4611

2. Einsla, B.R.; Hong, Y.T.; Kim, Y.S.; Wang, F.; Gunduz, N.; McGrath, J.E. *J. Polym. Sci.: Part A: Polym. Chem.* **2004**, 42, 862-874.

3. Watari, T.; Fang, J.; Tanaka, K.; Kita, H.; Okamoto, K. *ACS Polym. Mat.: Sci. & Eng. (PMSE)* **2001**, 85, 334.

4. A.L. Rusanov, *Adv. Polym. Sci.* **1994**, 111, 115-175.

5. Genies, C.; Mercier, R.; Sillion, B.; Petiaud, R.; Cornet, N.; Gebel, G.; Pineri, M. *Polymer* **2001**, 42, 5097-5105.

6. Savadago, O.. *J. New Mater. Electrochem. Systems* **1998**, 1, 47-66.

7. Genies, C.; Mercier, R.; Sillion, B.; Cornet, N.; Gebel, G.; Pineri, M. *Polymer* **2001**, 42, 359-373.

8. Brian R. Einsla, Yu Seung Kim, Michael A. Hickner, Young-Taik Hong, Melinda L. Hill, Bryan Pivovar, James E. McGrath. *Journal of Membrane Science* **2005**, (accepted)

SYNTHESIS OF (POLY(ARYLENE ETHER SULFONE)-SUBSTITUTED POLY(*P*-PHENYLENE)) MULTIBLOCK COPOLYMERS FOR PROTON EXCHANGE MEMBRANE

*Hang Wang, James E. McGrath**

Department of Chemistry
Virginia Polytechnic Institute and State University
Blacksburg, VA 24061
*jmcgrath@vt.edu

Introduction

The proton exchange membrane (PEM) is a key component in solid polymer electrolyte fuel cells. Currently the most used PEM is Nafion, which exhibits high conductivity and good chemical and thermal stability. However, it exhibits low conductivity at low water content. Other drawbacks include relatively low mechanical strength, moderate glass transition temperature and high cost[1]. Phase-separated hydrophilic-hydrophobic multiblock copolymers are promising materials that can be used as alternate PEMs. This is particularly due to their ability to form unique morphologies, such as: the spherical, cylinder, and lamellar shape. The morphology of these multiblock copolymers may play an important role in providing good conductivity even at low water content and determining the membranes' mechanical strength and water uptake.

Poly (*p*-phenylene) (PPP) soluble amorphous derivatives are a promising class of high-performance polymers because of their excellent thermal and mechanical properties[2]. We have previously reported synthesis of poly(2,5-benzophenone) derivatives via nickel-catalyzed coupling polymerization of 4'-substituted 2,5-dichlorobenzophenones[3]. These polymers were proven to be highly thermo-oxidative stable materials with good solubility and excellent mechanical properties. However, they do not form good films perhaps due to their extremely rigid rod-like chains.

A series of sulfonated poly (arylene ether sulfone) random copolymers (PAES) have been synthesized in our group in the past few years[4]. These high molecular weight sulfonated copolymers had excellent film forming behavior, high glass transition temperatures and high proton conductivities of greater than 0.1 S/cm, which was equivalent to Nafion control membranes.

This paper describes the synthesis and characterization of PAES-*b*-PPP multiblock copolymers, which are hoped, will combine the excellent thermal, mechanical properties, good proton conductivity and good film-forming ability.

Experimental

Materials. The synthesis of monomers via Friedel-Craft benzoylation of 1,4-dichlorobenzene has been previously reported. Triphenylphosphine (Aldrich) was recrystallized from Et_2O. Zn powder (Aldrich) was washed with acetic anhydride, filtered, washed with dry Et_2O, and dried under vacuum at 150°C. 2,2'-Bipyridine (BPY; Aldrich) and Dichlorobis(triphenylphosphine)nickel(II) (Aldrich) were used as received. Dimethylacetamide (DMAC) were dried over calcium hydride, distilled under vacuum and stored under nitrogen before use. 4,4'-dichlorodiphenylsulfone (DCDPS) and 4,4'-biphenol were obtained from BP Amoco and Eastman Chemical, respectively. The sulfonated comonomer, 3,3'-disulfonate-4,4'-dichlorodiphenylsulfone (SDCDPS) was synthesized in-house from DCDPS according to a modified literature method[5].

Synthesis of telechelic substituted poly(phenylene) and poly(arylene ether sulfone) oligomers. A 100mL Schlenk flask was first charged with $NiCl_2(Ph_3)_2$ (1.047g, 1.6mmol), PPh_3 (0.8387g, 3.2mmol) , Zn (3.2438g, 49.6mmol), 2,2'-Bipyridine (0.2504g, 1.6mmol) and a magnetic stir bar. The flask was sealed with a rubber septum, evacuated under flame for 10 minutes, and placed under an N_2 atmosphere by filling with N_2 followed by three evacuation-fill cycles. THF (10mL) was added via syringe through the rubber septum to initiate the reaction. The solution became deep red after 10 minutes. Then 2,5-dichloro-4'-phenylbenzophenone (3.7667g, 15mmol) and the end-capping agent 4-chloro-4'-flurobenzophenone (0.2346g, 1mmol) were charged under N_2 flow. The mixture was stirred and heated at 65°C for 24 h. After cooling to room temperature, the reaction mixture was poured into 40% HCl/methanol solution. The resulting precipitate was collected by filtration and washed with 10% sodium bicarbonate solution (3 times) and deionized water (3 times). After drying in a vacuum oven at 100°C overnight, the light yellow polymer was isolated and gave a yield of 95%.

The synthesis of hydroxyl terminated sulfonated poly (arylene ether sulfone) was reported earlier[6].

Copolymerization. The aromatic nucleophilic step was conducted in a 3-neck flask equipped with mechanical stirrer, nitrogen inlet and a Dean Stark trap. In a typical polymerization, biphenol (0.3742g, 2mmol), SDCDPS (0.7970g, 1.6224mmol) and potassium carbonate (0.4146g, 3mmol) were added to the flask. Dry DMAc and toluene were used as the solvents. The reaction mixture was heated under reflux at 150°C for 4 hours, which stripped off most of the toluene to dehydrate the system. The temperature was then raised slowly to 165°C for 36 hours. After that, poly (4'-phenyl-2,5-benzophenone) telechelic oligomer (1.051g, Mn=5800) was dissolved in 10 mL dry DMAc and added drop wise into the flask within one hour. The reaction was kept at 165°C for another 48 hours. The viscous polymer solution was cooled to room temperature, diluted with DMAc and filtrated to remove most of salts. The polymer was isolated by precipitation in isopropanol (IPA). It was washed extensively with deionized water several times to quantitatively remove the inorganic salts and finally vacuum dried at 120 °C for 24 hours.

Characterization. ^{1}H-NMR experiments were performed using a Varian 400MHz instrument in deuterated chloroform. The intrinsic viscosity (IV) of the polymers was measured in NMP with 0.05M LiBr at 25°C using a Cannon Ubbelohde viscometer. Number average molecular weights (Mn) and molecular weight distributions (MWD) of polymers were determined by gel permeation chromatography based on polystyrene standards. Glass transition temperatures were estimated by DSC using a Perkin Elmer Model DSC 7. Second-heat T_g values are reported.

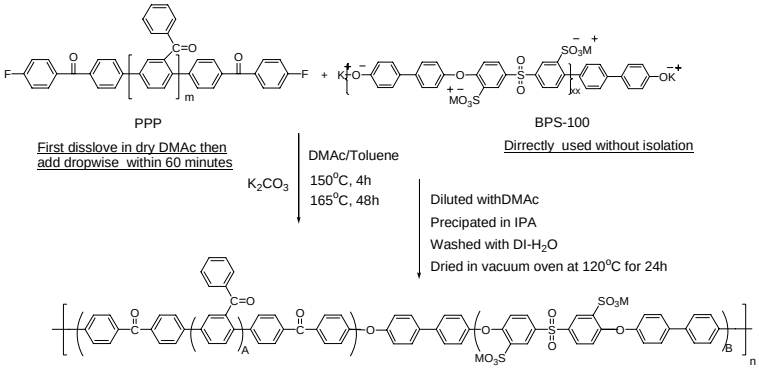

Scheme 1. Synthetic Scheme for Sulfonated Multiblock copolymers

Results and Discussion

A series of poly (4'-phenyl-2,5-benzophenone) telechelic oligomers with different molecular weights, shown in Table 1, were first synthesized by Ni (0) catalytic coupling of 2,5-dichloro-4'-phenylbenzophenone and the end-capping agent 4-chloro-4'-flurobenzophenone, following early procedure of Sheares, et al[2]. Molecular weight of telechelic oligomers were readily controlled by varying the stoichiometric ratio of end-capping agents and monomer. All telechelic oligomers were recovered by vacuum suction filtration in yields exceeding 95% after workup in a 40% hydrochloric acid/methanol solution to remove excess zinc. Carbon-13 NMR spectra were used to determine the degree of polymerization of telechelic oligomers, which were in good agreement with the target values. The peak assigned for the terminal carbonyl was compared with the peak corresponding to the carbonyl group on the benzophenone side groups for this calculation. In addition, both glass transition temperatures and intrinsic viscosities of these telechelic oligomers increase with increasing molecular weight as expect. Therefore, it is safe to say the poly (4'-phenyl-2, 5-benzophenone) telechelic oligomers with controlled molecular weight were successfully synthesized. More important, these telechelic oligomers have fluorine functional group at each end, which should be reactive in nucleophilic aromatic substitution reaction.

Table 1. Characterization of Poly (4'-phenyl-2,5-benzophenone) Telechelic Oligomers

No.	Stoichiometric Ratio between Monomer and End-capping Agent	M*n* (g/mol) (Target)	DP_n, (Target)	DP_n (C^{13} NMR)	IV (dl/g)	T_g (^oC)
1	5:1	2200	10	9.0	0.16	150
2	10:1	4000	20	16.5	0.21	161
3	15:1	5600	30	23.6	0.32	169
4	20:1	7600	40	36.9	0.46	182
5	25:1	9400	50	--	0.48	189

* The intrinsic viscosity (IV) of the polymers was measured in NMP with 0.05M LiBr at 25°C

** Glass transition temperatures were estimated by DSC using a Perkin Elmer Model DSC 7. Second-heat T_g values are reported.

To prepare the PAES-*b*-PPP multiblock copolymers, potassium phenoxide terminated oxide sulfonated poly (arylene ether sulfone) was first synthesized and, without isolation, previous made poly (4'-phenyl-2,5-benzophenone) telechelic oligomers were added in dry DMAc and the reaction was maintained at 165°C for 48h. This afforded a light- yellow copolymer in high yield (90%). A series of multiblock copolymers with various hydrophilic-hydrophobic length were made in this way. ^{1}H NMR showed characteristic peaks of both PAES and PPP oligomer. The multiblock copolymers gave intrinsic viscosity values as high as 0.94 dl/g in NMP with 0.05 LiBr at 25°C.

Atomic force microscope was used to study the morphology of these multiblock copolymers. From the phase image, channels and networks between the hydrophilic phases (darker) were observed, indicating some phase separation exists in these multiblock copolymers.

Conclusions

A series of poly (4'-phenyl-2,5-benzophenone) telechelic oligomers with different molecular weight were successfully synthesized by Ni (0) catalytic coupling reaction. These telechelic oligomers were then copolymerized with phenylate terminated sulfonated poly (arylene ether sulfone)s by nucleophilic aromatic substitution reaction in an attempt to form phase-separated hydrophilic-hydrophobic multiblock copolymers. High molecular weight multiblock copolymers with different block length were successfully synthesized and characterized.

Acknowledgements. The authors would like to thank the National Science Foundation "Partnership for Innovation" Program (HER-0090556) and the Department of Energy (DE-FC36-01G01086) for support of this research effort.

Reference:

(1) Hickner, M. A.; Ghassemi, H.;Kim, Y. S.; Einsla, B. R.; and McGrath, J. E. *Chem. Rev*. 2004, 104, 4587-4612

(2) (a) Schluter, A. D. *J Polym. Sci Part A: Polym Chem* 2001, 39, 1533-1556; (b) Phillips, R. W.; Sheares, V. V.; Samulski, E. T.; DeSimone, J. M. *Macromolecules* 1994, 27, 2354-2356; (c) Wang, Y.; Quirk, R. P. *Macromolecules* 1995, 28, 3495-3501; (d) Percec, V. Zhao, M.; Bae, J.; Hill, D. *Macromolecules* 1996, 29, 3727-3735; (e) Bloom, P. D.; Sheares, V. V. *J Polym. Sci Part A: Polym Chem* 2001, 39, 3505-3512

(3) (a) Ghassemi, H.; McGrath, J. E. *Polymer* 2004**,** 45, 5847-5854; (b)Ghassemi, H; Ndip, G; McGrath, J. E. Polymer, 2004, 45, 5855-5862

. (c) Ghassemi, H.; Harrison, W.; Zawodzinski, T. A., Jr.; McGrath, J. E. *Polymer Preprints* (American Chemical Society, Division of Polymer Chemistry) (2004), 45(1), 68-69; (d) Ghassemi, H.; Ndip, G.; McGrath, J. E. *Polymer Preprints* (American Chemical Society, Division of Polymer Chemistry) (2003), 44(1), 814-815.

(4) Wang, F.; Hickner, M.; Kim, Y. S.; Zawodzinski, T. A.; McGrath, J. E. *J. Membr. Sci*. 2002, 197, 231

(5) M. Ueda, H. Toyota, T. Ochi, J. Sugiyama, K. Yonetake, T. Masuko, T. Teramoto, J. Polym. Sci., Polym. Chem. Ed. 1993, 31, 85.

(6) Ghassemi, H.; Harrison, W.; Zawodzinski, T. A., Jr.; McGrath, J. E. *Polymer Preprints* (American Chemical Society, Division of Polymer Chemistry) (2004), 45(1), 68-69

SYNTHESIS AND CHARACTERIZATION OF SULFONATED POLYIMIDE COMPOSITE MEMBRANES FOR FUEL CELLS

Veena Choudhary and Pooja Chhabra

Centre For Polymer Science & Engg, Indian Institute of Technology, Delhi, India, I.I.T.Hauz Khas, New Delhi-110016, India

Abstract

The paper describes the synthesis and characterisation of sulfonated polyimides prepared by reacting 1,4,5,8-naphthalene tetracarboxylic dianhydride (NTDA),3,3,4,4-benzophenone tetracarboxylic dianhydride(BTDA) sulfonated diamine (4,4'-diaminodiphenylether-2,2'-disulfonic acid (ODADS)and common non-sulfonated diamines. A one step high temperature catalysed polycondensation in m-cresol was used for the synthesis of sulfonated copolyimides. Several samples were prepared by taking mixture of NTDA:BTDA (3:1 molar ratio) and by varying the molar ratio of sulfonated to nonsulfonated diamines in the initial feed. The structural characterisation of the copolymers was done using FTIR and elemental analysis.Ion exchange capacity and water uptake increased with increasing amount of sulfonated diamine. Thermal stability of the copolymers as determined using thermogrametric analyser in nitrogen atmosphere was found to be dependent upon the structure of diamines and the copolymer composition.

MODELING CONDUCTIVITY IN POLYELECTROLYTES

Morton Litt

Macromolecular Science Dept.
Case Western Reserve University, Cleveland, OH 44106

Introduction

Polyelectrolyte membranes are very important in fuel cell development. Most of the work has been on Nafion®, both as-is and with many different materials included[1]. More recently, aromatic sulfonic acid containing polymers have been receiving much attention[2]. One of the main requirements is high conductivity, which is facilitated by water absorption in the materials. A major problem is that, while conductivity is satisfactory at 100% relative humidity, for most materials it drops rapidly as humidity is reduced and water content decreases[1,3]. A second problem in comparing materials is that they vary greatly in composition and equivalent weight. A third problem is that morphology affects conductivity greatly at equivalent water content. In addition, fluorocarbon sulfonic acids are much stronger acids than the aromatic sulfonic acids. The aromatic sulfonic acids can revert to the neutral form as water is removed.

Intrinsic conductivities of polyelectrolyte membranes can be compared if one considers only the aqueous phase in each polymer. This removes the complication of widely differing equivalent weights for different PEMs. It does not compensate for the differing morphologies and acidities, but by removing one complicating factor, it may be easier to understand the influence of the other factors on conductivity. This paper represents a first attempt at this analysis, for fully ionized systems.

Discussion

Basic modeling approach and application to HCl solutions. When one considers the question of proton conduction versus that of any other ion, it is obvious that it is much higher[4], e.g. the limiting ionic conductance at 18°C for H^+ is 315.8 S*cm.^{2}/equiv. while that of Li^+ is 33.4. This is usually explained by the Grothus effect, a proton jumping along a chain of H-bonded water molecules. Since the Li^+ ion solvates about the same number of water molecules as H^+ [5], this implies that the jump length is about 9 to 10 water molecules. The drop in ionic conductance with increasing electrolyte concentration is usually explained by assuming that the ion activity coefficient drops as concentration increases. However, there is another way of looking at the question that may be fruitful. A very primitive model is given below.

As ion concentration increases, jumps are obstructed because a jump requires reorganization of the solvent shell around nearby ions. This is especially true for the proton, since it can jump large distances if unobstructed. One can model this by postulating that the Grothus jump length becomes proportional to λ^{-1} (possibly to an exponent other than -1) as the ion concentration increases; this replaces the activity coefficient approximation. This is shown in Eq. 1 for fully ionized systems. (When the same approach is applied to fluorocarbon sulfonic acid polyelectrolytes, there are further complications that will be discussed later.)

$$C = C_0 * (1 - Pj_{G0}) / (1 - Pj_{G0} * (1 - \lambda^{-a})) \qquad (1)$$

Figure 1. H^+ Equivalent Conductance, HCl solution, Exp. vs Calc. using Eq. 1

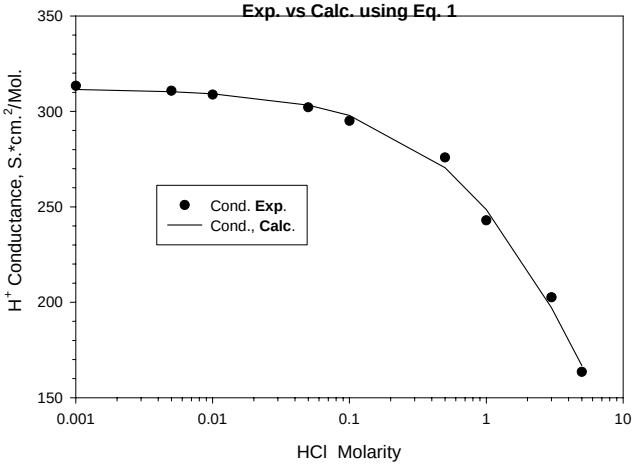

Here C is conductance at a given λ, C_0 is conductance at infinite dilution, Pj_{G0} is the probability of a proton transfer from one water to an adjoining H-bonded water molecule (part of a Grothus jump). λ is the ratio of water molecules to protons and a is a coefficient (near 1). This approach was applied to HCl solution conductance[6], subtracting the Cl^- contribution. The results are shown in Fig. 1 and Table 1.

Table 1. Best parameter values using Eq. 1

Parameter	Value	Standard Error	95% Dev. (S plane)
C_o, S*cm^2/Mol	312.0	2.6	~9.8
Pj_{G0}	.70	.03	~0.11
a	.72	.05	~0.19

The same approach can be applied to recent ^{1}H NMR determinations of the H^+ diffusion constant as a function of HCl concentration[7], Figure 2.

Figure 2. ^{1}H NMR Diffusion Constant for H^+, Exp. vs. Calc. using Eq. 1.

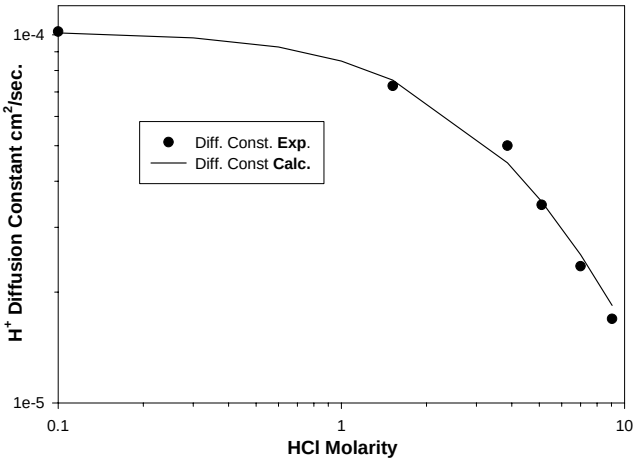

Table 2. B**est values for H^+ diffusion using Eq. 1**

Parameter	Value	Standard error	95% Dev. (S plane)
D_o *cm.*^{2}*/sec.*	1.02E-4	4.0E-6	~2E-5
Pj_{G0}	0.949	.017	~0.09
a	1.30	0.15	~0.8

The parameter values overlap at the 95% confidence level. However, parameter values are somewhat coupled and they can be varied over a relatively large range with little change in the fit. Also, slight changes in the procedure for calculating λ produce swings in the values. Almost as good fits can be obtained if *a* is fixed at 1. Pj_{G0} for Table 1 is then 0.90, and for Table 2 is 0.945, with a 1 σ overlap. The calculated values for a dilute solution Grothus jump length range from 3 to 20 water molecules. At a = 1, Table 1 fits well with the value of 9 to 10 obtained when the Li/H conductance values are compared[4].

Application to Nafion® and other fluorocarbon sulfonic acids. When this approach is applied to water insoluble polyelectrolytes, many other factors must be included. First, does the fraction of ionized acid change with water content? This is certainly true for aromatic sulfonic acids, and further complicates the problem. Fluorocarbon sufonic acids are superacids and are almost fully ionized even at λ's of 2 to 3[8]. Secondly, this is a two phase system, and Paddison has shown that the water dielectric constant decreases near the non-polar wall of the second phase[8]. Because of this, the average proton mobility will depend on the phase morphology. For a given λ the fraction of water as a function of distance from the wall differs if one considers "planar" micelles versus "cylindrical" pores. Using pore morphology, Paddison has calculated that the dielectric constant increases linearly from a low value at the wall to the bulk dielectric constant at about 0.5 nm away from the wall[8]. Proton mobility near the wall can be diminished for two reasons. First, a proton near the wall experiences less shielding from the discrete negative charges at the wall surface; the attraction is no longer homogeneous and there can be low energy wells that increase the activation energy for proton mobility. Second, the low dielectric constant implies lower entropy for the local water; the structure is more "rigid". This might decrease the Grothus jump length. One last point, the local phase orientation restricts the proton movement to specific directions which may not be parallel to the electric field direction.

The system can be modeled very crudely using the factors discussed in the previous paragraph. Litt[9] first proposed a lamellar model for Nafion®, while most investigators use some version of Gierke's model[5], approximately spherical domains interconnected by pores. Both lamellar and pore structures can be modeled using the same concepts, outlined below.

- Polyelectrolytes cannot be compared directly since only their aqueous phase participates in proton conduction. Measured conductivity is therefore proportional to the aqueous volume fraction of a particular system. This must be normalized by considering only the aqueous phase behavior in order to follow what happens as the water content is varied, and to compare different systems.
- Proton jump frequency is lowest at the water/electrolyte interface and rises with increasing dielectric constant to the bulk value, about 0.5 nm. from the interface. For want of better information, it is assumed that the mobility (jump length times frequency) is proportional to the dielectric constant. Mobility is constant when dielectric constant is constant, but depends on the ion concentration.
- Jump length in the whole system decreases as the proton concentration increases, as was postulated for bulk systems.
- The protons are approximately uniformly distributed in the aqueous phase.

Two regimes must be considered. At low λ, the dielectric constant is less than its bulk value throughout the whole system. At higher values of λ, the central aqueous region has the bulk properties. The volume of a single pore or lamella, per acid group, depends on λ. As λ increases, proton concentration decreases. The bulk conductivity reflects this. In the broader picture, the average area per acid group as well as the morphology will determine the aqueous layer thickness for a given λ.

Lamellar micelle model: The area per sulfonic acid was estimated to be about 0.6 nm^2, the cross-sectional area of two PTFE chains in the crystalline phase[9]. This does not change with changing λ, only the micelle spacing changes. If Padison's estimate of the distance from the wall to achieve the bulk dielectric constant holds here, this amounts to a λ of ~10 to 15. Let this be called λ_0. σ_0 represents the conductivity if there were no Grothus effect, the jump distance of a single water molecule. The equations for the different regimes are given below.

For $\lambda < \lambda_0$:

$$\sigma = (\sigma_0 / 2) / (1 - Pj_{G0} * (1 - \lambda^{-a})) \qquad (2)$$

For $\lambda > \lambda_0$:

$$\sigma = (\sigma_0 * \lambda_0^{\,2} / 2) / (\lambda^2 * (1 - Pj_{G0}(1 - \lambda^{-a}))) + \sigma_0 * \lambda_0 * (\lambda - \lambda_0) / (\lambda^2 * (1 - Pj_{G0}(1 - \lambda^{-a}))) \qquad (3)$$

The data used were taken from Gottesfeld and Zadowinski[1] for water in membranes first swollen in water or super-swelled in hot glycerol. Data for a Dow800 film are also included. They fall on the same curve once the aqueous volume fractions due to different equivalent weights are normalized. The data and calculated curve, for the normalized aqueous fractions, are shown in Table 3 and Figure 3.

Table 3. Parameter values for Nafion/Dow aqueous conductivity

Parameter	Value	St. Dev.	95% Dev.
σ_0, S/cm.	0.108	0.035	0.11
Pj_{G0}*	0.81	0.04	0.13
a	1.0	0.47	1.5
λ_0	16.3	4.3	14

Figure 3. Aqueous Phase Conductivity of Fluorosulfonic Acid Membranes, Experimental vs. Calculated Values, Eqs. 2 & 3

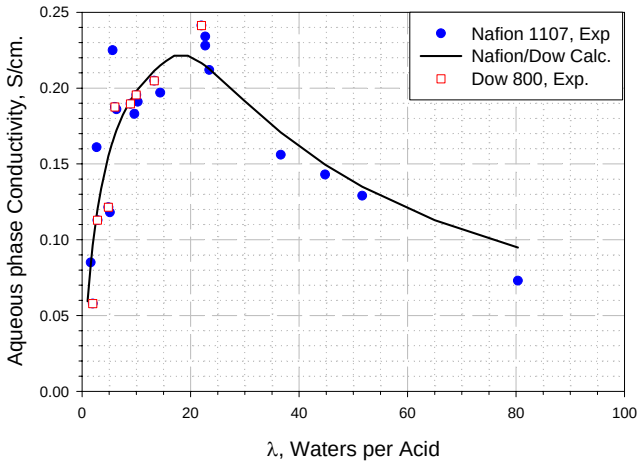

The limiting conductance for H^+ is calculated to be 160 $S*cm^2$/mole for a Grothus jump length of 5. For a Grothus jump length of 10, the limiting conductance is 320, essentially that of the literature value[4], 316.

Space is too limited to show the results of the calculations for a pore morphology. Whether one postulates that the surface charge density does not change or that the number of charges in the pore circumference does not change as λ changes, no fit can be found. The curves cannot reproduce the initial rise of conductivity as λ increases.

Conclusions

A very primitive model has been applied to aqueous proton conductivity, both in the bulk and in fluorocarbon sulfonic acid polyelectrolytes. The major feature is that the Grothus jump length decreases as λ decreases (acid concentration increases). For Nafion®, a very good fit was found using the lamellar micelle model; no fit was seen using a pore model. Using this model, the proton limiting conductance in Nafion® was calculated to be about that found for an aqueous proton. This shows that the model has some validity. The estimate for the limiting Grothus jump length is about 10, as is discussed by Kreuer[3].

References

1. Gottesfeld, S. and Zawodzinski, T. in *Advances in Electrochemical Science and Engineering, Volume 5*, Eds. Alkire, R. C., Gerischer, H., Kolb, D. M. and Tobias, C. W. Wiley, VCH, pp. 195-301
2. See for example, Kreuer K. D., Paddison S. J., Spohr E. and Schuster M., *Chem. Rev*. **2004**, *104*, 4637
3. Kreuer, K. D., Dippel, T. and Meier, J. in *Proton Conducting Membrane Fuel Cells I*, Eds. Gottesfeld, S. Halpert, G. and Landgrebe, A. *The Electrochemical Society, Pennington*, **1995**, 21
4. *Lange's Handbook of Chemistry (15th Edition)*, Ed. Dean, J. A., **1999**, McGraw-Hill p **8**.157
5. Gierke, T. D., Munn, G. E. and Wilson, F. C., J. *Polymer Sci. Part B-Polymer Physics* **1981**, *19(11)*, 1687-1704
6. *Lange's Handbook of Chemistry (15th Edition)*, Ed. Dean, J. A., **1999**, McGraw-Hill, pp **8**.164,165
7. Dippel, T. and Kreuer, K. D. *Solid State Ionics*, **1991**, *46*, 3
8. Paddison, S. *Annu. Rev. Mater. Res*. **2003**, *33*, 289
9. Litt, M. H., *ACS Polymer Preprints*, **38(1)**, April, 1997 p.80

MECHANISM OF ION TRANSPORT IN A SOL-GEL BASED ANHYDROUS PROTON CONDUCTING ELECTROLYTE

Jason E. Ritchie, Braja Ghosh, and Kyle Lott*

Department of Chemistry & Biochemistry, The University of Mississippi, University, MS 38677

Introduction

Proton conducting polymer electrolytes have important electrochemical applications in fuel cells and electrochromic displays. Nafion is the most widely used proton exchange membrane because of its mechanical and chemical stability, and its high H^+ conductivity when wet. However, Nafion requires hydration which limits its maximum operating temperature to around 100°C. Thus, a new electrolyte material is needed that can operate at high temperatures and low relative humidities.

We strive to gain a fundamental understanding of the mechanism of proton conductivity in our $MePEG_n$ polymer (scheme 1).[1-4] There are two general mechanisms for proton conductivity: the vehicle mechanism (which relies on the physical transport of a vehicle) and the Grotthus mechanism (which involves the proton being handed off from one hydrogen bonding site to another).[5] The Grotthus mechanism of H^+ conductivity is similar to Li^+ conductivity in PEG materials which rely on segmental motions and polymer reorganization.

Our group has shown an concentration dependence of ionic conductivity in a mixture of $MePEG_7SO_3H$ acid and our $MePEG_7$ polymer that seems to indicate a change in the mechanism of conductivity as a function of added acid concentration.[1] Our hypothesis is that the H^+ transport is accomplished primarily through a Grotthus mechanism and that H^+ transport is dependant on the volume fraction of polyethylene glycol (PEG) present with the Grotthus mechanism dominating at high PEG contents.

This work is important because, our system is a member of the relatively rare class of polymeric materials that display H^+ conductivity in the absence of water or plasticizing solvent.

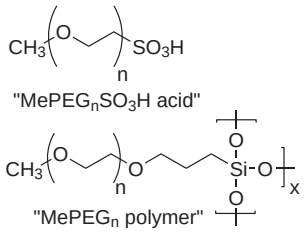

Scheme 1. Structures of $MePEG_n$ polymer and $MePEG_nSO_3H$ acid.

Experimental

The synthesis of the $MePEG_nSO_3H$ acids and $MePEG_n$ polymers have been described.[2] The densities were measured gravimetrically using tared micropipettes. Concentrations were calculated by dividing the density (g/mL) of the neat acid by its molecular weight (g/mol), yielding mol/mL.[2]

Electrochemical measurements were made with a PAR 283 potentiostat equipped with a PE 5210 Lock-in amplifier for AC-impedance.[1,2] GPC measurements were made with a Polymer Laboratories ELS-2100 detector and PL Mixed-D columns calibrated with PS MW standards (PL-EasiCal PS-2).

Results and Discussion

Synthesis. The MePEG polymer precursors synthesized for this study were prepared from a hydrosilation reaction between triethoxysilane and various length allyl-PEGs (Scheme 1).[2] This approach is similar to methods used by Hooper,[6] Zhang,[7] Allcock,[8] and Shriver[9] to prepare Li^+ conducting polymers.

The $MePEG_n$ polymer precursors were hydrolyzed and condensed to form the $MePEG_n$ polymer. This use of different PEG chain lengths allow for the control of volume fraction of PEG in the resulting polymer. In addition, we have prepared $MePEG_nSO_3H$ acids with 7, 12, and 16 repeat units which are miscible with the $MePEG_n$ polymers. These chain lengths are designed to allow us to control the mobility of the $MePEG_nSO_3^-$ ions by changing their physical size and to test the hypothesis that our proton conductivity is primarily through the Grotthus mechanism.

Ionic Conductivity. AC-impedance measurements were performed on anhydrous mixtures of polymers and acids. Figure 1 shows the activation of ionic conductivity (σ) for three different size $MePEG_nSO_3H$ acids (n=7,12,16) dissolved in the small $MePEG_3$ polymer at a low (0.26M) and high concentration (1.32M). As expected, the higher concentration of the acids produce larger ionic conductivities. However, the relationship between the conductivity and acid size reverses from high to low concentration. For example, the large $MePEG_{16}SO_3H$ acid has the largest ionic conductivity of the three MePEG acids at high concentration (1.32M), and the smallest ionic conductivity of the three MePEG acids at low concentration (0.26M). We attribute this conductivity dependence to the $MePEG_nSO_3H$ acid adding fluidity to the polymer & acid mixture.

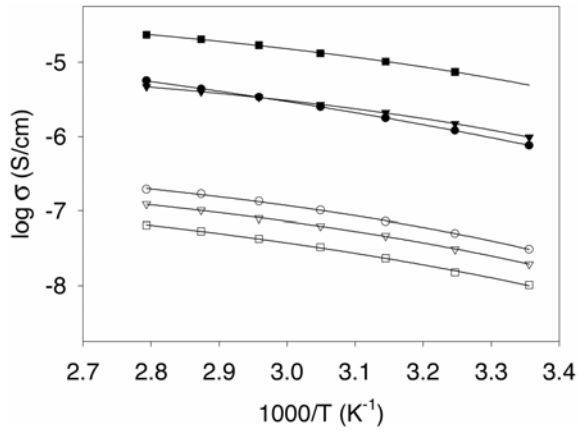

Figure 1. Activation of ionic conductivity (σ) of $MePEG_nSO_3H$ acids dissolved in the small $MePEG_3$ polymer at high (1.32M–$\lambda\tau\nu$) and low concentrations (0.26M–$\mu\nabla\rho$). $MePEG_7SO_3H$ ($\lambda\mu$), $MePEG_{12}SO_3H$ ($\tau\nabla$), $MePEG_{16}SO_3H$ ($\nu\rho$).

This increased fluidity in the mixture of $MePEG_{16}SO_3H$ acid and $MePEG_3$ polymer allows for both an increased rate of physical diffusion of the $MePEG_{16}SO_3H$ acid and an increased rate of motion of the segmental units of the polymer. This may result in a higher mobility of both the H^+ and $MePEG_{16}SO_3^-$ charge carriers, resulting in a larger overall ionic conductivity and a larger contribution from the vehicle mechanism of conductivity.

However, at the low concentration (0.26M), the $MePEG_nSO_3H$ acids are present at much lower weight fractions where it is expected that the fluidity of the mixture will be dominated by the high weight fraction $MePEG_3$ polymer. Figure 1 shows that the trend of ionic conductivity vs. $MePEG_nSO_3H$ acid size is reversed from high to low concentration yielding a trend where conductivity decreases with increased size of the acid. It is possible that this result indicates that

the mobility of the $MePEG_nSO_3^-$ anion is important to the overall ionic conductivity at this low concentration (i.e. the vehicle mechanism may be important). The higher ionic conductivity with the small $MePEG_7SO_3H$ acid may indicate that this acid has a larger D_{phys} than the larger acids.

Volume Fraction of PEG. Our hypothesis is that conductivity occurs through the Grotthus mechanism in the PEG region of the polymer and is dependant on the volume fraction of PEG. The calculation of volume fractions has been described.[2]

Figure 2 shows the dependence of equivalent conductivity (Λ) vs. the number of PEG units in the $MePEG_nSO_3H$ acids (n=7,12,16) dissolved in three $MePEG_n$ polymers (n=3,7,12). This plot shows that low concentration (0.26M) mixtures of the MePEG acids in the large $MePEG_{12}$ polymer have higher conductivities than mixtures of $MePEG_nSO_3H$ acids in the small $MePEG_3$ polymer. This dependence is likely due to the increase in the volume fraction of PEG units in a MePEG polymer with long PEG chains. In addition, the equivalent conductivity is larger in the high concentration point for each matching low (0.26M) and high (1.32M) concentration data point indicating that the mobility of one or both of the ions has increased in the high concentration samples. One possibility for this behavior is the increase in volume fraction of PEG in the high concentration samples leads to an increase in the mobility of the H^+ cation.

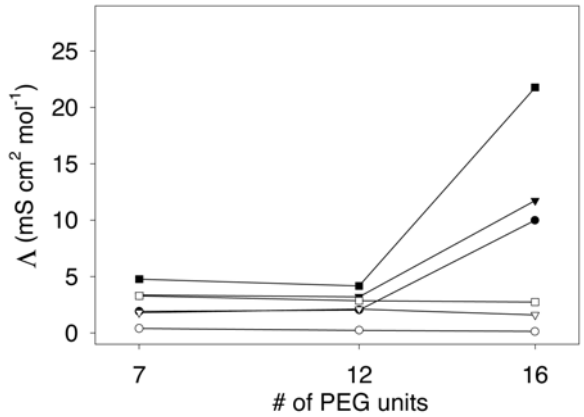

Figure 2. Dependence of equivalent conductivity (Λ) on the # of PEG units in the $MePEG_nSO_3H$ acid at high (1.32M–λτν) and low concentrations (0.26M–μ∇ρ). Samples are mixtures of $MePEG_nSO_3H$ in: the $MePEG_3$ polymer (λμ), $MePEG_7$ polymer (τ∇), and $MePEG_{12}$ polymer (νρ). All data points are at 55°C.

Low concentrations (0.26M) of the $MePEG_nSO_3H$ acids in the $MePEG_n$ polymers have no dependence on the size of the $MePEG_nSO_3H$ acid and a slope that is not significantly different than zero. This suggests that, at low $MePEG_nSO_3H$ acid concentrations, the mobility of the acid is not playing an important role in ionic conductivity. That is, the vehicle mechanism of H^+ conductivity is likely not important here.

Figure 3 shows the log of equivalent conductivity (Λ) vs. the inverse of volume fraction of PEG for a series of mixtures of $MePEG_nSO_3H$ acids and $MePEG_n$ polymers. Here, the results of experiments with four different concentrations of $MePEG_nSO_3H$ acids (0.26M, 0.43M, 1.05M, and 1.32M) are presented. According to free volume theory, diffusivity is exponentially related to the inverse of free volume,[10,11] and this type of plot has been used to determine the role of free volume in ion transport.

In Figure 3 the largest equivalent conductivities (i.e. ionic mobilities) are obtained for mixtures with the largest volume fraction of PEG (higher concentrations of the $MePEG_nSO_3H$ acid give mixtures with larger V_f of PEG). Linear regression gives a line with a slope of –5.37±0.55. While the correlation coefficient is somewhat small (r^2=0.751) and the scatter in the data appears large, an analysis of the residuals and a runs test indicate that the scatter is random, and that the regression line is not significantly non-linear. We conclude that the volume fraction of PEG in the mixtures is a good indicator of the overall ionic mobility in mixtures of our $MePEG_nSO_3H$ acid and $MePEG_n$ polymers.

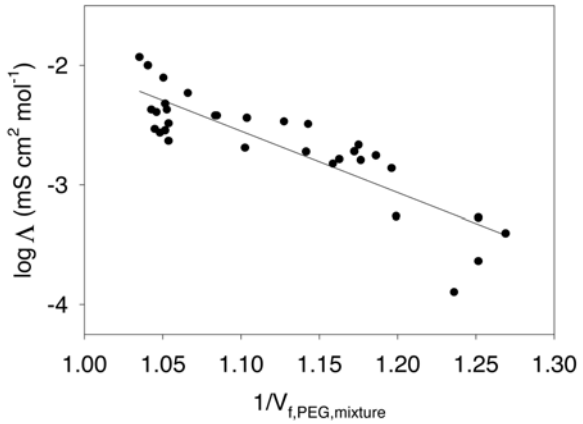

Figure 3. Dependence of equivalent conductivity (Λ) versus the inverse of volume fraction of PEG ($1/V_{f,PEG,mixture}$) in mixtures of the $MePEG_nSO_3H$ acids with the $MePEG_n$ polymers at 55°C.

Conclusions

Mechanism of H^+ Conductivity. Figure 2 clearly shows the lack of a dependence of the equivalent conductivity on the size of the $MePEG_nSO_3^-$ anion. This result strongly suggests that, at low $MePEG_nSO_3H$ acid concentrations, the mobility of the acid is not related to ionic conductivity, and that the low concentration trend in Figure 1 is due to some other factor. That is, the vehicle mechanism is not important at low concentrations.

More importantly, this system has shown an overall dependence on the free volume of the mixtures as measured by the V_f of PEG. In Figure 3, the V_f of PEG is correlated to the equivalent conductivity (i.e. ionic mobility). We conclude that the V_f of PEG in the mixtures is in control of ionic mobility. The V_f of PEG is important, because the Grotthus mechanism of H^+ conductivity in this system would be controlled by the rearrangement of ethylene oxide segments. Thus, the importance of V_f of PEG strongly suggests that the Grotthus mechanism is primarily responsible for conductivity in this system.

Acknowledgements. This research was supported in part by the NSF through the EPSCoR program (EPS-0132618).

References.

(1) Ritchie, J. E.; Crisp, J. A. *Anal. Chim. Acta* **2003**, *496*, 65-71.
(2) Ghosh, B. D.; Lott, K. F.; Ritchie, J. E. *Chem. Mater* **2005**, *17*, 661-669.
(3) Ghosh, B. D.; Lott, K. F.; Ritchie, J. E. *Macromolecules* **2005**, submitted.
(4) Lott, K. F.; Ghosh, B. D.; Ritchie, J. E. *Electrochem. Sol. St. Lett.* **2005**, submitted.
(5) Kreuer, K. D. *Chem. Mater.* **1996**, *8*, 610-641.
(6) Hooper, R.; Lyons, L. J.; Mapes, M. K.; Schumacher, D.; Moline, D. A.; West, R. *Macromolecules* **2001**, *34*, 931-936.
(7) Zhang, Z.; Sherlock, D.; West, R.; West, R.; Amine, K.; Lyons, L. J. *Macromolecules* **2003**, *36*, 9176-9180.
(8) Allcock, H. R.; O'Conner, S. J. M.; Olmeijer, D. L.; Napierala, M. E.; Cameron, C. G. *Macromolecules* **1996**, *29*, 7544-7552.
(9) Siska, D. P.; Shriver, D. F. *Chem. Mater.* **2001**, *13*, 4698-4700.
(10) Dickinson, E.; Masui, H.; Williams, M. E.; Murray, R. W. *J. Phys. Chem. B.* **1999**, *103*, 11028-11035.
(11) Cohen, M. H.; Turnbull, D. *J. Chem. Phys.* **1959**, *31*, 1164-1169.

INVESTIGATION OF PEM FUEL CELL BEHAVIOR: SWELLING AND VISCOELASTIC PROPERTIES

M.B. Satterfield, J.B. Benziger

Princeton University, Department of Chemical Engineering,
Princeton NJ 08544

Abstract

Recent work on PEM fuel cells has demonstrated the importance of membrane mechanical properties and swelling behavior on cell performance. Indeed, mechanical properties and swelling should be considered as integral factors when developing new membranes, improving cell design and creating models. The existence of two stable ignited states in autohumidified fuel cells and the cells' responses to dynamic conditions have revealed chemical-mechanical coupling in which the membrane's mechanical properties are changed by its water content which in turn changes cell performance and water production. This work presents several examples of fuel cell behavior for which mechanical properties and swelling are believed to be responsible and discusses the mechanical properties of membranes determined thus far and their relevance to cell performance.

Introduction

Previously we have presented results from auto-humidified PEM fuel cell operation, in which all feeds are dry and the water produced by the fuel cell is the only source of humidification. Under these conditions, complex phenomena caused by membrane chemical-mechanical coupling are observed. The cell's performance (water production) and the membrane hydration, conductivity, volume and stiffness continuously affect each other. This coupling shapes the cell's start-up behavior and response to dynamic operating conditions and enables the existence of two distinct stable ignited states. These behaviors have been previously reported and discussed,[1-3] and are examined here in light of membrane mechanical properties.

Figure 1 depicts the start-up behavior of a cell with different initial membrane water contents.

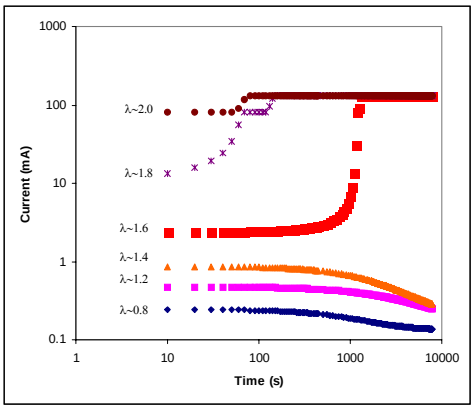

Figure 1. Autohumidified PEM fuel cell start-up behavior at 50°C with 10mL/min H_2 and O_2 flow rates and a 5 Ω load resistance. Initial water contents ($\lambda=H_2O/SO_3$) vary. The current through the external load was recorded every 10 s for 6 h. [3]

The figure shows the dependence of cell performance on membrane water content as well as the long time scale necessary for the cell to reach a true steady-state. In particular, the λ=1.6, 1.8 and 2.0 curves show a significant delay before igniting, as well as a partial ignition and delay in λ=1.8. These long time scales and response shapes are also observed when other parameters such as feed flow rates, load resistance and temperature are changed abruptly during operation, with no other perturbations to the system. The behavior is believed to be due to the viscoelastic relaxation of the polymeric membrane under the stress of both mechanical (clamping) and chemical (osmotic or swelling) pressure.

Figure 2 illustrates the existence of two ignited steady states, showing two steady-state polarization curves (each point equilibrated for 3-4 hours), one corresponding to a higher water content, the other to a lower. Between load resistances (RL) of 5Ω and 11Ω, there is a hysteresis where either state can exist, depending on the direction of approach.

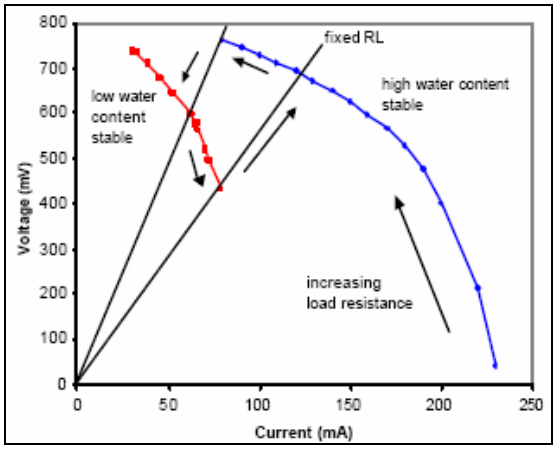

Figure 2. Steady state polarization curves for the autohumidified PEM fuel cell at 95ºC with H_2 and O_2 flows of 10 mL/min. The higher water content curve was taken after establishing steady state with a 2 Ω load resistance. The low curve was taken after establishing steady state with a 20 Ω load resistance.[1]

We believe that the existence of the lower ignited state is a result of the membrane water content being controlled by applied pressure. The force with which the cell is clamped together squeezes the membrane, reducing its potential water content.[4] The extent to which the membrane can swell against the applied pressure depends on its Young's Modulus and the swelling or osmotic pressure, which is related to the difference in chemical potential between water in the membrane and in the surrounding electrode space.

Experimental

Viscoelastic Properties. To address the cell's dynamic behavior, viscoelastic properties of the membrane are investigated. Constant-strain stress-relaxation and constant-stress creep experiments are performed at varying temperatures and humidities. Typical results appear in Figures 3 and 4 below.

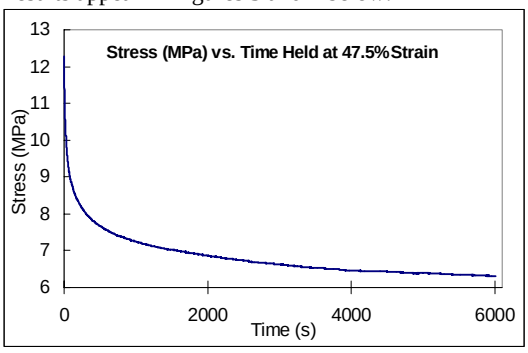

Figure 3. Stress Relaxation of Nafion 115 held at 47.5% strain for 6000 seconds under ambient temperature and humidity conditions.

For stress-relaxation experiments, the sample is quickly strained in the tensile direction by an Instron 1122 and held while the resultant stress is recorded over time. For creep experiments a free-hanging sample is loaded and strain is measured over time.

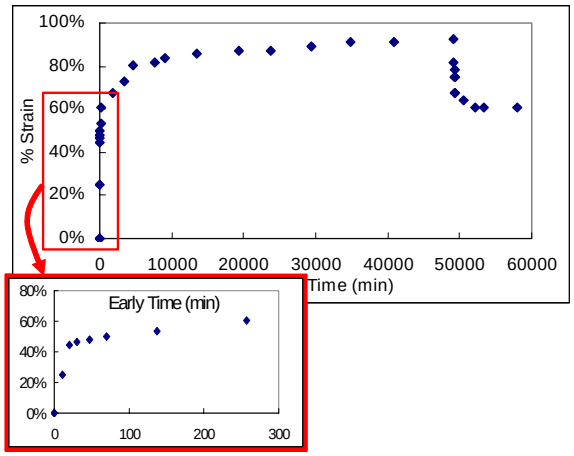

Figure 4. Creep behavior of Nafion 115 under 3.7 MPa of stress at 45C in 100% relative humidity. The bulk of the creep response occurs in the first 9000 seconds (150 min).

These data show considerable amounts of polymer creep and stress-relaxation, factors that should be considered in the design and operation of PEM fuel cells. More importantly, they exhibit time scales on the order of those witnessed in fuel cell dynamic responses, supporting the notion that polymer viscoelasticity is behind the cells' dynamic responses. Work is ongoing to quantify trends in behavior with temperature and relative humidity and to characterize membrane properties under fuel cell conditions. Both experiments are performed within an oven and a vapor barrier. As discussed below, humidity and temperature *significantly* affect membrane mechanical behavior.

Swelling Behavior. The membrane swelling behavior can be correlated to its stiffness or Young's Modulus. Tensile stress-strain tests were performed on Nafion 115 with an Instron 1122 at strain rates of 1-2 in/min and with varying temperatures and preconditioned water contents. Results for the Young's Modulus as it depends on water content (λ) and temperature appear in Figure 5.

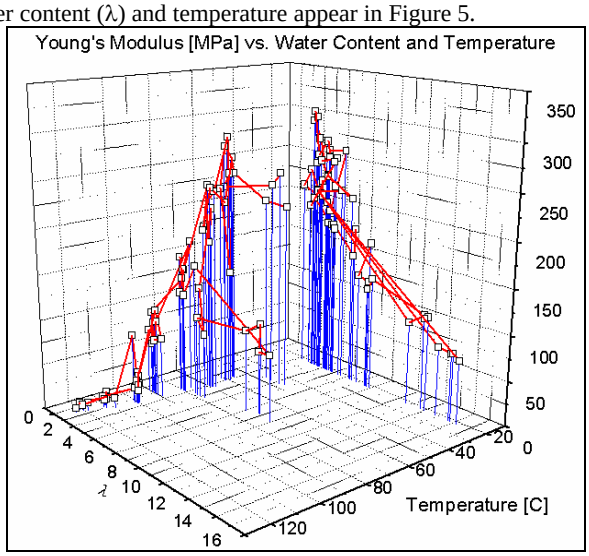

Figure 5. Dependence of Nafion 115 Young's Modulus (units in MPa) on test temperature and membrane water content ($\lambda=H_2O/SO_3$).

Clearly, increased temperature and water content dramatically reduce the membrane's Young's modulus, softening it from ~300 MPa to ~10 MPa over the range of conditions examined. This effect is important to note, as PEM fuel cell conditions necessarily involve elevated temperature and humidity, which together decrease the stiffness even further.

Of interest to swelling is the membrane's volume response to pressure, or compressibility β:

$$\beta = -\frac{1}{V}\left(\frac{\partial V}{\partial P}\right)_T$$

This compressibility can be found from the Young's modulus E by the simple relation

$$E = 3(1-2\nu)/\beta$$

were ν is Poisson's Ratio, typically 0.2-0.4 for polymers. The experimentally determined Young's modulus values yield compressibility values ranging from 0.002 to 0.2 MPa^{-1}. These values are compared to the osmotic pressure, p_{osm}:

$$p_{osm} = \frac{RT}{\bar{V}_{H_2O}} \ln\left(\frac{a_{H_2O}^{outside\ membrane}}{a_{H_2O}^{inside\ membrane}}\right)$$

The activity of water inside the membrane is calculated from the energy of mixing between the water and acid groups.

The membrane's compressibility is of the same order of magnitude as the calculated osmotic pressure, a result consistent with the finding that the membrane swells up to 20% when fully hydrated.[5] The result also indicates the potential for applied (clamping) pressure to control the membrane's swelling, thus causing the hysteresis in water content and ignited steady states, as witnessed in Figure 2.

Membrane swelling and water uptake under applied pressure is being further investigated with a controlled temperature and humidity compression device. This apparatus measures the membrane's water uptake and swelling pressure exerted over time under an applied pressure.

Acknowledgement. The National Science Foundation: CTS–0354279 and DMR-0213707 through the Materials Research and Science Engineering Center at Princeton.

References

(1) Benziger, J.; Chia, E.; Moxley, J. F.; Kevrekidis, I. G., *Chem. Eng. Sci.* **2005,** *60*, (6), 1743-1759.
(2) Benziger, J.; Chia, E.; Karnas, E.; Moxley, J.; Teuscher, C.; Kevrekidis, I. G., *Aiche J.* **2004,** *50*, (8), 1889-1900.
(3) Moxley, J. F.; Tulyani, S.; Benziger, J. B., *Chem. Eng. Sci.* **2003,** *58*, (20), 4705-4708.
(4) Escoubes, M.; Pineri, M.; Robens, E., *Thermochimica Acta* **1984,** *82*, 149-160.
(5) Morris, D. R.; Sun, X., *J. Appl. Polym. Sci.* **1993,** *50*, (8), 1445-1452.

STATES OF WATER- INVESTIGATING THE WATER-POLYMER INTERACTIONS AND TRANSPORT PHENOMENON IN PROTON EXCHANGE MEMBRANES

[1]Abhishek Roy , [2]Michael Hickner, [1]Tom Glass,[1]Yanxiang Li,
[1]Brian Einsla, [1]K.B. Wiles, [1]Xiang Yu
and [1]James E. McGrath (jmcgrath@vt.edu)

[1] Macromolecular Science and Engineering Program,
Macromolecules and Interfaces Institute
Virginia Polytechnic Institute and State University, Blacksburg, VA 24061
[2] Sandia National Laboratories, Albuquerque, NM 87123-0734

Introduction

Sulfonated copolymers studied in our laboratory phase separate to form a nano-scale hydrophilic and hydrophobic domain morphology[1]. The hydrophilic phase where in the sulfonic acid moieties reside absorbs water. Water confined in hydrophilic pores in concert with the sulfonic acid groups serve the critical function of proton (ion) conduction in these systems. It has been observed that the diffusion coefficients of both water and protons change with the water content of the pore. This change in proton and water transport mechanisms with hydration level has been attributed to the solvation of the acid groups and the amount of bound and bulk-like water within a pore. Water is known to reside in hydrophilic polymers in at least three different states as defined by the state's thermal properties[1]. *Non-freezing bound water* that is strongly associated with the polymer, shows no thermal transition by differential scanning calorimetry, but depresses the T_g of the copolymer. *Freezable bound water* which is weakly bound to the polymer (or weakly bound to the non-freezing water), displays a broad melting behavior around 0°C. *Free water* shows a sharp melting point at 0°C.

Synthesis of a controlled series of materials in both ion content and chemical composition, structure/property relationships between the functionality of the polymer backbone, the state of water, and the membrane transport has been achieved. It is anticipated that sulfone, ketone, phosphine oxide, and fluorine moieties incorporated within the polymer backbone will have a large influence on the state of water through the nano phase separation characteristics of the copolymers as well as direct interaction between the functional groups and water molecules.
The state of water in the copolymers is being quantified and characterized by differential scanning calorimetry and NMR T_2 & T_1 relaxation experiments. Self diffusion coefficients of water in a variety of copolymers were determined using pulse gradient NMR technique as a function of diffusive length.

Experimental Section.

a. Copolymer synthesis. Synthesis of hydroquinone based disulfonated poly (arylene ether sulfone)s copolymers (HQSH-xx ; xx: mole percent of disulfonated monomers) was carried out successfully via nucleophilic aromatic substitution[3]. To compare the effect of the functional group, 6F bisphenol based disulfonated poly(arylene ether ketone) copolymers with mono(Bxx) and diketone (PBxx) functional groups were synthesized .The structures of these three series of polymers are given below .

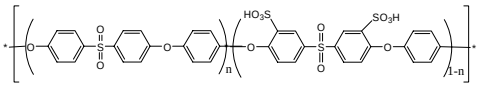

HQSH polymer in acid form

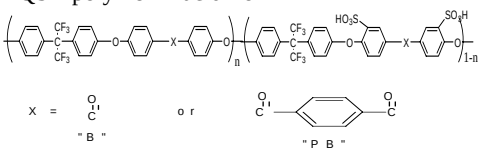

Ketone B & PB series in acid form.
The disulfonated copolymer membranes in their salt form were converted to the acid form by treating with 0.5 M sulfuric acid for 2 hours followed by immersion in deionized water for 2 hr .

b. Differential Scanning Calorimetry. The DSC experiments were performed in a TA DSC instruments using liquid nitrogen as cooling medium for sub ambient operation. The HQSHxx, Bxx and PBxx samples were equilibrated at various hydration level (from fully hydrated to 0% RH). The samples were placed in thermally sealed pans capable of withstanding pressure of 100 atm. Samples were cooled down to -70°C and then heated at a rate of 5°C per min under N_2 atmosphere.

c. T_2 relaxation measurements. The proton spin relaxation times, T_2, were measured in Varian Inova 400 MHz spectrometer using Carr-Purcell-Meiboom-Gill pulse sequence. The 90° pulse was of 13.8μs and the 180° pulse of 27.6μs. Total of 200 decay points were collected over 4 ms. Samples were equilibrated at room temperature in water. Just before the experiment they were removed from water and placed in the NMR probe

d. Determination of Self Diffusion Coefficient of water using pulse gradient stimulated echo NMR techniques[4]. Water self diffusion coefficients are measured in Varian Inova 400 MHz (for protons) nuclear magnetic resonance spectrometer with a 30 G/cm gradient diffusion probe. Total 16 points are normally collected and the signal to noise ratio is enhanced by co-adding 4 scans.

Results and Discussions

Fig 1 represents the thermograms of HQSH 35 at increasing water uptakes showing evolution of water melting endotherm and Tg depression. The transition from free water to loosely bound water is seen from the negative shift in the melting endotherm. The depression in melting point indicates interaction between the loosely bound water and the copolymer.

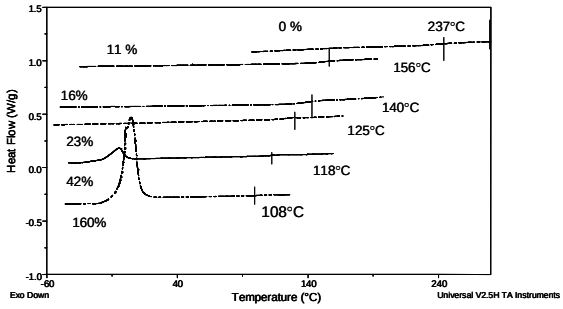

Figure 1. - Melting endotherm of HQSH 35

The tightly bound water can be correlated to the maximum amount of water for which there is no melting endotherms

The NMR T_2 relaxation measurements were also conducted on the fully hydrated samples. The experimental results were fitted

into a tri, bi or mono exponential decay function depending upon the type of water present[2] . Both DSC and NMR results were evaluated in proper quantification of three types water.

The integrated Δ H of fusion, the total amount of free plus loosely bound water and tightly bound water are reported in Table I.

Table I. H of fusion of water and quantification of states of water.

Sample HQSH	IEC (meq/g of SO_3H	Δ H (J/gm of water)	Total water λ (N H_2O/SO_3H)	Free +loosely bound water (λ)	Tightly bound water (λ)
20	1.2	50	14	5	9
30	1.6	130	29	20	9
35	1.8	180	48	39	9

It can be seen that the Δ H of fusion for water increases with increase in sulfonation level and free water content, which is likely due to better water-water interactions.

Self Diffusion coefficient of water. In a hydrated PEM, ^1H nuclei exchange rapidly between H_2O and H^+ environments. Accordingly the measured ^1H diffusion coefficient is a weighted average of the diffusion coefficient for separate environments. For a system having three states of water, the types of water differ from each other in their diffusive lengths. Thus the diffusion coefficient measured as a function of diffusion time will show a decay curve. Fig 3 represents the plot of diffusion coefficient as a function of effective diffusion time for the HQSH series. The effective diffusion time was varied by varying the Δ- term. It appears that the diffusion coefficient of HQSH 35 is higher than HQSH 30 and 25. This is in agreement with the amount of free water present in the sample.

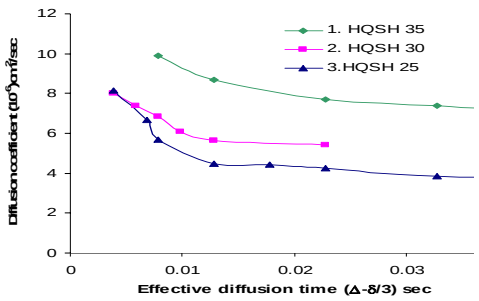

Figure 2. Diffusion coefficient of water as a function of effective diffusion time and copolymer composition.

Conclusions

The states of water were characterized for ion containing copolymers with DSC and NMR relaxation experiments. The of fusion for the free and loosely bound water was calculated and was found to increase with IEC and with free and loosely bound water content. Self diffusion coefficient was calculated using PGSE NMR experiments and was related to the different states of water. Further discussion of the results will be presented.

Acknowledgements. The authors would like to thank the National Science Foundation "Partnership for Innovation" Program (HER-0090556) and the Department of Energy (DE-FC36-01G01086) for support of this research effort.

References

1.Hickner,M.;Ghassemi,H.;Kim,Y.S.;McGrath,J.E., Chem. Rev. **2004**,*104(10)*,4587-4611
2. Kim, Y. S.; Dong, L.; Hickner, M. A.; Glass, T. E.; Webb, V.; McGrath, J. E.,Macromolecules **2003**, *36(17),* 6281.
3.Roy,A.; Einsla,B.;Harrison,W.L.;Hickner,M.;McGrath,J.E., Preprint of Symposia-American Chemical Society, Division of Fuel Chemistry **2004**,*49(2)*,614-615
4.Stejskal, E.O.; Tanner ,J.E., J. Chem. Phys **1965**, *42*, 288.

VISCOMETRIC BEHAVIOR AND MOLECULAR WEIGHT CHARACTERIZATION OF SULFONATED POLY(ARYLENE ETHER SULFONE) COPOLYMERS

*Juan Yang, Yanxiang Li, Hang Wang, Melinda Hill, Xiang Yu, Kenton B. Wiles, Hae-Seung Lee, James E. McGrath**

Department of Chemistry, Virginia Polytechnic Institute and State University, Blacksburg, VA 24061
*jmcgrath@vt.edu

Introduction

Proton exchange membrane (PEM), the key component of fuel cell, is responsible for the proton transport from the anode to the cathode, therefore directly determining the performance of the fuel cell. PEMs must have good mechanical, thermal and chemical stabilities and still have high proton conductivity. Many families of polymers with differing chemical structures and various strategies for incorporation of sulfonic acid groups have been explored as PEM materials. Sulfonated poly(arylene ether sulfone)s are promising candidates due to their good acid and thermal oxidative stabilities, high glass transition temperatures and excellent mechanical strengths. Our group has reported synthesis of poly(arylene ether sulfone) copolymers by directly copolymerizing sulfonated monomers.[1] This procedure is more preferable relative to post modification method since it is easy to control the degree of sulfonation and avoid the side reactions. However, this new synthetic route brought a whole new challenge in determining the molecular weight of the final polymer product. Molecular weight is a critical parameter defining PEM durability and this has not been properly characterized for any PEM membranes including Nafion, which is probably the most glaring omission in new ion conducting polymer research.[2] In the post modification method, sulfonic acid groups are formed by chemical modification of polymeric precursors and MW characterization of precursors is usually performed. The aim of this work was to study dilute solution behavior and develop techniques for the proper MW characterization of the ion-containing PEMs.

Experimental

Materials. *Tert*-butylphenyl terminated sulfonated poly(arylene ether sulfone) copolymers with different molecular weight (20 kg/mol ~ 50 kg/mol) were prepared by direct polymerization of the activated halides, biphenol and a t-butylphenyl endcapping reagent as shown in Scheme 1.[3] For all copolymers, the mole ratio of 4,4'-dichlorodiphenylsulfone(DCDPS) to 3,3'-disulfonated 4,4'-dichlorodiphenylsulfone (SDCDPS) was fixed to

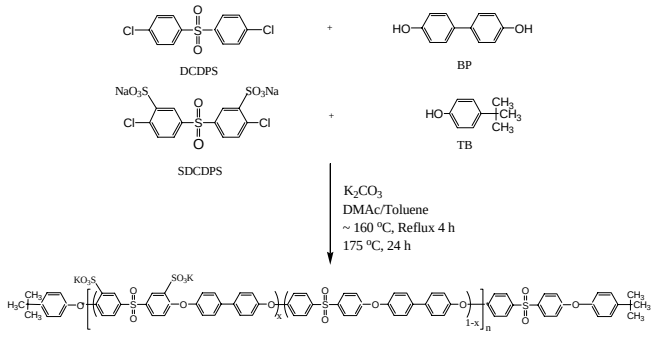

x=0.35 BPS35_20K, BPS35_40K, BPS35_50K

Scheme 1. Synthesis of tert-butylphenol terminated poly(arylene ether sulfone)s containing sulfonate groups 6.5/3.5. The molecular weight determined from ^{1}H NMR spectra was consistent with the theoretical values.

BPS35-control copolymer, with SDCDPS/DCDPS of 3.5/6.5 was also prepared from biphenol, DCDPS and SDCDPS under the similar polymerization condition without endcapping agent, in which the stoichiometry between dihalide monomers and biphenol was maintained at 1:1. GPC and intrinsic viscosity measurement show that it has higher molecular weight than all the other endcapped BPS35 as expected.

Intrinsic Viscosity Measurement. Viscosity measurements were carried out with a Cannon Ubbelholde viscometer with a flow time of about 98s for pure NMP at 25^{o}C. The temperature was regulated at 25 ± 0.1^{o}C. Each solution for viscometry was freshly prepared and was kept at 25.0 ± 0.1^{o}C for 10 min prior to the measurement. All the solutions were filtered in order to remove undissolved particles before introduction into the viscosimeter. The polymer concentration were suitably chosen to obtain relative viscosities in the appropriate range. After each determination, the viscometer was flushed at least 3 times with distilled water before rinsing with acetone prior to drying in the oven. This procedure was important because acetone is a precipitant for the copolymer. For the same reason, acetone vapor must be thoroughly removed before the introduction of the next solution.

GPC Measurement. GPC experiments were performed on a liquid chromatograph equipped with a Waters 1515 isocratic HPLC pump, Waters Autosampler, Waters 2414 refractive index detector and Viscotek 270 dual detector. LiBr/NMP was used as the mobile phase. The column temperature is maintained at 60^{o}C because of the viscous nature of NMP. Both the mobile phase solvent and sample solution were filtered before introduction to the GPC system.

Results and Discussion

Figure 1 presents the evolution of the reduced viscosity and inherent viscosity versus concentration of BPS35-control sample in salt-free NMP and in 0.05M LiBr/NMP respectively. The solution properties of BPS35 in the polar medium NMP with and without added salt are radically different. A polyelectrolyte effect is clearly observed. As one dilutes a charged macromolecule, they experience molecular coil expansion, exhibiting higher reduced viscosity as the concentration is reduced due to the charge repulsion along the polymer backbone.[4] The presence of small electrolyte LiBr, which determines the solution ionic strength, screens out charges and the repulsive interactions, affords a linear plot and enables us to obtain conventional extrapolations to dilute solution viscosity. Thus the key for the dilute solution viscosity measurements for ion-containing PEM is the introduction of a low molar mass salt, which is often quite appropriately able to screen the charges. However, based upon the consideration that the optimum salt concentration might depend upon the chemical structure, molar mass range, charged density etc., dilution viscosity measurements of different MW BPS35 samples in NMP containing various concentrations of LiBr from 0.01M to 0.1M were also performed. Linear plots were obtained for all the samples in all these salt concentrations. Intrinsic viscosity data obtained for different concentrations of salt were presented in table 1. One trend can be observed from the tabulated data. Increasing of the salt level decreases the intrinsic viscosity. It is clearly shown that the intrinsic viscosity drops significantly from the salt level of 0.01M to 0.05M for all the samples. Obviously 0.01M LiBr is not enough to screen the charges of BPS35. Furthermore, for the samples with the MW lower than 50K there shows only small decrease of intrinsic viscosity, probably within the experimental error, from the salt level of 0.05M to 0.1M. For the samples with MW equal or higher than

50K, there shows still further decrease of intrinsic viscosity from the salt level of 0.05 to 0.1M.

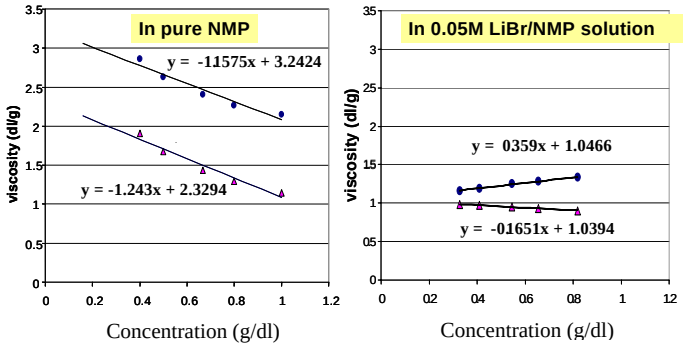

Figure 1. Evolution of the reduced viscosity and inherent viscosity versus concentration of BPS35-control sample in salt-free NMP and in 0.05M LiBr/NMP respectively.

Table 1. Summary of Intrinsic Viscosity Result of BPS35 at Different Salt Levels.

Sample	[η] [dl/g] 0.01M LiBr	[η] [dl/g] 0.05M LiBr	[η] [dl/g] 0.1M LiBr	$[\eta]_\infty$ [dl/g] (salt-free) Liberti-Stivala equation
BPS35_20K	0.51	0.43	0.41	0.43
BPS35_40K	0.70	0.56	0.52	0.54
BPS35_50K	0.95	0.74	0.68	0.59
BPS35_control	1.41	1.04	0.93	0.91

For salt-free polyelectrolyte solutions, an empirical analysis could also be performed to extract the intrinsic viscosity by extrapolation to infinite concentration using the Liberti-Stivala equation[5,6]

$$\eta_{red} = [\eta]_\infty + k\frac{[\eta]_\infty}{\sqrt{c}}$$

Where $[\eta]_\infty$ represents the intrinsic viscosity when the charges are shielded to the extent that the macromolecule behaves as a non-charged chain and is determined from the extrapolation to infinite concentration. Figure 2 shows the evolution of reduced viscosities for BPS35 with different molecular weights in salt-free NMP. The plot of η_{red} versus $c^{-1/2}$ is presented in Figure 3. The viscosity of BPS35 solutions is well represented by the Liberti-Stivala equation since a linear behavior is obtained. $[\eta]_\infty$ values of BPS35 samples with different molecular weights obtained by linear extrapolation were listed in Table 2.

The GPC measurement of BPS35 was also performed using NMP/LiBr as the mobile phase. The existence of charged groups in the copolymer coil may causes some specific problems in interpreting the results of GPC because, in addition to size exclusion, some additional mechanism might be involved.[7] Our result shows that GPC coupled with the light scattering detection seems to be a very promising way to characterize the MW of ion-containing PEMs. The detailed GPC data will be presented in the meeting.

Conclusions

Intrinsic viscosity measurements of BPS35 with different molecular weights were conducted in NMP with different concentration levels of LiBr. The salt (LiBr) was used to shield the polyions from intramolecular expansion and afforded linear plots. For salt-free BPS35 solutions, the viscometric behavior is shown to fit well with the Liberti-Stivala equation.

Acknowledgements

The authors would like to thank the Department of Energy for support of this research effort.

References

(1) Wang, F.; Hickner, M.; Kim, Y.S.; Zawodzinski, T.; McGrath, J.E.; *J. of Membr. Sci*, **2002**, 197,231-242

(2) Hickner, M. A.; Ghassemi, H.; Kim, Y. S.; Einsla, B. A.; McGrath, J.E.; Alternative polymer systems for proton exchange membranes (PEMs), *Chem. Rev.*, **2004**, 104, 4587

(3) Wang, F.; Glass, T., Li, X.; Hickner, M.; Kim Y.S.; J.E. McGrath, *Polymer Preprint*, **2002**, 43(1), 492-493

(4) Cohen, J.; Priel, Z.; Rabin, Y.; *J. Chem. Phys*. **1988**, 88, 7111

(5) Yan, L.; Dougherty, T. J.; Stivala, S. S.; *J. Polym. Sci. Part A2*, **1972**, 10, 171

(6) Aldebert, P.; Gebel, G.; Loppinet, B.; Nakamura, N.; *Polymer*, **1995**, 36, 431-434

(7) Blagodatskikh, I. V.; Sutkevich, M. V.; Sitnikova, N. L.; Khokhlov. A. R.; *J. Chromatography A*, **2002**, 976, 155-164

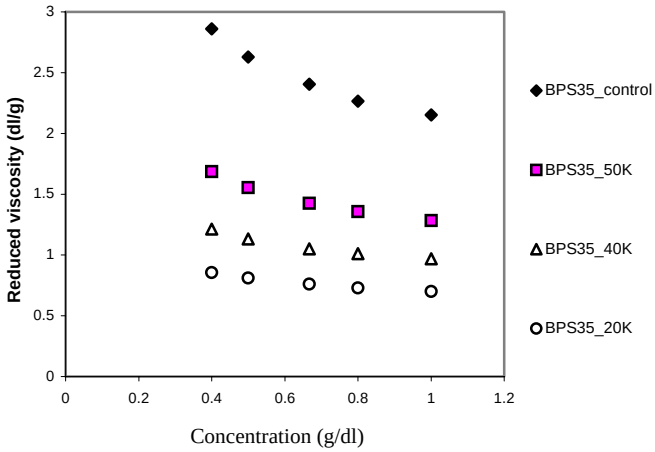

Figure 2. Concentration dependence of reduced viscosity of BPS35 in salt-free NMP

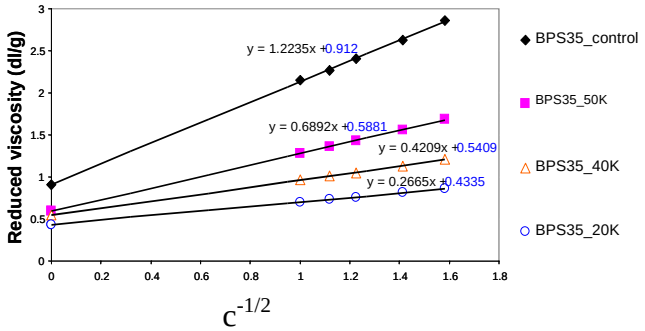

Figure 3. η_{red} versus $c^{-1/2}$ of BPS35 solutions in salt-free NMP

MORPHOLOGICAL ANALYSIS BY ATOMIC FORCE MICROSCOPY (AFM) OF PARTIALLY FLUORINATED DISULFONATED POLY(ARYLENE ETHER SULFONE) COPOLYMERS

*Anand S. Badami, Brian Einsla, Melinda Hill, Kenton B. Wiles and James E. McGrath**

Department of Chemistry
Macromolecules and Interfaces Institute
Virginia Polytechnic Institute and State University
Blacksburg, VA 24061, USA
*jmcgrath@vt.edu

Abstract

The realization of proton exchange membrane (PEM) fuel cells as commercially available energy conversion sources for a variety of applications depends largely upon the development of PEMs whose properties are enhanced over current perfluorinated sulfonic acid PEMs. An essential key to developing such materials lies in understanding how the morphology of a membrane affects its properties relevant to PEM usage such as proton conductivity and hydrolytic stability. The present study evaluates the relationship between the morphologies and select membrane properties of partially fluorinated poly(arylene ether sulfone) copolymers with disulfonation levels ranging from 10 to 60 mol%. Morphology was characterized by tapping mode atomic force microscopy. Molecular weight was estimated by intrinsic viscosity, and the water uptake and protonic conductivities of the polymers were also quantified. For disulfonation levels at or below 45 mol%, water uptake and conductivity were shown to scale proportionally with changes in morphological phase separation of the polymers. Analysis of two 35 mol% disulfonated membranes of different molecular weight suggested that molecular weight influences copolymer phase separation during membrane fabrication, but further study is required to elucidate the relationship between molecular weight, morphology, and membrane properties.

Introduction

The proton exchange membrane (PEM) fuel cell is fuel conversion technology for applications ranging from automobiles, homes, and portable electronic devices. PEMs must possess several characteristics to be viable, like high protonic conductivity, good mechanical properties, hydrolytic stability, low fuel permeability, and cost effectiveness [1]. While Nafion®, a perfluorinated sulfonic acid polymer, is currently the standard for use in PEMs, its limitations, which include cost and fuel permeability, have prompted research into alternative PEM materials. A promising alternative to Nafion® may be sulfonated poly(arylene ether sulfone) (BPSH) copolymers, which display good chemical/mechanical stability and proton conductivity, as well as reduced fuel permeability [2]. Sulfonated poly(arylene ether sulfone) copolymers synthesized with fluorinated comonomer (4,4'-hexafluoroisophenylidene diphenol or 6F-bisphenol) possess the positive membrane characteristics of BPSH copolymers and bond well to Nafion® electrodes. Understanding how the morphology of a membrane is related to its PEM properties is a necessary, but largely overlooked, step in developing new PEM materials. Consequently, the present study evaluates the relationship between morphology and membrane properties of partially fluorinated disulfonated poly(arylene ether sulfone) copolymers.

Experimental

Materials. Partially fluorinated poly(arylene ether sulfone) random copolymers with varying amounts of disulfonation (6FS-x; where x equals 10, 25, 35, 45, or 60 mol%) were synthesized as previously reported [3]. N,N-Dimethylacetamide (DMAc; EMD Chemicals, Gibbstown, NJ) was used as received.

Film Casting and Membrane Acidification. Copolymers in their potassium sulfonate salt form were dissolved in DMAc (7.5% (w/v) for microscopy, 10% (w/v) for all other characterizations). Solutions were syringe filtered through 0.45 μm Teflon® filters and cast onto clean glass substrates. The transparent solutions were dried under a 120V, 250W infrared lamp for 24 h and the resultant films were dried under vacuum at 60 °C for 12 h. Films were lifted from their substrates by immersion in deionized water. The 6FS-60 film was converted to its acid form (6FSH-60) by immersion in 1.5 M sulfuric acid for 24 h followed by rinsing and then immersion in deionized water for 24 h, which has been termed "Method 1" [2]. All other films were boiled in 0.5 M sulfuric acid for 2 h, rinsed, and then boiled in deionized water for 2 h, termed "Method 2" [2].

Characterization

Intrinsic viscosities of the potassium sulfonate salt form of the copolymers were obtained in NMP with 0.05 M LiBr at 30°C using an Ubbelohde viscometer. Conductivity measurements of acidified membranes were performed at 30 °C in water using a Hewlett-Packard 4192A impedance/gain-phase analyzer over a frequency range of 10 Hz-1 MHz. The cell geometry was chosen to ensure that the membrane resistance dominated the response of the system. The resistance of the film was taken at the frequency that produced the minimum imaginary response. To obtain water uptake values, membranes were dried for 24 h at 100 °C, weighed, and immersed in deionized water at room temperature for 24 h. The wet membranes were blotted dry and immediately weighed again. Water uptake was calculated as the ratio of the difference between wet and dry membrane weight divided by dry membrane weight and expressed as a weight percent. Atomic force microscopy (AFM) images were obtained using a Digital Instruments Dimension 3000 microscope in tapping mode, with micro-machined cantilevers with force constants of 40 N/m or 5 N/m. Samples were dried under vacuum at 60 °C for 12 h and then equilibrated at 50% relative humidity for at least 12 h before being imaged immediately at room temperature in a relative humidity of approximately 35%.

Results and Discussion

A series of partially fluorinated poly(arylene ether sulfone) copolymer (Figure 1) membranes with varying amounts of disulfonation (6FSH-x; where x equals 10, 25, 35, 45, or 60 mol%) were imaged using tapping mode AFM (Figure 2).

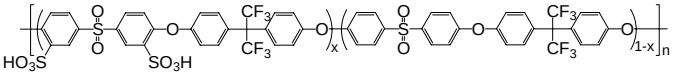

Figure 1. Chemical structure of partially fluorinated poly(arylene ether sulfone) copolymers.

The AFM images show that these 6FSH-x copolymers display a hydrophilic/hydrophobic phase separated morphology, with the hydrophilic sulfonated domains appearing darker than the hydrophobic domains. This is expected because BPSH copolymers have been shown to display similar phase separated morphology as a result of their direct copolymerization of biphenol units with hydrophobic diphenyl sulfones and hydrophilic disulfonated diphenyl sulfones [4]. 6FSH-x copolymers are synthesized similarly to BPSH, but with 6F-bisphenol instead of biphenol, which introduces fluorination into their structure.

Water uptake of the 6FSH-x copolymers was measured (Figure 3). There are two distinct parts of the water uptake vs. disulfonation plot. In the first part, regime I, water uptake gradually increases with an increase in disulfonation. The AFM images in

Figure 2 corroborate this observation because the connectivity of the hydrophilic (dark) domains appears to increase slightly with level of disulfonation, reaching a maximum between 35 and 45 mol% disulfonation.

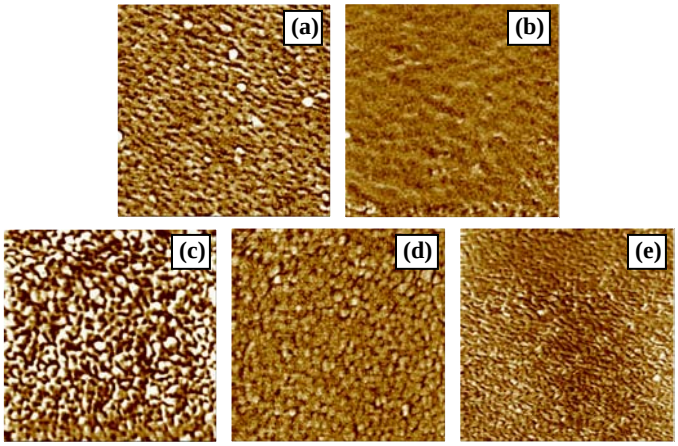

Figure 2. Tapping mode AFM phase images of 6FSH-x membranes with varying levels of disulfonation (mol%): (a) 10 (b) 25 (c) 35 (d) 45 and (e) 60. Scan sizes: 1µm, *Z* ranges: (a) 25° and (b-e) 8°.

In the second part of the graph, regime II, the water uptake increases dramatically as disulfonation increases to 60 mol%. This phenomenon has been observed before for BPSH membranes [4]. The swelling accompanying such a large water uptake would make BPSH-60 undesirable for use as a high-performance PEM.

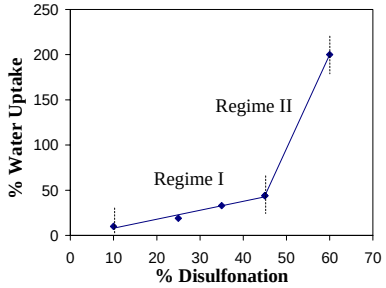

Figure 3. Effect of level of disulfonation on water uptake of 6FSH-x membranes.

Proton conductivity measurements were also made on the 6FSH-x copolymer series (Figure 4). Unlike water uptake, conductivity increases proportionally with level of disulfonation. Only the 6FSH-60 membrane displayed a proton conductivity above 0.08 S/cm, which is desired for high-performance fuel cell PEMs.

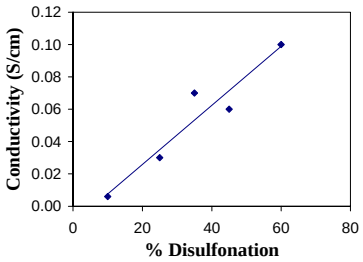

Figure 4. Effect of level of disulfonation on conductivity of 6FSH-x membranes.

A second 6FSH-35 membrane with a lower molecular weight than the one in Figure 1 was also imaged by tapping mode AFM. (Figure 5). The two 6FSH-35 copolymers have distinctly different molecular weights as indicated by their intrinsic viscosities (Table 1). Despite this difference, the water uptake and conductivity data for the two 6FSH-35 copolymers are essentially the same (Table 1). However, the difference in molecular weight is manifested in the multiphase morphology of the two membranes (Figure 5).

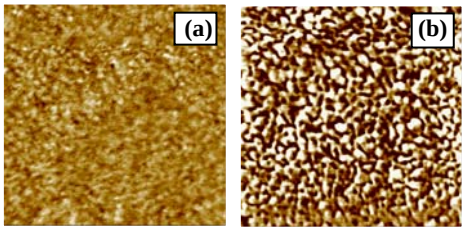

Figure 5. Tapping mode AFM phase images of 6FSH-35 membranes of (a) low and (b) high molecular weights (intrinsic viscosity data in Table 1). Scan sizes: 1µm, *Z* ranges: 6° and 8°.

Table 1. Properties of 6FSH-35 Membranes

6FSH-35 Membrane	Intrinsic Viscosity (dL/g)	Water Uptake (%)	Proton Conductivity (S cm^{-1})
low MW	0.50	33	0.07
high MW	1.01	30	0.07

The 6FSH-35 copolymer of lower molecular weight possesses smaller hydrophobic (bright) and hydrophilic (dark) domain structures than its higher molecular weight counterpart. This suggests that while molecular weight influences the phase separation of the ionomeric copolymers during membrane fabrication, it may or may not have as pronounced of an influence on membrane properties like water uptake and conductivity. Further study is required to assess whether molecular weight plays a greater role in affecting phase separation during membrane casting or acidification.

Conclusions

At low levels of disulfonation (≤45 mol%), both water uptake and proton conductivity of 6FSH-x membranes increase proportionally with disulfonation. These increases correspond to an increase in connectivity of the hydrophilic sulfonated domains in the morphologies of the membranes. While conductivity is favorable for PEM usage at 60 mol% disulfonation, water uptake is too high, preventing the membranes tested from being immediate candidates for high-performance PEMs. Morphological analysis of two 6FSH-35 membranes of two different molecular weights suggests that molecular weight influences copolymer phase separation during membrane fabrication, but it may or may not have as pronounced of an influence on all membrane properties. Further study is required to elucidate the relationship between molecular weight, morphology, and membrane properties.

Acknowledgement. The authors wish to thank the National Science Foundation "Partnership for Innovation" Program (HER-0090556) and IGERT Program (DGE-0114346), and the Department of Energy (DE-FC36-01G01086) for supporting this research.

References

(1) Hickner, M.A.; Ghassemi, H.; Kim, Y.S.; Einsla, B.R.; McGrath, J.E.. *Chem. Rev.* **2004**, *104*, 4587.
(2) Kim, Y.S.; Wang, F.; Hickner, M.; McCartney, S.; Hong, Y.T.; Harrison, W.; Zawodzinski, T.A.; McGrath, J.E. *J. Polym. Sci., Part B: Poly. Phys.* **2003**, *41*, 2816.
(3) Harrison, W.; Wang, F.; Mecham, J.B.; Bhanu, V.; Hill, M.; Kim, Y.S.; McGrath, J.E. *J. Polym. Sci., Part A: Polym. Chem.* **2003**, *41*, 2264.
(4) Wang, F.; Hickner, M.; Kim, Y.S.; Zawodzinski, T.A.; McGrath, J.E. *J. Membr. Sci.* **2002**, *197*, 231.